



Deliverable D4.2:

Report on information fusion and decision support



Project information

Project Acronym:	TEMA
Project full title:	Trusted Extremely Precise Mapping and Prediction for Emergency Management
Call identifier:	HORIZON-CL4-2022-DATA-01-01
Type of action:	HORIZON Research and Innovation Actions
Start date:	1 December 2022
End Date:	30 November 2026
Grant agreement No.:	No. 101093003

Deliverable D4.2: Report on information fusion and decision support			
Executive summary :	This deliverable outlines critical technological components developed in TEMA that automate and enhance situational awareness and decision-making capabilities for NDM. It discusses methods for advanced fusion of data including satellite analysis results, semantic, sentiment, spatial and temporal information from social media and multi-source web data. By integrating diverse data sources, automating processes, fusing data and generating actionable insights these innovations improve disaster response. The document serves as a foundation for ongoing integration and evaluation within TEMA for a holistic approach to disaster management.		
WP:	WP4		
Author(s):	Monika Friedemann, Martin Mühlbauer, Fabian Henkel, Dmitriy Shutin, Victor Scott Prieto Ruiz, Patrick Hinsen, Thomas Wiedemann		
Editor:			
Leading Partner:	DLR-DFD		
Participating partners:	All partners		
Version:	1.0	Status	final
Deliverable type:	R – Document, report	Dissemination level	PU - Public
Official submission date :	30/05/2025	Actual Submission Date	05/06/2025

Disclaimer

This document contains material, which is the copyright of certain TEMA contractors, and may not be reproduced or copied without permission. All TEMA consortium partners have agreed to the full publication of this document if not declared “Confidential”. The commercial use of any information contained in this document may require a license from the proprietor of that information. The reproduction of this document or of parts of it requires an agreement with the proprietor of that information.

The TEMA consortium consists of the following partners:

No.	Partner Organisation Name	Partner Organisation Short Name	Country
1	ARISTOTELIO PANEPISTIMIO THESSALONIKIS	AUTH	GR
2	DEUTSCHES ZENTRUM FUR LUFT – UND RAUMFAHRT EV	DLR	DE
3	ENGINEERING - INGEGNERIA INFORMATICA SPA	ENG	IT
4	ATOS IT SOLUTIONS AND SERVICES IBERIA SL	ATOS IT	ES
4.1	ATOS SPAIN SA	ATOS SP	ES
5	UNIVERSIDAD DE SEVILLA	USE	ES
6	TECNOSYLVA SL	TSYL	ES
7	NORTHDOCKS GMBH	ND	DE
8	INTERDISCIPLINARY TRANSFORMATION UNIVERSITY AUSTRIA	IT:U	AT
9	THE LISBON COUNCIL FOR ECONOMIC COMPETITIVENESS ASBL	LC	BE
10	LATITUDO 40 SRL	LAT40	IT
11	NELEN & SCHUURMANS TECHNOLOGY BV	NS	NL
12	FRAUNHOFER GESELLSCHAFT ZUR FORDERUNG DER ANGEWANDTEN FORSCHUNG EV	FHHI	DE
13	UNIVERSITA DEGLI STUDI DI MESSINA	UNIME	IT
14	KAJAANIN AMMATTIKORKEAKOULU OY	KAMK	FI
15	KAINUUN HYVINVOINTUALUE	KAHY	FI
16	KENTRO MELETON ASFALEIAS	KEMEA	GR
17	DIMOS MANTOUDIYOU - LIMNIS - AGIAS ANNAS	D.MALLIAN	GR
18	REGIONE AUTONOMA DELLA SARDEGNA*RAS	RAS	IT
19	BAYERISCHES ROTES KREUZ	BRK	DE

Document revision history

Version	Author/Editor	Summary of Changes Made
v0.1	DLR-DFD	First Draft
v0.8	DLR-DFD	Version for review
v0.9	ND	Reviewed version
v1.0	DLR-DFD	Final version

Contributing author(s)

Name(s)	Partner
Monika Friedemann	DLR
Martin Mühlbauer	DLR
Fabian Henkel	DLR
Dmitriy Shutin	DLR
Victor Scott Prieto Ruiz	DLR
Jose Ramiro Martinez de Dios	USE
Abdalraheem Abdullah Ijeh	USE
David Hanny	IT:U
Miguel Navarrete	TSYL
Joost van Dijk	NS
Joep Grispen	NS
Margareta Mihalic-Dogan	BRK
Joachim Perschbacher	ND

Table of Contents

Executive Summary	10
1. Introduction	12
1.1 Purpose and Scope of the Document	12
1.2 Structure of the Document	12
2. Summary of the work carried out.....	13
2.1 Objectives	13
2.2 Summary of the work carried out with respect to the objectives	13
3. Information Fusion	15
3.1 Introduction	15
3.2 Novelties of TEMA Information Fusion.....	15
3.3 Main Activities Performed (Months 19-30)	17
3.4 The TEMA Information Fusion Framework.....	18
3.5 Web Application Design and Implementation of the Information Fusion (IF) Module	27
3.6 Comprehensive Fusion Workflow in TEMA Technology PDM-tech-05.....	33
3.7 Summary (Key Outcomes)	48
3.8 Fusing Information Derived from Social Media	51
4. Decision Support Service for Remote Sensing	58
4.1 Main Activities Performed (Months 13–30)	58
4.2 State of the Art and Advancements Made	59
4.3 Technical Design and Implementation of PDM-tech-06.....	62
4.4 Performance in Real Events	74
4.5 Impact and Future Prospects.....	76
5. Conclusions	77
References	78
Annex A: Usage of the Decision Support Endpoint	82
Annex B: Related publications.....	85

List of Figures

Figure 1: Asynchronous occupancy grid mapping approach.....	19
Figure 2: The established coordinate systems including inertial (X_I, Y_I, Z_I), Drone, (X_D, Y_D, Z_D), gimbal (roll, yaw, pitch), and the camera (X_C, Y_C, Z_C) frames.	25
Figure 3: The ray tracing setup.	26
Figure 4: Information Fusion interaction diagram.	28
Figure 5: Deployment and Operational Workflow of the Cloud-based Web Application. This diagram highlights the integration of Data Sources, the Web Application, and Storage & Context Broker components, all orchestrated using Docker and Kubernetes for scalable and resilient operations.	34
Figure 6: Received Alert notification.	36
Figure 7: Creation of Maps4Flood and Maps4Objects after extracting Area of Interest (AOI) from an Alert notification.	37
Figure 8: Example of a Unmanned Aerial Vehicle (UAV) segmentation mask before and after georeferencing.	37
Figure 9: Example of a UAV segmentation mask before and after georeferencing.....	38
Figure 10: Example of a UAV segmentation mask before and after georeferencing.....	38
Figure 11: Fusion of FireSegmentation and BurntSegmentation masks into the Maps4Fire occupancy grid (inset shows the local update).	39
Figure 12: Original satellite-derived flood extent mask for the historical Ahrtal flood scenario (TFA-tech-08).	40
Figure 13: Cropped and resampled flood segmentation for the historical Ahrtal event, aligned to the 20m cells of Maps4Flood.	41
Figure 14: Comparison of the Maps4Flood occupancy grid before (left) and after (right) fusing the satellite-derived flood mask for the historical Ahrtal event.	41
Figure 15: Fusion of rasterized HotspotResult metrics into the Maps4Fire grid for the flood case scenario of Ahrtal.....	42
Figure 16: Occupancy grid fusion for the Ahrtal flood scenario.	43
Figure 17: Prediction at the first hour.	44
Figure 18: Prediction at the second hour.	45
Figure 19: Prediction at the third hour.	45
Figure 20: Prediction at the fourth hour.	45
Figure 21: Prediction at the fifth hour.	46
Figure 22: Georeferenced detections of the SinglePostResult.	47
Figure 23: Georeferenced detections out of TFA-tech-05 (PersonVehicleDetection).....	48
Figure 24: Predicted (blue) vs. Kalman-filtered (red) trajectories.....	49
Figure 25: Tolerance over time.	49
Figure 26: Methodological workflow of the JSTTS framework developed within TEMA	53
Figure 27: Learned weights of the trained (Geo-)GSOM networks in all three dimensions x, y (plotted on the axes) and z (colour) given the artificial training data	54

Figure 28: Visual representation of the multimodal Ahr Valley clusters identified as potentially flood-related, juxtaposed with respect to the associated sentiment (negative and neutral). The figure displays the convex hull of the clusters in geographic space, coloured by sentiment. The cluster labels in the format *cluster ID:name* were computed with the help of Llama-2-70b-chat and placed at the representative cluster location learned by the Geo-GSOM. The density of underlying posts is displayed using a heat map. To provide context, flooded areas identified by the Copernicus Emergency Management Service are depicted in blue..... 57

Figure 29: Comparison between state-of-the-art and proposed automated SEM workflow 60

Figure 30: Condensed timeline of the CEMS activation EMSR517 for Bad Neuenahr-Ahrweiler with time in UTC. 61

Figure 31: Architecture of PDM-tech-06 63

Figure 32: Prioritisation of satellite sensors for flood and wildfire from highly suitable (green), over suitable (yellow) to less suitable (red). S=Sentinel, L=Landsat, WV=WorldView, GE=GeoEye 65

Figure 33: Interactions of PDM-tech-06 in the context of the TEMA platform 66

Figure 34: Different time steps with various flood extents. 68

Figure 35: Possible geospatial map visualisation of an AOI derived from a manually ingested Ahrtal warning 69

Figure 36: Possible geospatial map visualisation of selected relevant satellite overpasses 70

Figure 37: Possible list visualisation of relevant satellite overpass windows. The table shows for each satellite the prioritisation for the disaster event, overlap in percent, an indication whether the acquisition is "planned" or "acquired" and the acquisition time. 71

Figure 38: SmartDesk showing an official warning as issued by the German National Meteorological Service (DWD) in July 2021 for the Ahrtal valley, Germany. The box contains the warning text and the identified overlapping satellites. 72

Figure 39: SmartDesk showing the swaths of the two satellites Sentinel-2B and Landsat-8 relevant for the Ahrtal valley warning AOI. 73

Figure 40: E-Mail notification showing the analysis results in a human-readable format 74

Figure 41: Screenshot showing the list of public warnings captured by PDM-tech-06 and the resulting clustered AOIs in a map for the regional floods in Central and Eastern Europe in September 2024 utilizing a test Geographic Information System (GIS)..... 75

Figure 42: Screenshot showing the list of relevant satellite acquisition opportunities generated by PDM-tech-06 for the regional floods in Central and Eastern Europe in September 2024. In a test GIS app satellite windows are visualised in a table and on the map. 75

Figure 43: Main part of a proposal as provided via the Web API..... 83

Figure 44: Example of a satellite segment as listed for warning elements inside a proposal 84

List of Tables

Table 1: NGS-LD entities, formats, and approximate update intervals in the information fusion pipeline.	34
Table 2: Characteristics and occupancy-grid configurations of historical scenarios.	50
Table 3: Evaluation metrics for the clusters computed by the JSTTS model and an adversarial sequential approach.	56



List of Abbreviations

AOI	Area of Interest
API	Application Programming Interface
BM	Business Mission
CAP	Common Alerting Protocol
CDSE	Copernicus Data Space Ecosystem
CEMS	Copernicus Emergency Management Service
DEM	Digital Elevation Model
DLR	German Aerospace Center
DoA	Description of Action
DSS	Decision Support Service
DWD	German National Meteorological Service
ECO	Emergency On-Call Officer
EFAS	European Flood Awareness System
EO	Earth Observation
GDACS	Global Disaster Alert and Coordination System
GIS	Geographic Information System
GISCO	Geographic Information System of the Commission
GPS	Global Positioning System
IF	Information Fusion
IMU	Inertial Measurement Unit
JSTTS	Joint Spatio-Temporal Topic-Sentiment
KPI	Key Performance Indicator
LDA	Latent Dirichlet Allocation
LHP	Länderübergreifendes Hochwasserportal - Cross-border Flood Portal
MSL	Mean Sea Level
ND	Natural Disaster
NGSI-LD	Next Generation Service Interface – Linked Data
NDM	Natural Disaster Management
NS	Nelen & Schuurmans
NWP	Numerical Weather Prediction
OGM	Occupancy Grid Map
PSM	Processing System Management
RMS	Rapid Mapping Service
SEM	Satellite-based Emergency Mapping
TV	Target Value
UAV	Unmanned Aerial Vehicle
VHR	Very High Resolution
VPN	Virtual Private Network
ZKI	Center for Satellite-Based Crisis Information

Executive Summary

Deliverable D4.2 outlines the research and development achievements of the TEMA project's Work Package 4, with a dual focus on **Information Fusion (T4.3)** and **Data-Fusion-Based Decision Support and Process Triggering (T4.4)**. The deliverable introduces critical technological components that automate and enhance situational awareness and decision-making capabilities for Natural Disaster Management (NDM). This is achieved by integrating diverse data sources, automating processes, fusing data and generating actionable insights.

Section 2 details the progress in the development of the **Information Fusion (IF) Module**, a core element of the TEMA platform architecture, as well as of a multimodal geosocial-media analysis framework since the first report D4.1. The IF module integrates in real-time diverse analytical data such as drone image analyses, satellite imagery analyses, sentiment data from social media, and predictive models. Key features include UAV-based people and vehicles tracking, geosocial media integration, high-precision georeferencing and continuous real-time updates of actionable outputs. The IF technology improves disaster response by delivering timely, high-fidelity geospatial data, enabling faster, more informed decisions during crises, which directly contribute to OC2 (increase situational awareness in natural-disaster management) by combining multiple heterogeneous data sources into a single, coherent operational picture. The resulting high-fidelity geospatial output maps provide responders with timely, actionable information for faster, better informed decisions during natural disasters.

Another key innovation is the **Joint Spatio-Temporal Topic-Sentiment (JSTTS) framework**, which combines semantic, sentiment, spatial, and temporal analyses to create coherent clusters of disaster-related social media posts. It builds on the limitations of previous methods by using the Geo-GSOM algorithm to preserve spatial coherence, ensuring that clusters of social media posts are both geographically and emotionally consistent. The JSTTS model was tested on major disasters (e.g., Hurricane Harvey, Ahr Valley floods) and showed superior performance in topic quality and sentiment consistency compared to sequential methods. The JSTTS framework offers a flexible, scalable tool for improving disaster response by providing clearer, more cohesive insights from large-scale social media data. It specifically addresses TEMA objective OC2 (increasing situational awareness in NDM).

Section 3 of the deliverable describes the implementation of a **Decision Support Service (DSS) for Remote Sensing**. The DSS processes public warnings and intersects them with satellite acquisition opportunities. Additionally, FireSim and flood simulation outputs (T4.1) have been integrated as inputs. This tool provides emergency managers with a map-based decision proposal that includes information on available satellite acquisition opportunities for the AOI and their timing, thereby supporting faster and more informed responses. SmartDesk (T5.2), an interactive decision interface, visualises AOIs and satellite overpasses and enhances user interaction with warning data. Field evaluations included use cases such as floods in Lithuania, Bavaria, and Central/Eastern Europe, and Cyclone Chido in Mayotte. These tests validated the DSS's real-time performance and informed refinements to improve its responsiveness and reliability. Integration with automated email alerts further supports operational readiness for end users. Real-world trials in Germany and Finland are expected to demonstrate the system's ability to reduce the AOI identification and satellite correlation time to under two hours—a significant improvement over manual

workflows.

The DSS technology also contributes to the TEMA objectives OC1 (reducing latency between warning and map product delivery) and OC3 (reducing operator workload) by automating key steps in the Satellite-based Emergency Mapping (SEM) process. Future work includes automated targeted triggering of disaster-specific processors (e.g., flood, fire) and further quantifying processing time across the full SEM rapid mapping workflow.

Overall, D4.2 showcases the potential of integrated, multi-source information fusion and decision support technologies in disaster response, and lays a foundation for broader evaluation and integration of TEMA technologies in future disaster scenarios.

1 Introduction

1.1 Purpose and Scope of the Document

Deliverable D4.2 is the second deliverable of the fourth Work package (WP4) of the TEMA project. The main purpose of this document is to report the final research results of Tasks T4.3 Information Fusion and T4.4 Data-fusion-based Decision Support and Process Triggering until M30. More specifically, the research effort was focused on the following areas:

- Information fusion within TEMA
- Fusion of information derived from social media
- Decision support for remote sensing

1.2 Structure of the Document

This document is organised as follows: Section 2 summarises the main research efforts and key outputs, with respect to TEMA objectives. Section 3 describes the progress in the development of the IF module of the TEMA platform as well as of the JSTTS framework for the fusion of information derived from social media. Section 4 describes the content regarding decision support for remote sensing. The deliverable is concluded in Section 5. Finally, additional information is provided in Annex A: Usage of the Decision Support Endpoint and Annex B: Related publications.

2 Summary of the work carried out

2.1 Objectives

The main objective of TEMA tasks T4.3 "Information Fusion" and T4.4 "Data-Fusion-Based Decision Support and Process Triggering" (M13-M30) is to advance near real-time NDM by developing novel methods for information fusion, decision support, and automation. Key objectives include:

- Developing innovative information fusion techniques that quickly and accurately merge diverse data sources, including meteorological sensors, social media, and remote sensing.
- Creating a decision support service that improves the end user's situational awareness by dynamically and automatically generating decision proposals regarding Earth Observation (EO) data and product availability for emergencies like wildfires and floods.

Information fusion employs advanced filtering and tracking methods to coherently merge decentralised observations in real time, extending prior forest fire monitoring approaches to multiple types of emergencies. The decision support service integrates automated processing of web data (e.g., warnings, forecasts), satellite data acquisition timing, and optional social media data analysis to enhance rapid mapping and event awareness.

The specific TEMA objectives linked to Tasks T4.3, and T4.4 are derived from existing challenges in information fusion and SEM as well as from the socially relevant use-cases, i.e., regional floods, flash floods, and forest fires/wildfires. They are presented below, along with accompanying Key Performance Indicators (KPIs) and Target Values (TVs) as defined in Section 1.1.1 of Part B of TEMA's Description of Action (DoA). Task 4.3 contributes to TEMA objective OC2 "Increase situational awareness in NDM". Task T4.4 contributes to TEMA objectives OC3 "Reduce mental load for human operators in NDM" and OC1 "Reduce latency in NDM".

Section 2.2 summarises the research and development activities conducted under Tasks T4.3, and T4.4 by TEMA partners, aligned with TEMA objectives in their natural order.

2.2 Summary of the work carried out with respect to the objectives

Between M13 and M30, the following research and development work was carried out with respect to the objectives and KPIs of TEMA.

2.2.1 Information Fusion

The IF module developed in the TEMA project delivers robust, scalable, and real-time integration of heterogeneous data sources. The completely event-driven pipeline of the IF module asynchronously processes and integrates heterogeneous data sources into unified georeferenced occupancy and object maps, thereby sustaining multimodal awareness. Fused maps and tracked-object

overlays deliver high-fidelity, up-to-date insights, empowering emergency responders with actionable situational awareness that directly supports faster and more informed decisions in line with **OC2**.

Another innovation forms the JSTTS framework, which combines semantic, sentiment, spatial, and temporal analyses to create coherent clusters of disaster-related social media posts. The JSTTS model was tested on major disasters (e.g., Hurricane Harvey, Ahr Valley floods) and showed superior performance in topic quality and sentiment consistency compared to sequential methods. The JSTTS framework offers a flexible, scalable tool for improving disaster response by providing clearer, more cohesive insights from large-scale social media data. With social media data alone, IT:U is able to handle four modalities simultaneously, also addressing **OC2** within TEMA and significantly advancing the state-of-the-art in information fusion of geo-social media data. More details on the model's performance with respect to KPIs addressed by T3.3 are summarized in D3.2 in the counterpart of this section.

2.2.2 Decision Support

To reduce the delays in the standard Copernicus SEM workflow [1] between the first warning, the acquisition of satellite data and the availability of analysis results DLR developed the DSS for Remote Sensing. The tool automatically processes and fuses multi-source web data, identifies AOIs at risk and identifies relevant satellite image acquisition opportunities. The **automation of two steps** in the SEM process reduces the time required for AOI detection to 5-10 minutes on average and the total time for AOI detection and correlation of AOIs with satellite overpasses up to 1.5 hours addressing the "**Workload from retrieval of satellite position and acquisition data**" KPI of TEMA objective **OC3**. In combination with related achievements for the flood and burnt area processors made in T3.2 (documented in D3.1 and D3.2), the automation also supports the "**Latency between warning and map product delivery**" of TEMA objective **OC1**. Compared to the standard Copernicus SEM workflow, the KPI "**Transparency, automation and improvement of communication between service provider and end user**" of **OC3** is met through the generation of **transparent decision proposals** that include information on relevant satellite acquisition opportunities for the AOI and their timing.

3 Information Fusion

3.1 Introduction

This section provides a complete overview of the Information Fusion (IF) module within the TEMA platform architecture. Information Fusion constitutes a core module designed to optimally integrate outputs generated by WP3 analytics into a coherent, unified, and georeferenced representation, accurately reflecting the current status of the monitored natural disaster (Natural Disaster (ND)). This description completes the design and preliminary development of the Information Fusion (IF) module provided in TEMA Deliverable D4.1.

Information Fusion integrates in near real-time diverse analytical outputs, including drone image analyses (as developed in TEMA task T3.2), satellite imagery analyses (TEMA task T3.2), and geosocial analytics results (TEMA task T3.3). By merging these heterogeneous data streams with ND predictive models, the Information Fusion module continuously updates the state of the ND, offering critical insights into its evolving dynamics.

The outputs generated by Information Fusion are essential for understanding the progression of the ND and are integral to multiple other modules within the TEMA platform. Information Fusion is implemented in the TEMA architecture as technology PDM-tech-05.

The assumptions and end-user requirements that guide the design and implementation of the Information Fusion module have been described in Deliverable D4.1. Specifically, Section 3.3.1 of Deliverable D4.1 outlines the key assumptions underpinning the module, including data preprocessing expectations, georeferencing dependencies, temporal synchronisation, and the integration of predictive models. In addition, Section 3.3.2 of the same deliverable presents a summary of the end-user requirements identified in Deliverable D2.1, categorised into functional and non-functional aspects. These requirements have served as foundational references for all subsequent development phases. As these elements remain unchanged, for brevity, they are not reiterated in this document.

The structure of this section is organised as follows. Section 3.2 highlights the novel contributions introduced by TEMA in the field of information fusion for natural disaster management. Section 3.3 summarises the main activities carried out during the reporting period (Months 19–30). Section 3.4 details the fusion methodology, including the use of occupancy grid maps for spatial data integration. Section 3.5 describes the design and implementation of the web application supporting the fusion processes. Section 3.6 presents a comprehensive fusion workflow for the Information Fusion in TEMA. Finally, Section 3.7 presents a summary of the key outcomes achieved during this period.

3.2 Novelties of TEMA Information Fusion

The Information Fusion module constitutes one of the key technical components of the TEMA Project. It enhances the platform's ability to generate a coherent and updated representation of natural disaster (ND) situations by integrating diverse data sources in near real-time. Unlike

the conventional ND fusion frameworks that perform offline, sequential integration of limited data streams (as described in Section 3.2.1 of Deliverable D4.1), the Information Fusion module in TEMA concurrently assimilates all WP3 analytics, satellite processed images, drone processed data, geosocial feeds, and predictive model outputs in a unified real pipeline, eliminating manual preprocessing and dramatically reducing the information gaps [2, 3]. Moreover, by enforcing the rigorous timestamp synchronisation and native georeferencing of every input, it eradicates the spatial drift and clock-skew errors that still undermine state-of-the-art fusion platforms [4–6].

This section outlines the specific contributions introduced through the development and implementation of this module.

- **Multimodal Data Integration:** The module enables the fusion of heterogeneous data sources, including processed outputs from satellite images, drone imagery, and geosocial data analytics. By relying on the advanced analytics developed in WP3, the module operates on high-level, semantically rich inputs, synthesising a unified, georeferenced view of the disaster scenario. This integration improves the spatial and temporal completeness and contextual understanding of the ND event. Unlike previous frameworks that merge only a subset of sources or require batch preprocessing, the Information Fusion approach within TEMA simultaneously assimilates all available modalities, thereby reducing information gaps that commonly arise in existing systems.
- **Real-Time Fusion and Dynamic Updating:** A major advancement of Information Fusion is its ability to perform **continuous and real-time data fusion**, ensuring that the platform reflects the latest developments in the monitored environment. As new data becomes available from various sources, the Information Fusion module updates the system’s internal state representation accordingly, offering near-instantaneous situational awareness to end-users. This asynchronous, event-driven update cycle removes the latency inherent to state-of-the-art sequential or offline fusion pipelines and thus keeps decision makers permanently aligned with field realities.
- **Temporal and Geospatial Alignment:** The module introduces robust mechanisms to manage **temporal synchronisation and spatial consistency**. All input data is assumed to be timestamped, and the system adheres to a unified time reference across all modules. Additionally, the fusion process relies on accurate georeferencing of input data, including the use of drone image metadata (position, orientation, camera parameters) and Digital Elevation Models (Digital Elevation Model (DEM)) to derive precise spatial context. These alignment procedures eliminate the spatial drift and clock skew that still hamper many conventional disaster-monitoring platforms, yielding a more reliable common operational picture.
- **Integration with ND Prediction Models:** The Information Fusion module is designed to reflect the current state of the ND and support **forward-looking insights**. This is achieved by incorporating predictions from the forest fire and flood hydrodynamic models developed in TEMA task T4.1. The module merges these predictive outputs with observational data to build a forward-aware representation of the environment, enabling informed planning and early response actions. This enables increasing the accuracy of the estimation performed by IF, representing a significant advantage over the State of the Art.
- **Support for Operational Decision-Making:** By delivering a unified, continuously updated,

and georeferenced representation of the disaster scenario, the Information Fusion module plays a central role in supporting operational decision-making across the TEMA platform. Its outputs are consumed by multiple other components in the system and are tailored to align with the requirements expressed by end-users (as detailed in Deliverables D4.1 and D2.1). Consequently, operators receive a single, consistent feed instead of stitching together heterogeneous layers manually, streamlining workflows that previously depended on disparate tools and ad-hoc overlays.

3.3 Main Activities Performed (Months 19-30)

Building upon the initial design and conceptual framework established in Deliverable D4.1, the period from Month 19 to Month 30 focused on implementing, refining, and validating the Information Fusion module (PDM-tech-05) within the operational context of the TEMA platform. The activities carried out during this reporting period represent a critical phase in transitioning from design to deployment. The key efforts are outlined below:

- **IF Algorithm Refinement:** Significant effort was devoted to refining the core fusion algorithms first introduced in Deliverable D4.1. Based on the initial fusion logic described therein, the development team focused on improving the robustness and accuracy of information fusion under real-world data conditions. This included optimising the spatial and temporal alignment of data inputs, improving the handling of asynchronous updates, and ensuring stability when integrating predictive outputs with observed measurements. Moreover, enhancements were made to support a more seamless incorporation of georeferenced social media data, which was identified in Deliverable D4.1 as a key input stream. These activities have been summarised in Section 3.4 of this document.
- **Web Platform Development for the IF Module:** A major milestone during this period was the development of a scalable, web-based interface enabling real-time visualisation and interaction with the fused outputs. The platform acts as a centralised dashboard where outputs from multiple data producers, such as satellite analytics (TEMA task T3.2), drone image processors (T3.2), and geosocial analytics modules (T3.3), are aggregated, visualised, and managed. Additionally, Application Programming Interfaces (APIs) were implemented to ensure smooth interoperability between the web interface and predictive modelling components such as the forest fire and hydrodynamic flood models described in TEMA task T4.1. This bidirectional communication allows the platform not only to display real-time ND states but also to incorporate and visualise forecasted scenarios. These activities have been summarised in Section 3.5.
- **Adaptation for integration within the TEMA Platform:** Following the design principles and module interfaces described in Deliverable D4.1, substantial progress was made toward full system integration. This involved the alignment of the Information Fusion module with other TEMA components across the technical stack. Integration efforts ensured that input data flows, metadata standards (e.g., timestamps, data formats, and georeferencing), and model outputs were compatible across different partners' systems. The focus was on ensuring modular extensibility, minimal latency in data exchange, and compliance with the platform-

wide architectural guidelines outlined in TEMA Work Package WP5. These activities have been summarised in Sections 3.5 and 3.6.

- **Validation:** A series of integration tests were conducted to validate the end-to-end functioning of the Information Fusion module within the TEMA Platform. The first major integration test took place in Naples, Italy, in June 2024, serving as a baseline assessment of multi-partner interoperability. Following this, weekly virtual integration sessions were held to iteratively resolve technical issues, validate data exchange formats, and align module behaviour with user expectations. In addition, each general project meeting included dedicated hands-on testing sessions with live demonstrations of the platform. Most recently, an advanced in-field integration test was held at the DLR-KN facility in Munich, Germany, focusing on high-volume data fusion and cross-component responsiveness under simulated emergency scenarios. These activities have been summarised in Section 3.6.
- **Preparation for publications:** In parallel with system development and validation, efforts were initiated to disseminate the outcomes of the Information Fusion module through the preparation of academic journal publications. One paper is being prepared that describes the IF design and algorithms, end-to-end integration workflows, and validation results from the Ahrtal flood and Montiferru wildfire historical cases, and will be expanded to include findings from the June 2025 Sardinia experimental field trial.

These activities mark a critical transition from theoretical model development (as described in Deliverable D4.1) to the deployment of a functional, user-facing, and testable prototype within the TEMA platform. They have collectively contributed to the operational readiness of the Information Fusion module and its alignment with both technical requirements and end-user expectations.

3.4 The TEMA Information Fusion Framework

This section details the mathematical and algorithmic framework underlying our fusion process, implemented in the PDM-tech-05 module of the TEMA Platform. Our methodology seamlessly integrates occupancy grid mapping, updated via Bayesian filtering in the log-odds domain, with dynamic state estimation using a linear Kalman filter. To tackle the challenges associated with fusing heterogeneous sensor data, the IF framework processes asynchronous notifications in real-time, ensuring continuous and reliable updates.

Specifically, our Information Fusion framework process produces three distinct outputs:

- **Maps4Fire:** Monitors the propagation of forest fire by fusing processed segmentation data with predictive simulation outputs of forest fires.
- **Maps4Flood:** Monitors flood propagation by integrating processed segmentation data with flood simulation predictions. The Bayesian filtering framework continuously updates the grid map with asynchronous data.
- **Maps4Objects:** Tracks detected objects (persons and vehicles) by fusing individual detections with an object-tracking pipeline. This pipeline employs data association using the Hungarian

matching algorithm and updates object tracks via a linear Kalman filter.

By processing asynchronous notifications from diverse sensors, including UAV-processed imagery, satellite measurements, and geosocial media, the system continuously updates the occupancy grid maps and object tracks despite temporal heterogeneity. Figure 1 shows the asynchronous approach utilised in the information fusion.

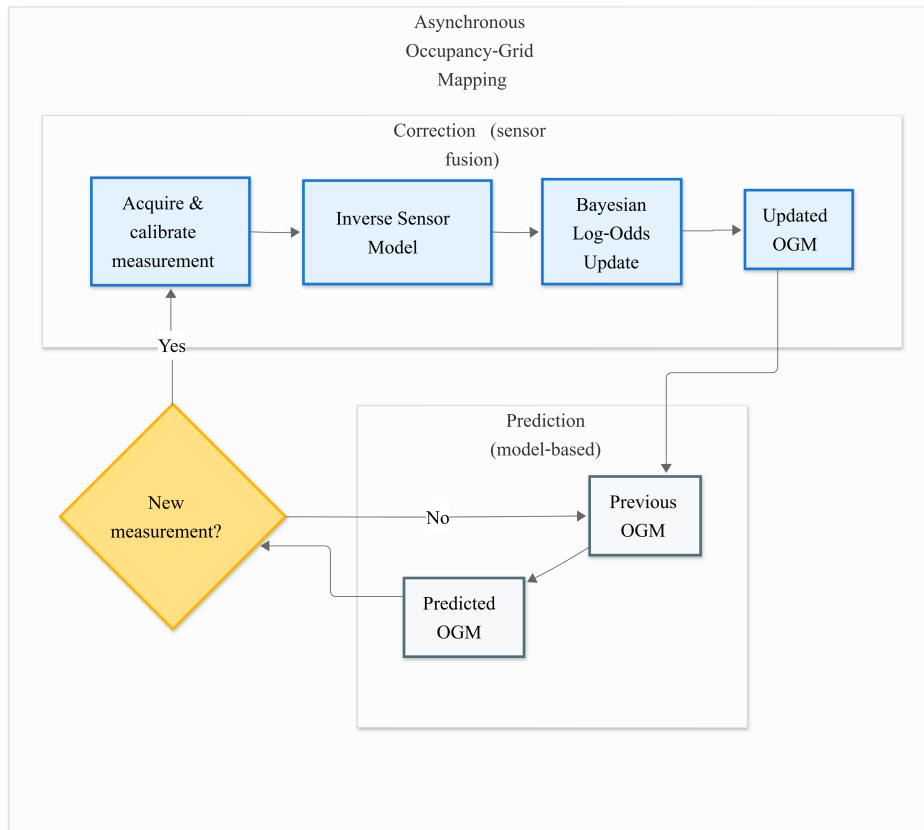


Figure 1: Asynchronous occupancy grid mapping approach.

This integrated, real-time fusion approach ensures that TEMA delivers dynamic and reliable situational awareness for disaster monitoring.

3.4.1 Challenges in Fusing Heterogeneous Data

Fusing data from multiple sensors introduces several significant challenges that have been addressed by different mechanisms within the IF Framework:

- **Data Heterogeneity and Calibration:** Data are collected from diverse modalities (e.g., UAV imagery, satellite sensors, social media inputs, simulation models), each with its own spatial resolution, format, and coordinate system. To ensure effective fusion, all inputs must be rigorously calibrated and, where necessary, georeferenced. In our system, for instance,

UAV images generated by TEMA technology TFA-tech-05/06 are georeferenced upon receipt within the information fusion module.

- **Temporal Synchronisation:** Sensors often operate at different sampling rates and may experience variable time delays. Achieving accurate temporal alignment, using techniques such as time-window matching, is crucial to ensure that the data being fused represents the same temporal instance of the monitored event.
- **Uncertainty Management:** Inherent sensor noise and environmental variability introduce significant uncertainty into the measurements. Our system explicitly incorporates this uncertainty into the state estimation process by employing probabilistic filtering methods, including Bayesian and Kalman filtering, to generate robust occupancy grid maps.
- **Computational Complexity:** Processing high-resolution occupancy grids in real time, particularly when fusing data from multiple sources, requires efficient algorithms and considerable computational power. Optimising these algorithms is critical to meeting real-time performance requirements.
- **Data Association:** For reliable object tracking, as implemented in `Maps4Objects`, it is essential to correctly associate incoming measurements with existing object tracks. Our approach utilises the Hungarian matching algorithm [7] to determine optimal correspondences, thereby ensuring that the Kalman filter updates the correct tracks.

3.4.2 Occupancy Grid Maps for Maps4Fire and Maps4Flood

The generation of `Maps4Fire` and `Maps4Flood` is based on occupancy grid mapping, updated asynchronously via Bayesian filtering [8]. The environment is divided into discrete cells, each cell m_i carrying a probability $P(m_i)$ that quantifies the likelihood of being occupied by a fire or flood. Each new sensor measurement is integrated immediately, ensuring that the occupancy grid maps are refined in real time despite the temporal heterogeneity of incoming data.

Bayesian Filtering and Log Odds Formulation: Given sensor measurements $z_{1:t}$ and sensor poses $x_{1:t}$ up to time t , Bayes' theorem updates the occupancy probability for cell m_i as:

$$P(m_i | z_{1:t}, x_{1:t}) = \frac{P(z_t | m_i, x_t) P(m_i | z_{1:t-1}, x_{1:t-1})}{P(z_t | z_{1:t-1}, x_{1:t})}. \quad (1)$$

The likelihood term $P(z_t | m_i, x_t)$ is supplied by an inverse sensor model that converts each incoming measurement into a per-cell occupancy likelihood. To enhance numerical stability, we convert this probability into log odds:

$$l_t = \log \frac{P(m_i | z_{1:t}, x_{1:t})}{1 - P(m_i | z_{1:t}, x_{1:t})}. \quad (2)$$

With a prior occupancy probability $P(m_i)$, the initial log odds is:

$$l_0 = \log \frac{P(m_i)}{1 - P(m_i)}. \quad (3)$$

Each new measurement increments the log odds additively:

$$l_t = l_{t-1} + \log \frac{P(z_t | m_i, x_t)}{P(z_t | \neg m_i, x_t)} - l_0, \quad (4)$$

such that the updated occupancy probability is

$$P(m_i | z_{1:t}, x_{1:t}) = \frac{1}{1 + e^{-l_t}}. \quad (5)$$

Fire Scenario (Maps4Fire): Maps4Fire denotes the occupancy grid map that stores fire-related probabilities. The system fuses multiple measurement inputs to derive the per-cell likelihood of fire occupancy:

- FireSegmentation (from TEMA technology TFA-tech-06) representing a per-pixel classification of actively burning areas in drone imagery,
- BurntSegmentation (from TEMA technology TFA-tech-06) representing a per-pixel mask of vegetation areas already consumed by fire in drone imagery,
- HotspotResult (from TEMA technology TFA-tech-11) representing aggregated geosocial activity metrics, such as post count, anomaly scores (Z-score), and statistical significance (p-value), computed over spatial cells to indicate perceived impact during a natural disaster,
- EOBurntArea (from TEMA technology TFA-tech-09), representing satellite-derived segmentation masks that outline burnt regions with per-pixel classification probabilities.

Each of these sources provides a per-cell probability (e.g., active fire or burnt area), which can be combined via a weighted sum [9] as in the following equation:

$$p_m(m_i) = w_{\text{fire}} p_{\text{fire}}(m_i) + w_{\text{burnt}} p_{\text{burnt}}(m_i), \quad w_{\text{fire}} + w_{\text{burnt}} = 1, \quad (6)$$

where $p_{\text{fire}}(m_i)$ and $p_{\text{burnt}}(m_i)$ represent the final probabilities derived by merging active fire measurements and burnt area measurements.

The resulting likelihood $p_m(m_i)$ is plugged into the Bayesian update equations (Equations (1)-(5)), ensuring that each asynchronous measurement incrementally refines the occupancy probability in Maps4Fire. Predictive model outputs from TEMA technology PDM-tech-01 (StandardArrivalTime) are likewise incorporated using the same log-odds update mechanism, yielding a continuously updated fire map that reflects the evolving fire scenario in real-time.

Flood Scenario (Maps4Flood): Maps4Flood is the analogue occupancy grid map for flood probabilities. For a flood scenario, the measurement inputs include:

- FloodSegmentation (from TEMA technology TFA-tech-06), representing UAV-derived flood segmentation masks that identify flooded areas.
- HotspotResult (from TEMA technology TFA-tech-11) representing aggregated geosocial activity metrics, such as post count, anomaly scores (Z-score), and statistical significance (p-value), computed over spatial cells to indicate perceived impact during a natural disaster,

- E0FloodExtent (from TEMA technology TFA-tech-08), representing satellite-based flood extent segmentation masks that provide broad-area flood detection with per-pixel classification probabilities.

Along with predictive model outputs (FloodCalculationResult) from TEMA technology PDM-tech-02. These data sources produce per-cell probabilities for flood occupancy, which are integrated in the same Bayesian filtering manner as Equations (1)-(5), thereby ensuring Maps4Flood remains accurate in real-time.

The Bayesian update equations (Equations 4-5) accommodate heterogeneous measurements for both fire and flood scenarios. Because the fusion process is asynchronous, each incoming measurement, whether from UAV-processed imagery, satellite-processed data, or geosocial media analysis, is incorporated immediately, providing a constantly refined and up-to-date occupancy grid map.

3.4.3 Linear Kalman Filter for Maps4objects

The Maps4objects layer maintains a dynamic, vector-based representation of tracked entities (persons and vehicles), each annotated with a class label and confidence score. Its core objective is to estimate and update the geospatial trajectories of these detected objects over time.

To achieve this, we employ a standard linear Kalman filter [8], which models the belief over an object's state as a multivariate Gaussian:

$$\text{bel}(x_t) = \mathcal{N}(x_t; \mu_t, \Sigma_t), \quad (7)$$

where μ_t is the mean state vector (e.g., latitude, longitude, and velocity components), and Σ_t is the associated uncertainty covariance.

We model each tracked object using a 6-dimensional state vector:

$$\mu_t = \begin{bmatrix} \lambda_t \\ \phi_t \\ h_t \\ \dot{\lambda}_t \\ \dot{\phi}_t \\ \dot{h}_t \end{bmatrix} \in \mathbb{R}^6, \quad \Sigma_t \in \mathbb{R}^{6 \times 6}, \quad (8)$$

where λ , ϕ , and h represent longitude, latitude, and elevation respectively, and $\dot{\lambda}_t$, $\dot{\phi}_t$, and \dot{h}_t are their corresponding velocities.

Prediction Step: In conventional Kalman filtering, the state evolves under the influence of a control input u_t . However, in our context, object motion is inferred solely from past estimated positions, without any known control actions. Thus, the prediction step simplifies to:

$$\bar{\mu}_t = A_t \mu_{t-1}, \quad (9)$$

$$\bar{\Sigma}_t = A_t \Sigma_{t-1} A_t^T + R_t, \quad (10)$$

where A_t is the state transition matrix (a constant-velocity model), and R is the process noise:

$$A = \begin{bmatrix} 1 & 0 & 0 & \Delta t & 0 & 0 \\ 0 & 1 & 0 & 0 & \Delta t & 0 \\ 0 & 0 & 1 & 0 & 0 & \Delta t \\ 0 & 0 & 0 & 1 & 0 & 0 \\ 0 & 0 & 0 & 0 & 1 & 0 \\ 0 & 0 & 0 & 0 & 0 & 1 \end{bmatrix}, \quad (11)$$

$$R = \sigma^2 \begin{bmatrix} I_3 & 0 \\ 0 & I_3 \end{bmatrix}, \quad (12)$$

where Δt is the elapsed time between steps.

The predicted state $(\bar{\mu}_t, \bar{\Sigma}_t)$ estimates the object's state prior to incorporating new measurements.

Correction Step: When a new georeferenced measurement z_t is available, the prediction is corrected as follows:

$$K_t = \bar{\Sigma}_t C_t^T (C_t \bar{\Sigma}_t C_t^T + Q_t)^{-1}, \quad (13)$$

$$\mu_t = \bar{\mu}_t + K_t (z_t - C_t \bar{\mu}_t), \quad (14)$$

$$\Sigma_t = (I - K_t C_t) \bar{\Sigma}_t, \quad (15)$$

where K_t is the Kalman gain and C_t is the observation matrix, Q_t is the measurement noise covariance:

$$C = \begin{bmatrix} 1 & 0 & 0 & 0 & 0 & 0 \\ 0 & 1 & 0 & 0 & 0 & 0 \\ 0 & 0 & 1 & 0 & 0 & 0 \end{bmatrix}, \quad Q = \sigma_{\text{meas}}^2 I_3. \quad (16)$$

The corrected state (μ_t, Σ_t) yields a more accurate estimate of the object's true location.

This configuration enables robust tracking of each object's full 3D position with uncertainty, even under noisy or asynchronous observations.

Data Association via Hungarian Matching: Since multiple detections can occur over time, an optimal data association step is critical to correctly match new measurements with existing object tracks. In our approach, each feature, whether from the current occupancy grid (Occupancy Grid Map (OGM) features) or new sensor measurements, contains geographic coordinates (longitude, latitude).

We first compute a cost matrix $C \in \mathbb{R}^{N \times M}$ where N is the number of existing features and M is the number of new measurements. Each element $C(i, j)$ is determined using the haversine distance [10] between the geographic coordinates of the i th OGM feature and the j th new measurement:

$$C(i, j) = \begin{cases} \text{haversine}((\lambda_i, \phi_i), (\lambda_j, \phi_j)), & \text{if } (\lambda_i, \phi_i) \text{ and } (\lambda_j, \phi_j) \text{ are valid,} \\ 10^{12}, & \text{otherwise.} \end{cases} \quad (17)$$

where (λ_i, ϕ_i) and (λ_j, ϕ_j) are the longitude-latitude pairs of the existing feature and the new measurement, respectively, and the haversine distance is given by:

$$d = 2r \arcsin \left(\sqrt{\sin^2 \left(\frac{\Delta\phi}{2} \right) + \cos \phi_1 \cos \phi_2 \sin^2 \left(\frac{\Delta\lambda}{2} \right)} \right), \quad (18)$$

with $\Delta\phi = \phi_2 - \phi_1$, $\Delta\lambda = \lambda_2 - \lambda_1$, and r as the Earth's radius.

Next, we formulate the linear assignment problem by defining a binary assignment matrix $X \in \{0, 1\}^{N \times M}$, where:

$$X(i, j) = \begin{cases} 1, & \text{if the } i\text{th OGM feature is assigned to the } j\text{th measurement,} \\ 0, & \text{otherwise.} \end{cases} \quad (19)$$

The objective is to minimise the total cost:

$$\min_X \sum_{i=1}^N \sum_{j=1}^M C(i, j) X(i, j), \quad (20)$$

subject to constraints ensuring that each OGM feature is assigned at most once and each measurement is assigned to at most one feature.

The optimal assignment is computed using the Hungarian algorithm [7, 11]:

$$\text{assignment} = \arg \min_{X \in \{0,1\}^{N \times M}} \sum_{i=1}^N \sum_{j=1}^M C(i, j) X(i, j). \quad (21)$$

Finally, the resulting assignment pairs (i, j) are filtered such that only those with a cost $C(i, j)$ below a predetermined distance threshold are retained. These final assignments are then used to update the Kalman filter for each object track, ensuring that only closely matched new measurements are used in the state correction.

3.4.4 Georeferencing module within Information fusion

Georeferencing is critical in TEMA for ensuring the accuracy and usability of images captured by aerial drones during disaster events. By assigning precise geographic coordinates to these images, georeferencing transforms [5] raw drone footage into spatially accurate data that can be effectively integrated into occupancy grid maps. These maps, which depict the probability distribution of disaster-affected regions, rely on the correct alignment of drone imagery with real-world locations to provide reliable measurements and insights for disaster response and management.

This process bridges the gap between visual data and actionable geospatial information, enhancing the precision of disaster assessment and resource allocation. In this section, we will detail the georeferencing procedure to illustrate its implementation within the TEMA framework.

We begin by defining the coordinate frames involved and deriving the necessary rotation matrices to relate these frames, enabling the projection of image data into the inertial reference system. Subsequently, we describe a ray tracing algorithm [12, 13] that leverages a digital elevation model (DEM) to map pixel coordinates to ground locations.

The process of georeferencing requires the transformation between several coordinate systems. Four coordinate frames are defined: the inertial frame, the drone body frame, the gimbal frame, and the camera frame. The inertial coordinate system (X_I, Y_I, Z_I) is defined with its X_I and Y_I axes aligned to the geographical longitude and latitude directions, respectively. The drone frame (X_D, Y_D, Z_D) is attached to the drone. In this frame, the X_D axis points forward along the drone's direction of motion, while the Z_D axis points downward, consistent with standard aviation conventions. In the home state, the inertial and drone frames are orthogonal, with the X_D and Y_D axes aligned to the latitude and longitude directions, as illustrated in Figure 2. The gimbal model includes yaw, pitch, and roll degrees of freedom. For the gimbal, the DLI Zenmuse H20 series is adopted, which uses the ZXY rotation convention. The camera frame (X_C, Y_C, Z_C) is oriented such that the X and Y axes align with the image plane's width and height, facilitating pixel-domain operations.

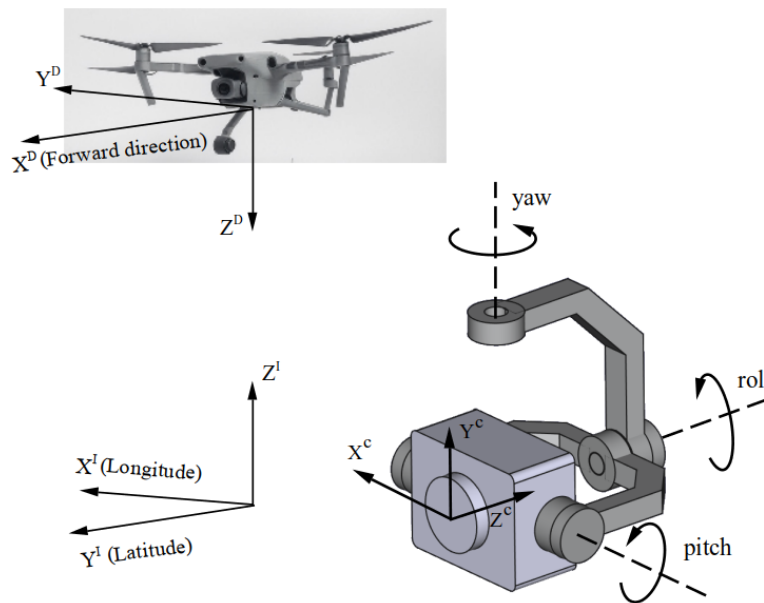


Figure 2: The established coordinate systems including inertial (X_I, Y_I, Z_I) , Drone, (X_D, Y_D, Z_D) , gimbal (roll, yaw, pitch), and the camera (X_C, Y_C, Z_C) frames.

The overall rotation matrix projecting a vector from the camera frame to the inertial frame is obtained by concatenating all intermediate rotation matrices:

$$\mathbf{R}_C^I = \mathbf{R}_D^I \times \mathbf{R}_G^D \times \mathbf{R}_C^G, \quad (22)$$

where \mathbf{R}_D^I , \mathbf{R}_G^D , and \mathbf{R}_C^G are rotation matrices from the inertial to the drone, from the drone to the gimbal, and from the gimbal to the camera frames, respectively as:

$$\begin{aligned} \mathbf{R}_D^I &= \mathbf{R}_{(Z)}(\pi/2) \times \mathbf{R}_{(X)}(\pi) = \begin{bmatrix} 0 & 1 & 0 \\ 1 & 0 & 0 \\ 0 & 0 & -1 \end{bmatrix}, \\ \mathbf{R}_G^D &= \mathbf{R}_{(X)}(\pi) \times \mathbf{R}_{(Z)}(\gamma) \times \mathbf{R}_{(X)}(\alpha) \times \mathbf{R}_{(Y)}(\beta), \\ \mathbf{R}_C^G &= \mathbf{R}_{(X)}(\pi/2) \times \mathbf{R}_{(Y)}(-\pi/2) = \begin{bmatrix} 0 & 0 & -1 \\ -1 & 0 & 0 \\ 0 & 1 & 0 \end{bmatrix}, \end{aligned} \quad (23)$$

where α , β , and γ are the gimbal's roll, pitch, and yaw angles, respectively. By eliminating the matrices in Eq. 22, the overall rotation matrix is obtained as:

$$\mathbf{R}_C^I = \begin{bmatrix} s_\beta & c_\beta s_\alpha & -c_\beta c_\alpha \\ c_\gamma c_\beta & -c_\gamma s_\beta s_\alpha - s_\gamma c_\alpha & c_\gamma s_\beta c_\alpha - s_\gamma s_\alpha \\ s_\gamma c_\beta & -s_\gamma s_\beta s_\alpha + c_\gamma c_\alpha & s_\gamma s_\beta c_\alpha + c_\gamma s_\alpha \end{bmatrix}, \quad (24)$$

where c and s represent $\cos()$ and $\sin()$ respectively.

The ray tracing setup for georeferencing is illustrated in Figure 3. The camera's position in the inertial frame is known at all times, derived from its latitude, longitude, and altitude above sea level using Global Positioning System (Global Positioning System (GPS)) data. The orientation components are also available from the Inertial Measurement Unit (Inertial Measurement Unit (IMU)).

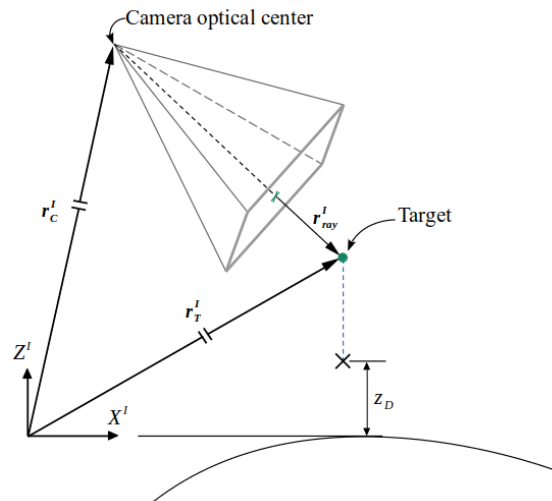


Figure 3: The ray tracing setup.

During the process, the image plane is systematically traversed pixel by pixel, casting a ray from the camera's optical centre in the direction corresponding to each pixel. This ray is traced iteratively

until it intersects with the digital elevation model (DEM). The unit direction vector of a ray in the camera frame for a pixel (x_p, y_p) is defined as:

$$\mathbf{dir}_{\text{ray}}^C = \frac{(x_p, y_p, f)^T}{\|(x_p, y_p, f)\|}, \quad (25)$$

where f represents the camera's focal length. To express this direction vector in the inertial frame, it is pre-multiplied by the rotation matrix:

$$\mathbf{dir}_{\text{ray}}^I = \mathbf{R}_C^I \mathbf{dir}_{\text{ray}}^C, \quad (26)$$

The ray's vector in the inertial frame is scaled by its length, R , to compute the extended ray vector:

$$\mathbf{r}_{\text{ray}}^I = R \mathbf{dir}_{\text{ray}}^I. \quad (27)$$

Consequently, the ray tip position in the inertial frame is given by:

$$\mathbf{r}_T^I = (X_T, Y_T, Z_T)^T = \mathbf{r}_C^I + \mathbf{r}_{\text{ray}}^I. \quad (28)$$

Let R_0 represent the distance from the camera's optical centre to the origin of the casted ray. The ray length is incremented iteratively as:

$$R = R_0 + \tau. \quad (29)$$

where τ is the step size. At each step, the ray's tip position is compared with the DEM altitude at the corresponding ground-projected location (X_D, Y_D, Z_D) . A hit is detected when the ray tip altitude falls below the DEM height:

$$Z_T < Z_D. \quad (30)$$

The ray tracing process is summarised in Algorithm 1, which illustrates the iterative mechanism for georeferencing.

3.5 Web Application Design and Implementation of the IF Module

The Information Fusion (IF) module has been developed as a core cloud native component within the TEMA platform. Designed to run in the TEMA cloud backend, it operates as an event-driven service that fuses heterogeneous data sources ranging from processed UAV and satellite images to geosocial media analysis and predictive models via Next Generation Service Interface – Linked Data (Next Generation Service Interface – Linked Data (NGSI-LD)) [14] notifications. Its primary role is to fuse these inputs into unified, georeferenced occupancy and object maps in near real-time. By leveraging the modern cloud infrastructure, the IF modules ensure scalability, responsiveness, and seamless integration with both the TEMA platform and other integrated services, enabling rapid, reliable, and context-aware decision support for effective disaster monitoring and response. Figure 4 illustrates the interaction flow of the IF module with various components of the TEMA architecture (for further architectural context, see Section 3.5.2 of Deliverable D4.1).

Algorithm 1 Adaptive ray tracing.

- 1: **Input:** DEM, Camera states
- 2: **Output:** Georeferencing dictionary key: pixel, value: ground location
- 3: Initialise georeferencing dictionary $G = \{\}$
- 4: Retrieve the camera's position and orientation from the camera states.
- 5: Compute the overall rotation matrix \mathbf{R}_C^l (Eq.22)
- 6: **for** each pixel (i, j) in the image **do**
- 7: Initialise $R = R_0$
- 8: Compute \mathbf{r}_T^l (Eq.28)
- 9: Compute ray tip projection altitude on terrain (Z_D)
- 10: **while** $Z_T \geq Z_D$ (no intersection) **do**
- 11: Compute ray tip projection on terrain (X_D, Y_D, Z_D)
- 12: Check intersection condition (Eq.30)
- 13: Extend \mathbf{r}_{ray}^l (Eq.29)
- 14: **end while**
- 15: Add pixel (i, j) and ground location (X_D, Y_D, Z_D) to G
- 16: **end for**
- 17: **Return** G

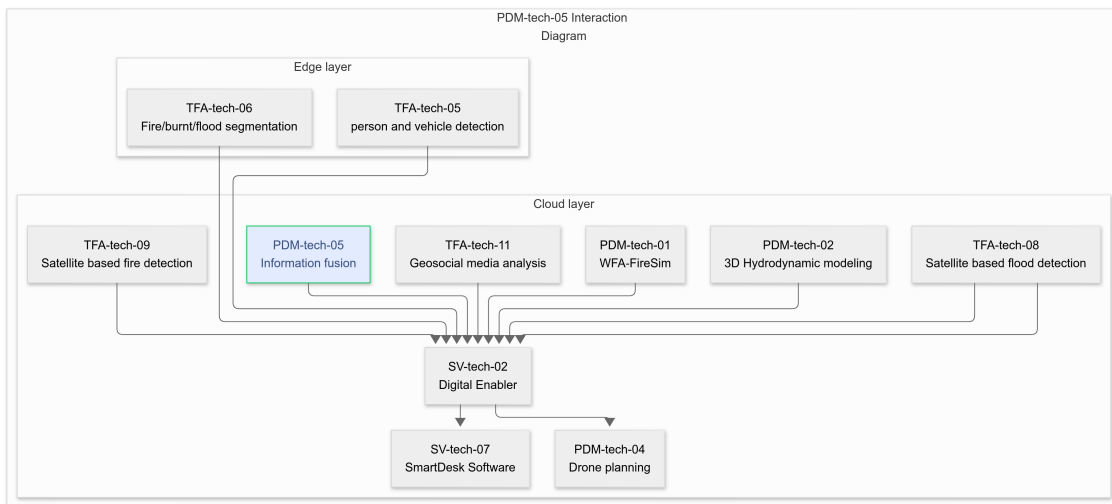


Figure 4: Information Fusion interaction diagram.

3.5.1 System Architecture and Technology Stack

The application is developed using the Flask framework and integrated with SocketIO [15], which provides robust support for real-time communication and asynchronous processing. This combination enables the application to serve dynamic data updates (e.g., status, logs, notifications) over the web, thereby supporting continuous monitoring and prompt feedback during disaster events.

3.5.2 Data Ingestion and Notification Handling

The web service is designed to ingest heterogeneous notifications from multiple sources by subscribing to various technology modules. This enables comprehensive and robust information fusion. In particular, the system integrates notifications from:

- **Alert Notifications:** These alerts trigger processing routines by updating a global cache with critical information such as the Area of Interest (AOI), disaster type, expiration timestamps, and ignition points. Alert notifications serve as the primary trigger for initiating the information fusion process.
- **Detection of Persons and Vehicles (TEMA technology TFA-tech-05):** This technology provides data on detected persons and vehicles in captured drone imagery, contributing real-time insights into on-ground activity during a disaster.
- **Segmentation Masks (TEMA technology TFA-tech-06):** The system ingests segmentation outputs, such as flood segmentation masks, fire segmentation masks, and burnt area segmentation masks. These masks are critical for accurately geo-referencing the impacted areas.
- **Satellite-based Flood Detection (TEMA technology TFA-tech-08):** Notifications from this module supply satellite-derived flood detection and assessment data, which are integrated to enhance situational awareness regarding flood extents.
- **Satellite-based Forest Fire Detection (TEMA technology TFA-tech-09):** This technology delivers satellite-based assessments of forest fire activity, broadening the scope of data available for disaster monitoring.
- **Geo-social Media Analysis (TEMA technology TFA-tech-11):** Geo-tagged social media data are processed to extract supplementary information on disaster impacts from the community, thereby supporting more comprehensive assessments.
- **Flood Simulation Predictions (TEMA technology PDM-tech-02):** Predictive models for flood simulations provide foresight into potential flood extents. These forecasts are crucial for updating and refining the occupancy grid maps used in disaster response.
- **Fire Simulation Predictions (TEMA technology PDM-tech-01):** Similarly, predictive models for fire simulations supply estimations of fire spread and intensity. The integration of these predictions helps in accurately assessing fire ND.

Together, these diverse data streams enable information fusion technology to generate high-fidelity occupancy grid maps and deliver precise, real-time situational awareness for effective disaster monitoring and response.

3.5.3 NGS-LD Entities and Context Broker Interactions

The application models key disaster monitoring data as NGS-LD entities, supporting dynamic status updates and seamless integration within the overall monitoring system:

- **Entity Representation:** Different aspects of disaster monitoring are represented as NGSI-LD entities such as:
 - Alert,
 - FloodCalculationResult,
 - StandardArrivalTime,
 - FireSegmentation,
 - BurntSegmentation,
 - FloodSegmentation,
 - PersonVehicleDetection,
 - HotspotResult,
 - SinglePostResult,
 - EOBurntArea,
 - EOFloodExtent.
- **Subscription Management:** During initialization, the system subscribes to these NGSI-LD entity types via a Context Broker.
- **Entity Updates:** Following the execution of the information fusion routines, the NGSI-LD entities `Maps4Fire`, `Maps4Flood`, and `Maps4Objects` are updated with new metadata, including processing timestamps and links to the generated GeoTIFF and GeoJSON files, ensuring that downstream systems can access the latest information.

3.5.4 Information Fusion: Role and Interactions with Other Technologies

The Information Fusion component is the central engine responsible for aggregating, processing, and integrating data from diverse NGSI-LD entities. It is designed to operate in different natural disaster scenarios, specifically fire and flood, by subscribing to specialized data sources and predictive modules. Based on the Business Mission (BM), the fusion process updates the corresponding occupancy grid map entities: `Maps4Fire`, `Maps4Flood`, and `Maps4Objects`.

Fire Natural Disaster Scenario (BM for Fire): In a fire scenario, the information fusion module takes its measurements from the following sources:

1. **TFA-tech-06 FireSegmentation:** Provides segmentation masks that outline fire-affected areas captured in drone imagery.
2. **TFA-tech-06 BurntSegmentation:** Supplies segmentation masks identifying burnt regions captured in drone imagery.

3. **TFA-tech-05** PersonVehicleDetection: Offers detection data for persons and vehicles captured in drone imagery.
4. **TFA-tech-11** HotspotResult: Delivers geospatial insights derived from hotspot detection.
5. **TFA-tech-11** SinglePostResult: Contributes additional geospatial data from social media posts.
6. **TFA-tech-09** EOBurntArea: Provides satellite-based assessments of burnt areas.

In addition, predictive outputs are obtained from:

- **PDM-tech-01** StandardArrivalTime: Supplies fire simulation predictions.

The fusion of these measurement inputs and predictive outputs results in two occupancy grid maps:

- Maps4Fire: Updated with measurement and prediction data specific to fire incidents.
- Maps4Objects: Contains refined tracks of the detected objects (persons and vehicles).

Flood Natural Disaster Scenario (BM for Flood): In a flood scenario, the measurements are obtained from the following sources:

1. **TFA-tech-06** FloodSegmentation: Provides segmentation masks that outline flood-affected areas captured in drone imagery.
2. **TFA-tech-05** PersonVehicleDetection: Offers detection data for persons and vehicles captured in drone imagery.
3. **TFA-tech-11** HotspotResult: Delivers geospatial insights derived from hotspot detection.
4. **TFA-tech-11** SinglePostResult: Contributes additional geospatial data from social media posts.

Predictive outputs are obtained from

- **PDM-tech-02** FloodCalculationResult: Provides flood simulation predictions.

The fusion process in this scenario produces two occupancy grid maps:

- Maps4Flood: Updated with measurement and prediction data tailored for flood events.
- Maps4Objects: Contains refined tracks of the detected objects (persons and vehicles).

Feedback Loop and NGSI-LD Updates Upon completion of the information fusion process, whether in a fire or flood scenario, the newly computed occupancy grid maps and object overlays are pushed back to the respective NGSI-LD entities. This continuous feedback ensures that the system's state remains updated in real-time with high-fidelity situational data for effective disaster response and management.

3.5.5 Initialization Process

Upon receiving an `Alert` notification, the Information Fusion module initiates a new BM tailored to the specific disaster scenario (fire or flood). The application then begins a multi-step process to prepare for subsequent data fusion:

- **Global Cache and Data Cleanup:** Outdated data in designated directories is cleared, and global variables are reset to ensure a pristine processing environment for the new BM.
- **AOI Determination and DEM Acquisition:** The system computes the polygon that defines the area of interest based on the alert notification details and retrieves the corresponding Digital Elevation Model (DEM) data from external services (e.g., the OpenTopography service).
- **Subscription Initialization:** NGS-LD subscriptions are established and validated for all relevant technology modules (e.g., TEMA technologies TFA-tech-05, TFA-tech-06, TFA-tech-08, TFA-tech-09, TFA-tech-11, PDM-tech-01, and PDM-tech-02), ensuring that data from these sources is reliably received and integrated into the information fusion process.

3.5.6 Real-Time Monitoring, Scalability, and File Management

The application is engineered to deliver high throughput and real-time monitoring capabilities, essential for effective disaster management. Its design incorporates advanced concurrency, dynamic data management, robust logging, and scalable file storage. Key elements include:

- **Concurrency and Event-Driven Processing:** The system leverages Python's `ThreadPoolExecutor` to manage a pool of worker threads that process incoming notifications and data fusion tasks in parallel. Event triggers and threading mechanisms ensure that high-priority `Alert` notifications are promptly processed, while computationally intensive tasks (such as occupancy grid map calculations or georeferencing operations) are executed asynchronously. This non-blocking approach facilitates rapid decision-making and enables the simultaneous handling of multiple data streams without performance degradation.
- **Dynamic Data Management and Logging:** Automated cleanup routines periodically clear outdated or temporary files from designated directories to prevent data clutter and resource exhaustion. The system incorporates comprehensive error handling and exception management across all processing routines. Centralized logging captures detailed operational information, including success and error states, which is made accessible via a dedicated logs endpoint.
- **MinIO Integration:** The system systematically uploads all fused outputs to a MinIO object storage service. Specifically, occupancy grid maps for `Maps4Fire` and `Maps4Flood` are stored as GeoTIFF files, while data for `Maps4Objects` is maintained in GeoJSON format. This centralized, scalable repository ensures that both processed data and its associated metadata are readily available for further analysis, downstream processing, and web-based visualization. The MinIO client efficiently manages file download and upload operations, which is vital for handling the large volumes of data generated during disaster monitoring.

Overall, the combination of advanced concurrency, proactive data management, centralized logging, and scalable file storage ensures that the system maintains high reliability and responsiveness under real-time, high-volume operational conditions.

3.5.7 Deployment and Operational Workflow

The application is deployed as a cloud-based service managed externally. The main entry point performs the following operations:

- **Subscription Initialization:** Establishes NGSI-LD subscriptions with the Context Broker, ensuring that updates from various disaster monitoring technologies are captured in real-time.
- **Real-Time Communication Setup:** Initializes Flask and SocketIO to support live logging and status updates.
- **Service Launch:** Starts the web server, continuously receiving, processing, and fusing heterogeneous data streams to generate timely disaster monitoring outputs.

To facilitate efficient deployment and scalability, the web application is containerized using Docker. The container image is built and pushed to the TEMA Git repository, enabling version-controlled and reproducible deployments. This Docker image is then deployed on a Kubernetes cluster, which manages resource allocation, load balancing, and scalability, ensuring that the application remains resilient and highly available even under varying operational loads.

Figure 5 illustrates the overall deployment and operational workflow of the system. The diagram shows the integration of the system's core components (Data Sources, Web Application, and Storage & Context Broker) and how the orchestration layer (implemented with Docker containers and a Kubernetes cluster) underpins continuous monitoring, dynamic scaling, and efficient resource management.

3.6 Comprehensive Fusion Workflow in TEMA Technology PDM-tech-05

In the following subsections, we will present how the system fuses incoming data to update occupancy grid maps for disaster monitoring (Maps4Fire and Maps4Flood) and to track detected objects (Maps4Objects) for the historical use case scenarios of the Ahrtal floods in Germany and the Moniferru wildfire in Sardinia, Italy.

Upon receiving a notification from any subscribed entity, the information fusion module initiates a comprehensive processing pipeline to integrate heterogeneous sensor data.

Table 1 presents a concise overview of the NGSI-LD entities ingested by the fusion module, their data formats, and typical refresh intervals. It highlights the wide range of input frequencies from sub-second processed UAV outputs to infrequent satellite products that the Information Fusion's event-driven architecture accommodates.

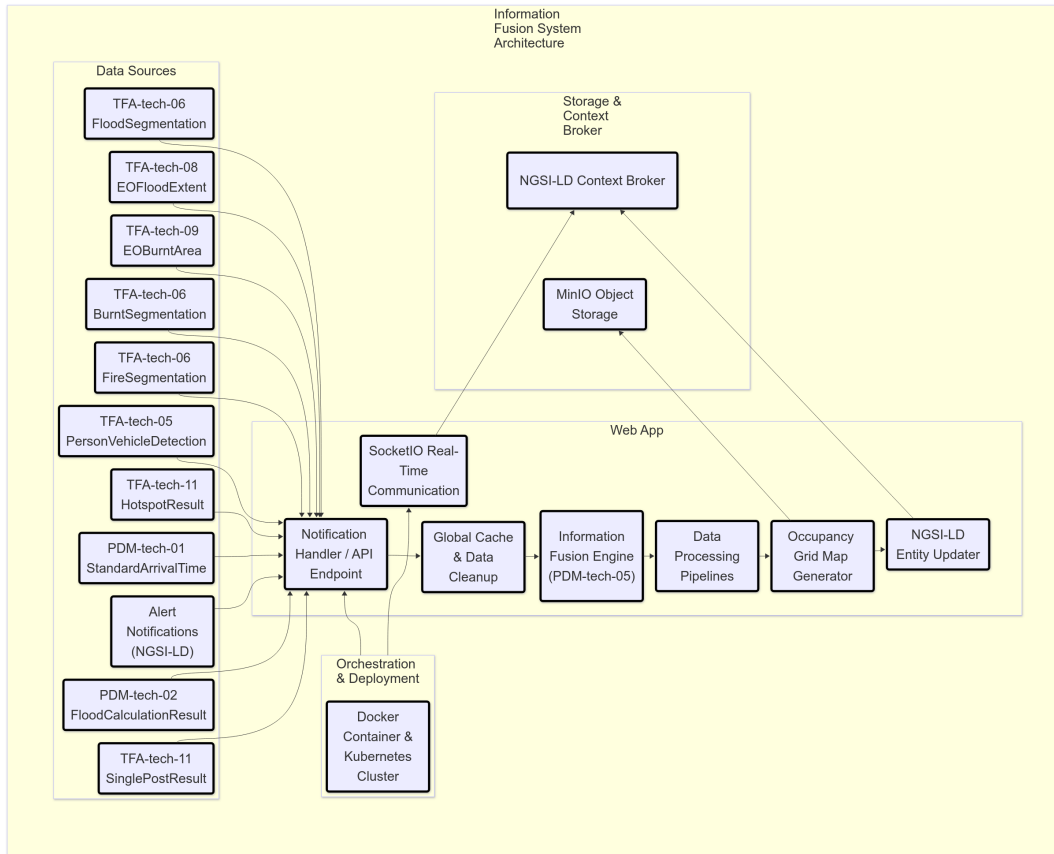


Figure 5: Deployment and Operational Workflow of the Cloud-based Web Application. This diagram highlights the integration of Data Sources, the Web Application, and Storage & Context Broker components, all orchestrated using Docker and Kubernetes for scalable and resilient operations.

Data Type	Entity	Format	Update Interval
Alert	Alert	JSON	Immediate (event-driven)
Segmentation Masks (Fire)	FireSegmentation	PNG / JPG	≈ 1 s
Segmentation Masks (Burnt)	BurntSegmentation	PNG / JPG	≈ 1 s
Segmentation Masks (Flood)	FloodSegmentation	PNG / JPG	≈ 1 s
Satellite Extent Mask (Flood)	EOFloodExtent	GeoTiff	≈ 12 h
Satellite Extent Mask (Burnt)	EOBurntArea	GeoJSON	≈ 12 h
Person/Vehicle Detections	PersonVehicleDetection	JSON	≈ 1 s
Hotspot Aggregation	HotspotResult	GeoJSON	≈ 60 min
Single Social-Media Post	SinglePostResult	GeoJSON	≈ 60 min
Fire Forecast	StandardArrivalTime	GeoTiff	≈ 60 min
Flood Forecast	FloodCalculationResult	GeoTiff	≈ 60 min

Table 1: NGSI-LD entities, formats, and approximate update intervals in the information fusion pipeline.

3.6.1 Alert Notification and Initial Setup

When an `Alert` notification arrives as shown in Fig. 6, the system immediately extracts key information, including:

- The type of the business mission ("`event`"), `Flood` or `Fire`.
- The AOI (`["area"] ["coordinates"]`), defined as a polygon.

Based on the extracted AOI, the system initialises an OGM for monitoring the natural disaster. For both `Maps4Fire` and `Maps4Flood`, all cells are set to an initial probability of 0.5, reflecting maximum uncertainty at the outset. The OGM's spatial resolution is also defined at this stage finer resolutions provide more detail but require higher computational effort.

In parallel, a separate OGM, `Maps4Objects`, is created for tracking detected objects (e.g., persons, vehicles). This map has two distinct bands: one for the probability of an object's presence and another for its label.

3.6.2 Fusing measurements on `Maps4Fire` and `Maps4Flood`

3.6.3 Fusing Processed UAV Imagery (TEMA technology TFA-tech-06)

When TFA-tech-06 provides segmentation outputs (e.g., `FireSegmentation`, `BurntSegmentation`, or `FloodSegmentation`), the system receives a notification and downloads the corresponding JSON metadata and segmented mask. Then, using the image metadata and DEM, the module in Section 3.4.4 ray-traces each mask pixel into the inertial frame, producing a georeferenced raster aligned to real-world coordinates. Figure 8 illustrates a historical flood scenario in the Ahrtal region, displaying the segmentation mask generated upon receiving a notification from the `FloodSegmentation` entity. Similarly, Figure 9 depicts a historical fire scenario in Montiferru, Sardinia, Italy, with the corresponding segmentation mask (indicating the active fire area) obtained via the `FireSegmentation` entity, while Figure 10 shows a segmentation mask of the burnt area from the same region following a notification from the `BurntSegmentation` entity.

Because drone segmentation masks typically have much finer spatial resolution than the occupancy grid (e.g. `Maps4Fire` or `Maps4Flood`), we first compute the mask's footprint polygon and intersect it with the grid's area of interest. The corresponding patch of the occupancy grid is then resampled, using nearest-neighbor interpolation on binary masks, so that its cell size matches the UAV raster resolution. Next, each binary mask value $m(i) \in \{0, 1\}$ is converted to a per-cell measurement likelihood, then we fused it into the existing log-odds grid via the Bayesian update equations (see Section 3.4.2), integrating the new, timestamped UAV measurement into the occupancy grid in real time. Figure 11 shows an example of fusing the `FireSegmentation` and `BurntSegmentation` masks from the historical SAR wildfire scenario in Montiferru, Sardinia, into the `Maps4Fire` occupancy grid. The main panel displays the full-area occupancy map with the area of interest highlighted; the inset zoom illustrates the precise area where the fire and burnt-area masks (outputs of TEMA technology TFA-tech-06 (`FireSegmentation` and `BurntSegmentation`)) are fused, demonstrating their combined effect on cell occupancy probabilities.

```
Entity urn:ngsi-ld:Alert:test5:flood011
{
  "area": {
    "coordinates": [
      [
        [6.996817325, 50.521793116],
        [6.982379622, 50.517755746],
        [6.976085293, 50.513526712],
        [6.980425116, 50.506469699],
        [6.995878527, 50.511398138],
        [6.996817325, 50.521793116]
      ]
    ],
    "type": "Polygon"
  },
  "areaDesc": "Flood in Ahrtal hystorical case",
  "bm_id": "c09868712235f4fa72d0993ca4aeb2ef",
  "category": "Met",
  "certainty": "Observed",
  "effective": "2021-07-14T14:31:39.034Z",
  "event": "Flood",
  "expires": "2025-04-09T16:02:14.106Z",
  "id": "urn:ngsi-ld:Alert:test5:flood011",
  "location": {
    "coordinates": [
      [
        [6.996817325, 50.521793116],
        [6.982379622, 50.517755746],
        [6.976085293, 50.513526712],
        [6.980425116, 50.506469699],
        [6.995878527, 50.511398138],
        [6.996817325, 50.521793116]
      ]
    ],
    "type": "Polygon"
  },
  "msgType": "Alert",
  "scope": "Private",
  "sender": "alert@tema-project.eu",
  "sent": "2025-04-08T16:02:14.106Z",
  "severity": "Severe",
  "status": "Exercise",
  "type": "Alert",
  "urgency": "Immediate"
}
```

Figure 6: Received Alert notification.

Fusing Processed Satellite Data (TEMA Technology TFA-tech-08/09): When new segmentation results arrive from the satellite-based modules (TEMA technology TFA-tech-08: EOfloodExtent and TEMA technology TFA-tech-09: EOBurntArea), the Information Fusion pipeline performs the following steps:

1. **Fetch georeferenced images:** Retrieve the GeoTIFF mask together with its timestamps and



(a) *Maps4Flood* at 20 m resolution.



(b) *Maps4Objects* at 1 m resolution.

Figure 7: Creation of *Maps4Flood* and *Maps4Objects* after extracting AOI from an *Alert* notification.



(a) *Flood Segmentation Mask*.



(b) *Georeferenced Flood Mask*.

Figure 8: Example of a UAV segmentation mask before and after georeferencing.

bounding boxes.

2. **AOI intersection:** Discard any mask that does not overlap the current occupancy-grid AOI polygon (from the latest *Alert*).
3. **Polygon-precise cropping:** Clip the georeferenced mask to the exact AOI polygon, preserving coordinate metadata.
4. **Resolution matching:** Resample the clipped mask to the occupancy grid's native resolution via nearest-neighbour, ensuring each grid cell aligns one-to-one.
5. **Likelihood assignment (soft mask):** For every grid cell i within the cropped AOI, take the resampled mask value $m(i) \in [0, 1]$ directly as the measurement likelihood $p_m(i) = m(i)$.
6. **Bayesian update:** apply the Bayesian update to the existing log-odds occupancy grid using the equations Eqs. 1–5 in Section 3.4.2.



(a) Fire Segmentation Mask.

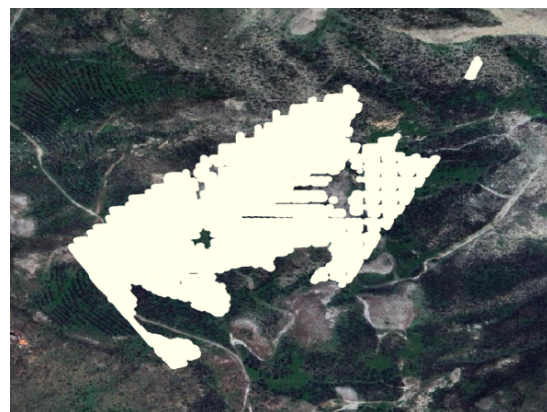


(b) Georeferenced Fire Mask.

Figure 9: Example of a UAV segmentation mask before and after georeferencing.



(a) Burnt Segmentation Mask.



(b) Georeferenced burnt Mask.

Figure 10: Example of a UAV segmentation mask before and after georeferencing.

In Figure 12 we show the raw satellite-derived flood extent mask for the historical Ahrtal flood event, as delivered by the NGSi-LD entity `EOFloodExtent` (TEMA technology TFA-tech-08). This GeoTIFF contains per-pixel inundation probabilities from the archived satellite pass, fully georeferenced in the project CRS.

Figure 13 presents the same historical mask after two key preprocessing steps: (1) cropping to the Alert-defined AOI polygon for this past event, and (2) resolution matching to the 20m grid of `Maps4Flood`. The result is a grid-aligned inundation mask, ready for direct Bayesian fusion with the occupancy grid.

Figure 14 illustrates how the soft-mask probabilities from the archived satellite flood extent (TEMA technology TFA-tech-08) modify our `Maps4Flood` grid:

- Prior state (left): All cells within the AOI start at a neutral probability of 0.5, indicating maximum uncertainty before integrating the satellite data.

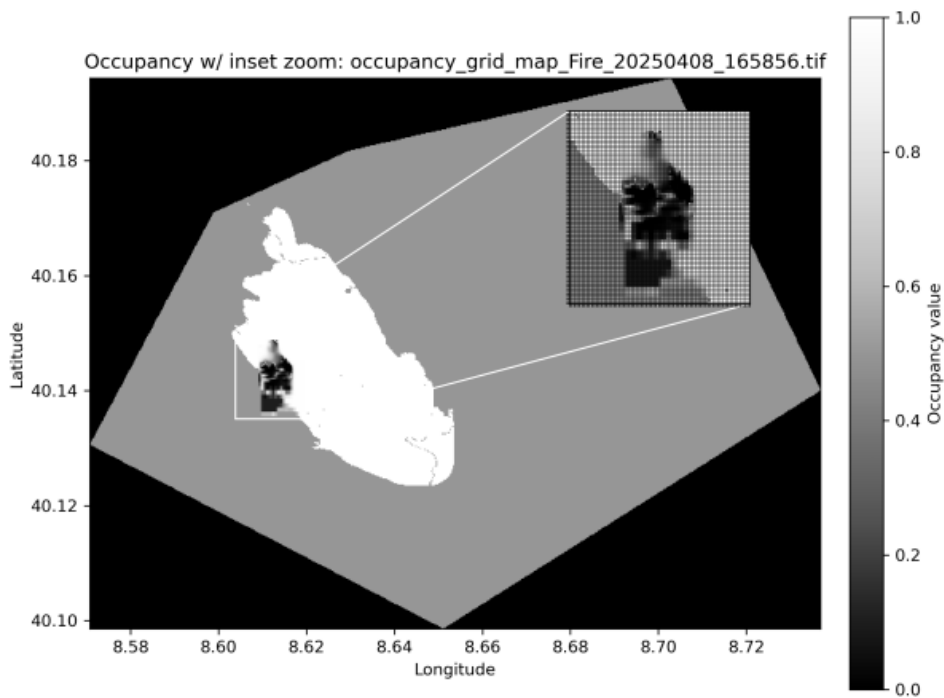


Figure 11: Fusion of FireSegmentation and BurntSegmentation masks into the Maps4Fire occupancy grid (inset shows the local update).

- Posterior state (right): Cells where the resampled soft-mask $m(i)$ was nonzero experience a Bayesian update, producing localised clusters of elevated occupancy probability. This precisely highlights the flood-affected subregions detected by the satellite.
- AOI overlay: The red polygon delineates the Alert-defined AOI. Only cells inside this boundary were considered in the fusion.

By directly plugging per-pixel mask values $m(i) \in [0, 1]$ into the log-odds update, we preserve continuous confidence information and obtain a more nuanced, data-driven flood map.

Fusing Geosocial Media Data (TEMA technology TFA-tech-11): The geosocial media data from TEMA technology TFA-tech-11 provides two distinct types of outputs: `HotspotResult` (aggregated regional metrics) and `SinglePostResult` (individual geolocated posts). Each offers complementary information to enhance our system’s occupancy grid maps and object tracking.

For updating the Maps4Fire and Maps4Flood, we fuse the processed `HotspotResult` data via Bayesian Update as follows.

HotspotResult fusion:

1. **Rasterize metrics:** Download the GeoJSON payload from `HotspotResult`, which contains per-cell $\{count, z_score, p_value\}$. Rasterize each metric to exactly match the occupancy

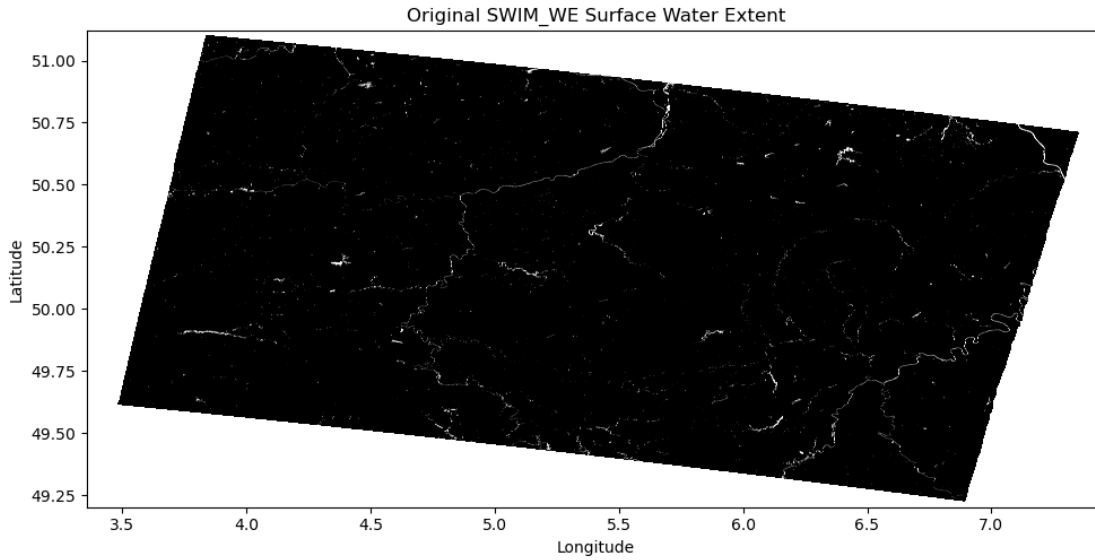


Figure 12: Original satellite-derived flood extent mask for the historical Ahrtal flood scenario (TFA-tech-08).

grid's extent, resolution, and CRS (see Section 3.4.2).

2. **Build Measurement Likelihood:** For each cell i , normalize and combine the three metrics into a single likelihood:

$$p_m(i) = w_c \frac{\text{count}(i)}{\max(\text{count})} + w_Z \sigma(Z(i)) + w_p [1 - p\text{-value}(i)], \quad (31)$$

where $\sigma(z) = 1/(1 + e^{-z})$ and $w_c + w_Z + w_p = 1$. Clamp $p_m(i)$ into $[\varepsilon, 1 - \varepsilon]$ to avoid infinite log-odds. As a simpler alternative, one can apply a threshold rule:

$$p_m(i) = \begin{cases} p_{\text{high}}, & p\text{-value}(i) < 0.05, \\ p_{\text{low}}, & \text{otherwise,} \end{cases} \quad \text{with } p_{\text{high}} = 0.8, p_{\text{low}} = 0.2. \quad (32)$$

3. **Bayesian Log-Odds Update:** Convert the prior occupancy probability $p_{\text{prior}}(i)$ into log-odds $\ell_{\text{prior}} = \ln \frac{p_{\text{prior}}}{1 - p_{\text{prior}}}$. Compute the log-likelihood ratio $\text{LLR}(i) = \ln \frac{p_m(i)}{1 - p_m(i)}$, then update as follows:

$$\ell_{\text{updated}}(i) = \ell_{\text{prior}}(i) + [\text{LLR}(i) - \ell_0], \quad \ell_0 = 0. \quad (33)$$

Finally, we recover the fused probability as follows:

$$p_{\text{updated}}(i) = [1 + e^{-\ell_{\text{updated}}(i)}]^{-1}. \quad (34)$$

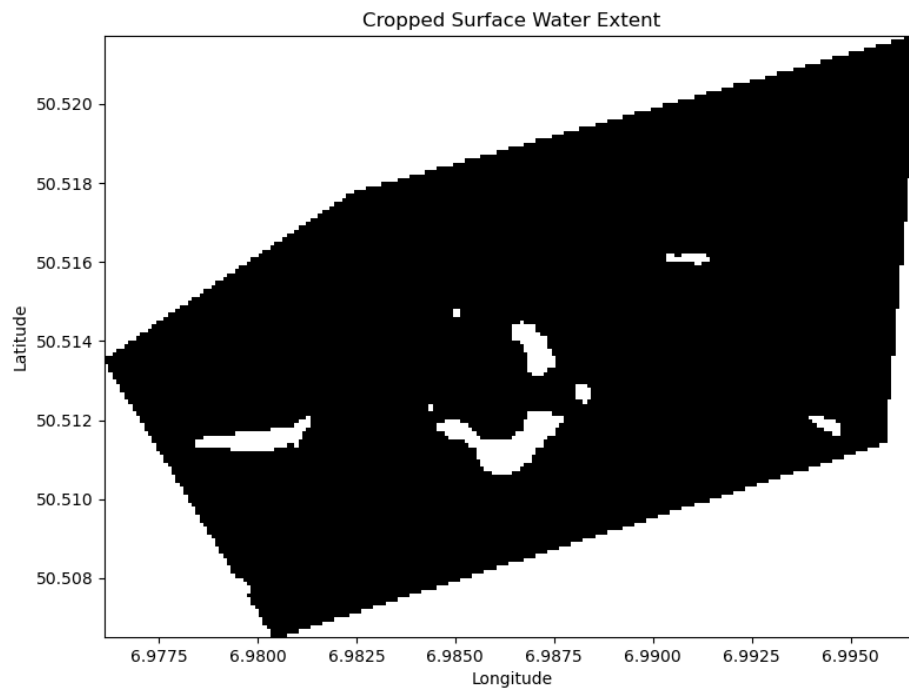


Figure 13: Cropped and resampled flood segmentation for the historical Ahrtal event, aligned to the 20m cells of Maps4Flood.

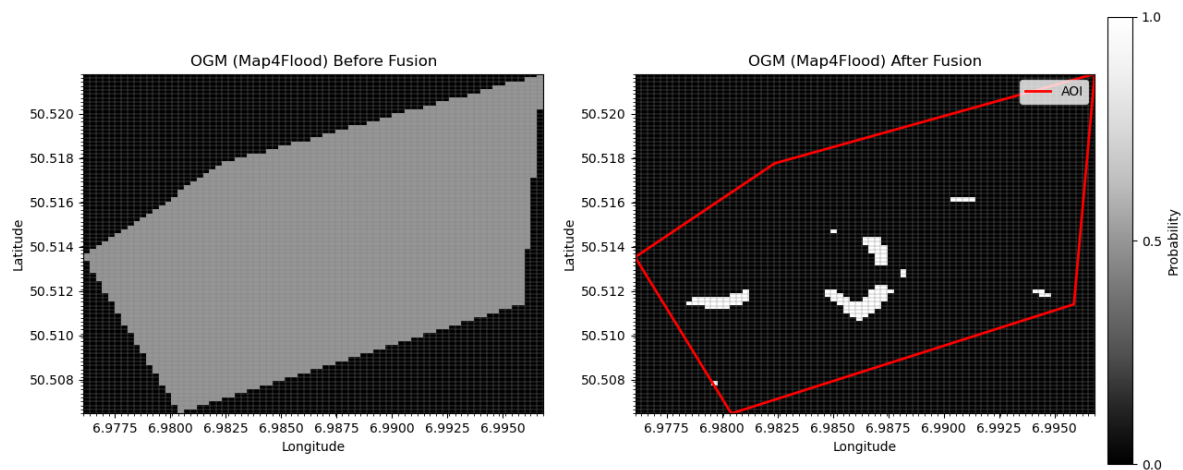


Figure 14: Comparison of the Maps4Flood occupancy grid before (left) and after (right) fusing the satellite-derived flood mask for the historical Ahrtal event.

Figure 15 displays the raw `HotspotResult` hex cell counts across the study area of the Ahrtal use case scenario:

- **Intensity scale:** Each hexagon’s fill color (from light pink to deep red) represents the total number of geotagged social-media posts in that cell, with darker hues indicating higher volumes of reporting.
- **Data coverage:** The hex-grid format makes it easy to see gaps in geosocial coverage—cells with zero posts stand out immediately, flagging areas with little to no crowd-sourced information.

The blue polygon drawn over the hex-cells marks the AOI used by our occupancy-grid model, indicating exactly which cells will be carried forward into the fusion process.

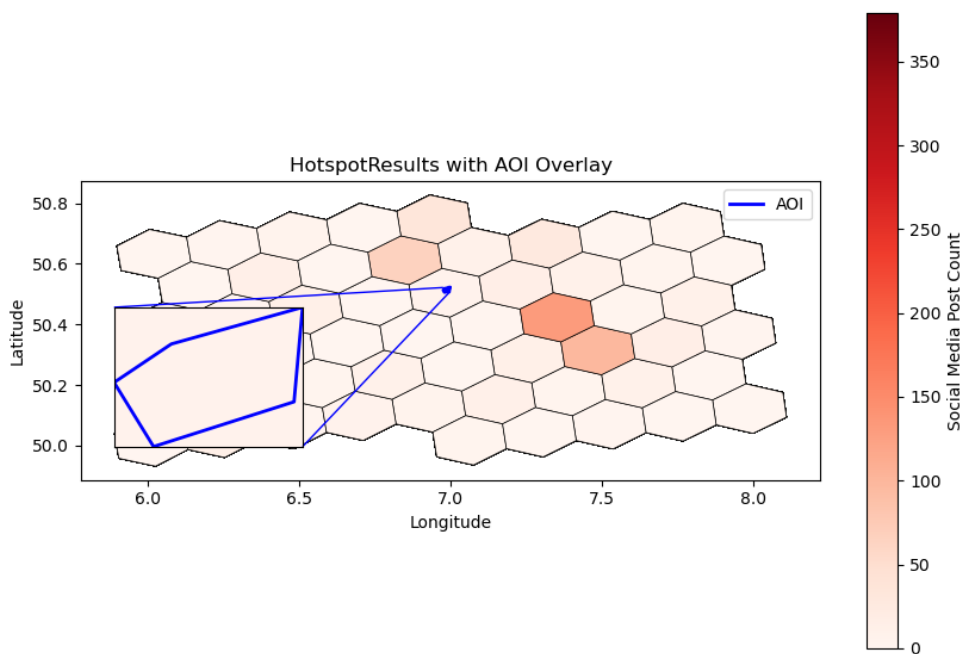


Figure 15: Fusion of rasterized `HotspotResult` metrics into the `Maps4Fire` grid for the flood case scenario of Ahrtal.

Figure 16 illustrates the effect of Bayesian fusion on the Ahrtal flood occupancy grid:

- **Prior (left panel):** All cells inside the AOI (red outline) are initialized to $p = 0.5$ (light gray), representing complete uncertainty, while cells outside are set to zero (black).
- **Posterior (right panel):** Only those AOI cells with significant social-media hotspots (count > 10 and p -value < 0.05) receive a log-odds update. Their probabilities increase (up to approx-

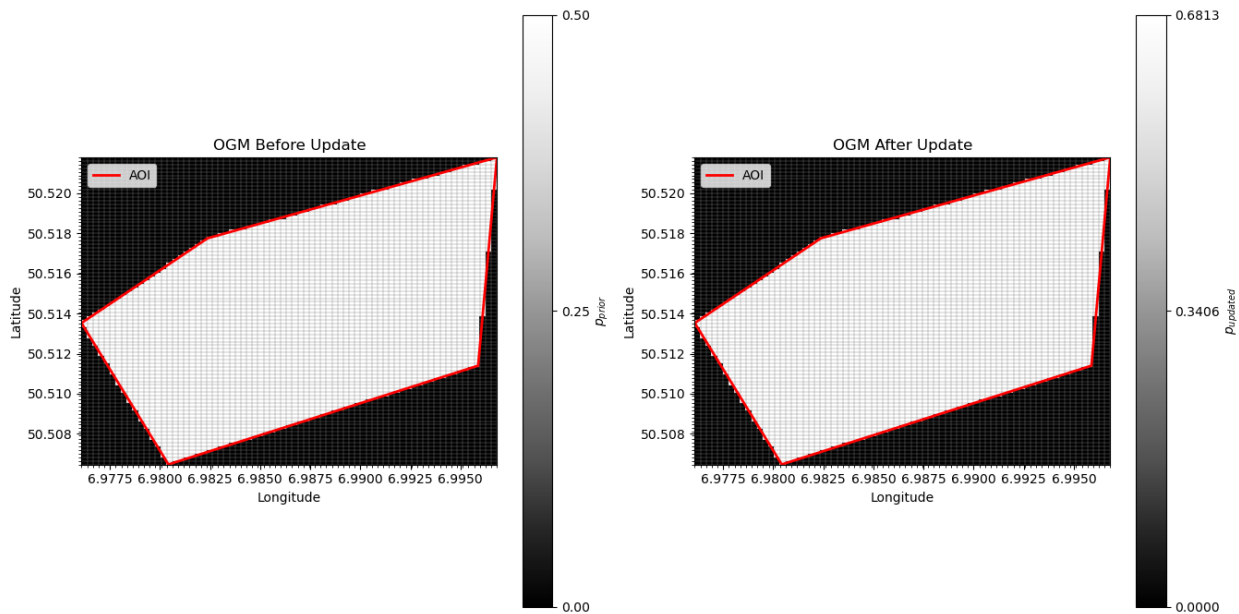


Figure 16: Occupancy grid fusion for the Ahrtal flood scenario.

imately 0.68, shown in brighter gray), whereas all other cells remain at zero.

- **Cell-by-cell update:** The fine gridlines make clear that the update is applied individually to each cell, focusing the map’s attention precisely where geosocial evidence exists.

This selective sharpening of the occupancy grid demonstrates how integrating HotspotResult metrics can enhance situational awareness by highlighting areas most likely affected according to social-media signals.

Fusing Predictive Model Outputs (TEMA technologies PDM-tech-01 and PDM-tech-02): Predictive simulation models generate forward-looking ND estimates that are integrated into the occupancy grid via our log-odds Bayesian framework.

In a fire scenario, the NGS-LD entity `StandardArrivalTime` (TEMA technologies PDM-tech-01), produced by the Wildfire Analyst FireSim module, provides per-cell fire arrival-time predictions. In a flood scenario, the NGS-LD entity `FloodCalculationResult` (TEMA technologies PDM-tech-02), generated by the 3Di Water Management simulator, yields a binary inundation mask indicating which cells are predicted to be flooded at the given forecast time.

These predictive outputs are fused with real-time sensor measurements as follows:

1. **Prediction retrieval:** For each grid cell m_i , obtain either:
 - Fire arrival time $t_{arr}(i)$ from `StandardArrivalTime`, or
 - Binary flood indicator $b(i) \in \{0, 1\}$ from `FloodCalculationResult`.

2. **Likelihood computation:** Convert the raw predictions into a normalized likelihood $p_{\text{pred}}(i) \in [0, 1]$:

$$p_{\text{pred}}(i) = \begin{cases} \max\left(0, 1 - \frac{t_{\text{arr}}(i) - t_{\text{current}}}{T_{\text{horizon}}}\right), & \text{(fire)} \\ b(i) p_f + (1 - b(i)) p_{\text{nf}}, & \text{(flood spread)} \end{cases} \quad (35)$$

- *Fire case:* We interpret the arrival-time prediction $t_{\text{arr}}(i)$ relative to the current time t_{current} . The term $(t_{\text{arr}}(i) - t_{\text{current}})$ gives the lead time until fire reaches cell m_i . Dividing by the forecast horizon T_{horizon} (e.g. 60 min) yields a normalized delay in $[0, 1]$. Subtracting from 1 produces higher likelihoods for cells predicted to burn sooner.
- *Flood case:* The binary mask $b(i)$ takes the value 1 for predicted flood cells and 0 otherwise. We assign a high likelihood p_f (e.g. 0.95) to inundated cells and a low likelihood p_{nf} (e.g. 0.05) to non-inundated cells. This avoids degenerate log-odds when computing $\log(p_{\text{pred}}/(1 - p_{\text{pred}}))$.

Then clamp:

$$p_{\text{pred}}(i) \leftarrow \min(1, \max(0, p_{\text{pred}}(i))). \quad (36)$$

3. **Occupancy Grid Update:** Incorporate $p_{\text{pred}}(i)$ into the existing log-odds occupancy grid using the Bayesian update equations (Eq. 1-5 in Section 3.4.2), producing the final fused map in Maps4Fire or Maps4Flood.

Figures 17 - 21 present successive FireSim occupancy grid snapshots taken at hourly intervals, illustrating the temporal evolution of the Maps4Fire prediction produced by the FireSim module (TEMA technology PDM-tech-01) for the historical RAS wildfire use case in Montiferru, Italy.

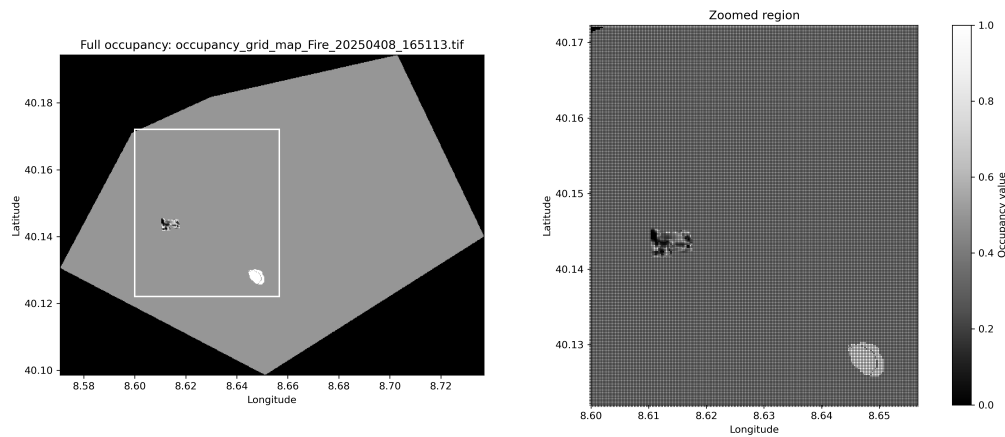


Figure 17: Prediction at the first hour.

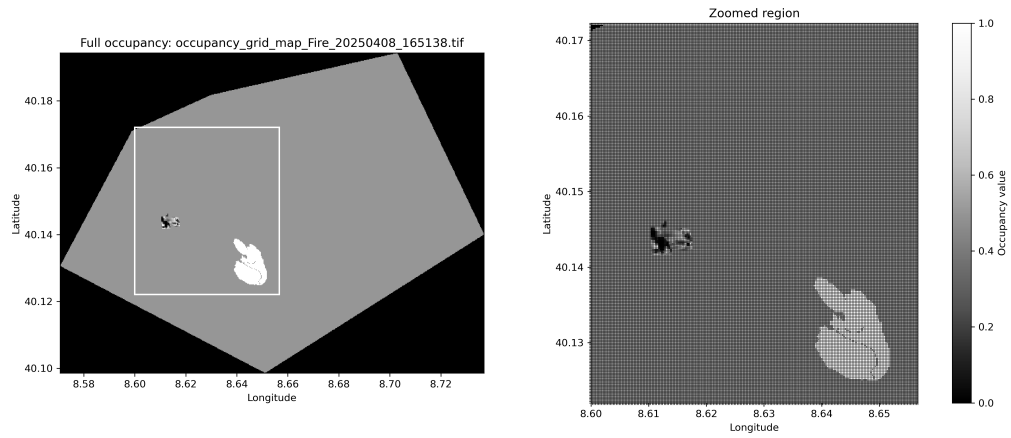


Figure 18: Prediction at the second hour.

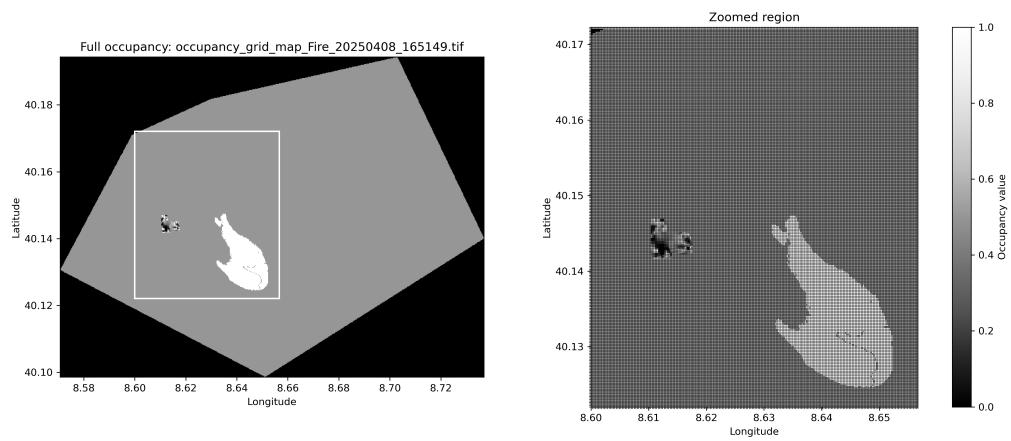


Figure 19: Prediction at the third hour.

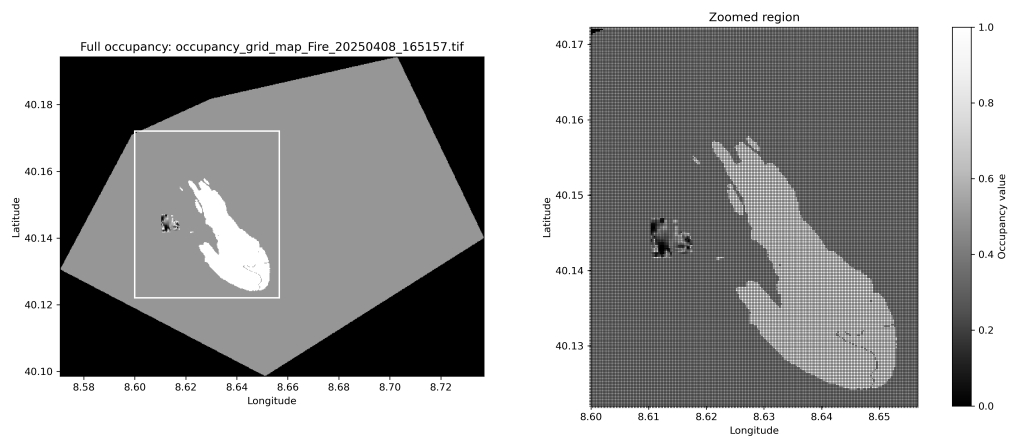


Figure 20: Prediction at the fourth hour.

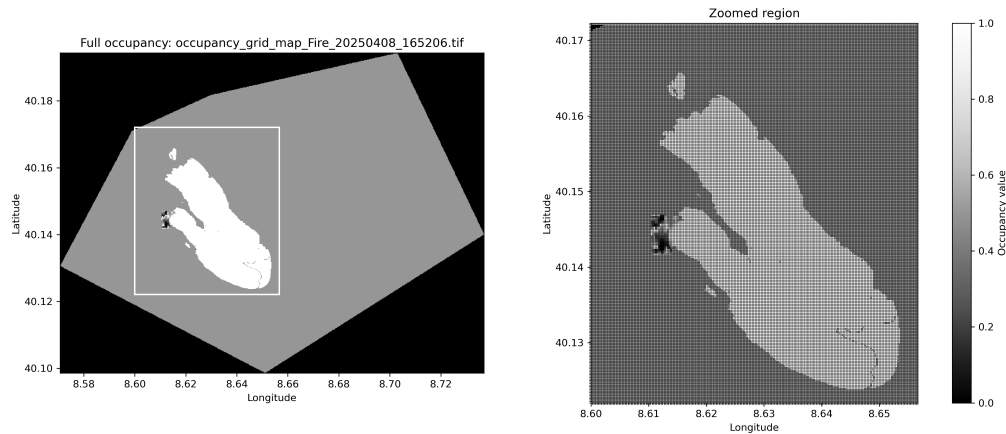


Figure 21: Prediction at the fifth hour.

This asynchronous fusion of predictive outputs with sensor data enhances map smoothness, reduces uncertainty, and improves forecast fidelity for real-time disaster monitoring and decision support.

3.6.4 Fusing measurements of Maps4Objects

Fusing Processed UAV Imagery (TEMA technology TFA-tech-05): The `PersonVehicleDetection` outputs from TFA-tech-05 provide both image metadata and bounding-box detections of people and vehicles. Upon receipt:

1. **Georeferencing:** Each bounding box is projected into the inertial frame using the pipeline described in Section 3.4.4, yielding precise ground coordinates for each detection.
2. **Measurement Extraction:** For each detected object, we compute the center-of-mass of the box and record its latitude/longitude, confidence score, and class label (`person` or `vehicle`).
3. **AOI and Temporal Filtering:** Detections outside the Alert-defined AOI or outside the current time window are discarded.
4. **Data Association:** Remaining measurements are matched to existing tracks via the Hungarian algorithm (see Section 3.4.3).
5. **Track Management:**
 - *Matched detections:* Update the corresponding Kalman filter state.
 - *Unmatched detections:* Initialize a new Kalman filter to begin tracking.

This procedure ensures that drone-processed images with detections continuously refine the `Maps4Objects` tracks in real time.

Fusing Geosocial Media Data (TEMA technology TFA-tech-11): The `SinglePostResult` stream delivers individual, geolocated social-media posts associated with the disaster. The Information fu-

sion utilizes the geolocated data, which provides the location of the persons in the places of the natural disasters. These detections provide explicit coordinates and are used to update the object tracking map (`Maps4Objects`). The processing involves:

- **Temporal and Spatial Validation:** Detections outside the Alert- defined AOI or outside the current time window are discarded.
- **Data Association:** The new detection is associated with existing tracks using the Hungarian matching algorithm (as detailed in Section 3.4.3).
- **Kalman Filter Update:** if the detection is associated with an existing track, its state is updated via the linear Kalman filter; otherwise, a new tracking filter is instantiated.

This method ensures that individual social media posts (`SinglePostResult`) contribute to accurate and continuous object tracking within the `Maps4Objects` output.

Figure 22 illustrates the TEMA technology TFA-tech-11 `SinglePostResult` posts for the historical Ahrtal scenario, overlaid on the Alert-defined AOI polygon that bounds the `Maps4Objects` output. Each marker represents a geolocated social-media post attributed to a person. Furthermore,

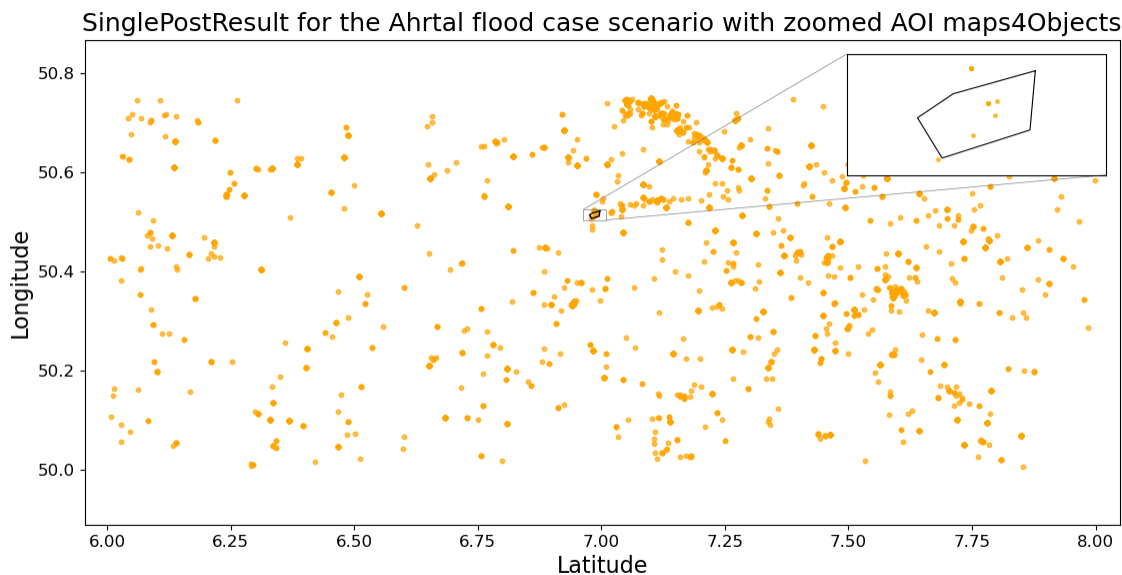


Figure 22: Georeferenced detections of the `SinglePostResult`.

Fig. 23 shows the TEMA technology TFA-tech-05 `PersonVehicleDetection` output for the historical Ahrtal scenario: each dot is a georeferenced detection that has a label as either “person” or “vehicle.”

In Fig. 24 we compare the “raw” predicted trajectory (blue) derived from the motion model alone against the “updated” trajectory (red) after each measurement fusion. Circles denote the respective



Figure 23: Georeferenced detections out of TFA-tech-05 (*PersonVehicleDetection*).

start points, and squares the end points. The raw prediction diverges slightly due to uncorrected process noise, whereas the updated path remains closer to the true (measured) positions.

Figure 25 shows plots that track the tracking “tolerance” (Euclidean error in metres) between the raw measurements and the Kalman-filter state estimate at each time step. The solid blue curve shows the instantaneous measurement-to-estimate distance, while the dashed red line marks the mean tolerance ($0.17m$). Early in the sequence (Steps 0 – 5), the filter quickly corrects large initial deviations, and thereafter the error fluctuates in the $0.1 - 0.3m$ range.

3.7 Summary (Key Outcomes)

This section consolidates the principal achievements and deliverables of the TEMA technology PDM-tech-05 Information Fusion module:

- **Multimodal data integration:** Seamless fusion of UAV segmentation (TEMA technologies TFA-tech-05/06), satellite segmented masks (TEMA technologies TFA-tech-08/09), geosocial analytics (TEMA technology TFA-tech-11), and predictive models (TEMA technologies PDM-tech-01/02) into a unified, georeferenced situational picture.
- **Real-time, asynchronous processing:** Event-driven pipelines and non-blocking threads ensure that each incoming measurement or forecast is immediately incorporated via Bayesian occupancy-grid updates and Kalman filter tracking.
- **Precise georeferencing:** A dedicated ray-tracing module aligns UAV segmented masks with a DEM, guaranteeing pixel-accurate geographic registration for all fused inputs.

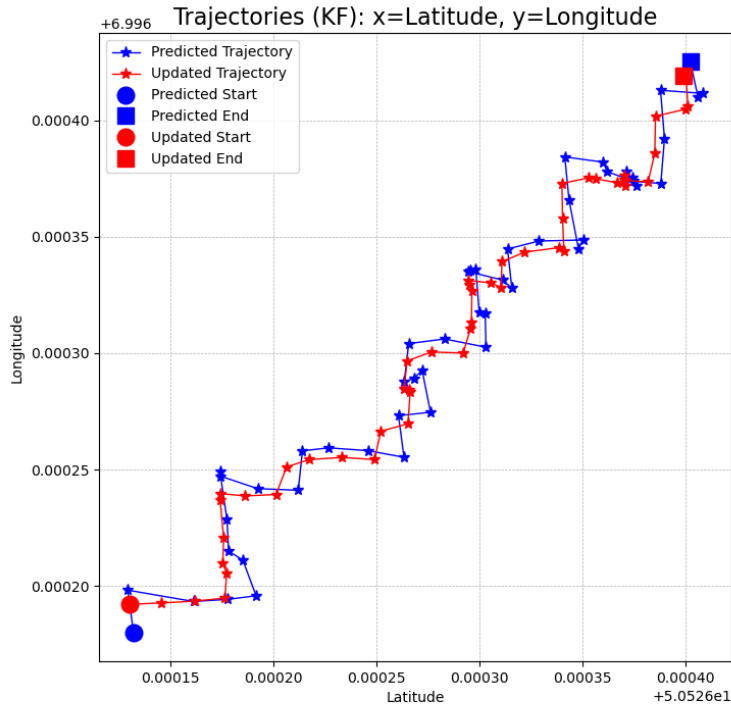


Figure 24: Predicted (blue) vs. Kalman-filtered (red) trajectories.

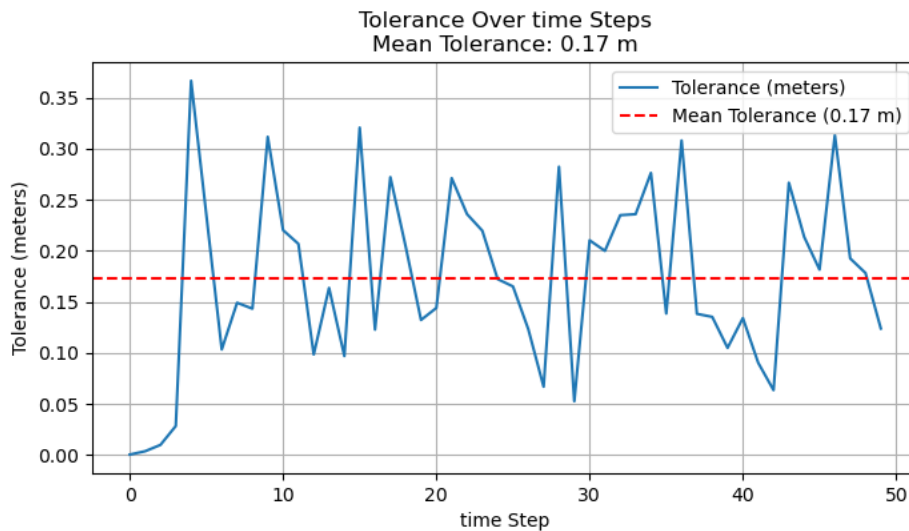


Figure 25: Tolerance over time.

- **Comprehensive outputs:** Generation of three occupancy maps, Maps4Fire, Maps4Flood, and Maps4Objects, continuously updated to reflect the latest observations and forecasts.

- **Web dashboard and NGSi-LD integration:** A Flask SocketIO interface subscribes to NGSi-LD entities, visualizes fusion outputs in real time, and exposes REST APIs for downstream consumption.
- **Scalable deployment and validation:** Containerized via Docker and orchestrated on Kubernetes, the service demonstrated end-to-end interoperability and performance in multi-partner tests.
- **Decision-support readiness:** The fused maps and tracked-object overlays deliver high-fidelity, up-to-date insights, empowering emergency responders with actionable situational awareness that directly support faster and more informed decisions in line with **OC2 “Increase situational awareness in NDM”**.

Table 2 summarises the two historical scenarios used to benchmark the Information Fusion pipeline. For the 2021 Ahrtal flood, the Alert-defined AOI covers about 1.5 km^2 . We therefore maintain fine resolutions 20m for the flood OGM (Maps4Flood) and 1m for the tracked object OGM (Maps4Objects), yielding sub-second refresh times. Furthermore, regarding the Montiferru wildfire, which spans a much larger AOI of 92 km^2 . Here Maps4Fire is kept at 20m , while the object grid is coarsened to 10m to limit computational load.

Table 2: Characteristics and occupancy-grid configurations of historical scenarios.

	Ahrtal Flood	Montiferru Fire
Location	Ahrtal, Germany	Montiferru, Sardinia
Monitored AOI (km^2)	≈ 1.47	≈ 91.6
<i>Spatial resolution of occupancy grids</i>		
Maps4Flood	20m	—
Maps4Fire	—	20m
Maps4Objects	1m	10m
<i>Average computation time per map</i>		
Maps4Flood	$\approx 1\text{s}$	—
Maps4Fire	—	$\approx 18\text{s}$
Maps4Objects	$\approx 1\text{s}$	$\approx 9\text{s}$

The following Algorithm 2 presents the complete event-driven pipeline of the IF module developed in the TEMA project, detailing how heterogeneous data sources are asynchronously processed and integrated into unified georeferenced occupancy and object maps, thereby sustaining the multimodal awareness required by **OC2 “Increase situational awareness in NDM”**.

In summary, the IF module delivers robust, scalable, and real-time integration of heterogeneous data sources, substantially advancing situational awareness and fulfilling **OC2 “Increase situational awareness in NDM”** within the TEMA platform.

Algorithm 2 Event-driven fusion loop (PDM-tech-05)

Require: asynchronous NGS-LD stream \mathcal{N}

```

1: global activeBM  $\leftarrow$  false                                ▷ no business mission yet
2: global ROI  $\mathcal{P} \leftarrow \emptyset$ 
3: for all  $n \in \mathcal{N}$  asynchronously do
4:   if  $n.type = \text{Alert}$  then
5:     extract disaster type  $\mathcal{D}$ , ROI  $\mathcal{P}$ 
6:     initialise  $\text{Maps4Flood/Fire} \leftarrow 0.5$ ;  $\text{Maps4Objects: score} = 0$ ,  $\text{label} = \emptyset$ 
7:     activeBM  $\leftarrow$  true                                    ▷ gate opens
8:     continue                                                ▷ next notification
9:   end if
10:  if not activeBM then
11:    skip notification                                        ▷ ignore until an Alert arrives
12:    continue
13:  end if
14:  if  $n.type \in \{\text{FireSegmentation, BurntSegmentation, FloodSegmentation}\}$  then
15:    georeference  $\rightarrow$  crop to  $\mathcal{P} \rightarrow$  resample
16:    Bayesian update with  $p_m = m(i)$ 
17:  else if  $n.type \in \{\text{EOBurntArea, EOFloodExtent}\}$  then
18:    crop to  $\mathcal{P}$ , resample; Bayesian update
19:  else if  $n.type = \text{SinglePostResult}$  then
20:    validate time/ROI; associate  $\rightarrow$  Kalman update / new track
21:  else if  $n.type = \text{PersonVehicleDetection}$  then
22:    georeference; associate  $\rightarrow$  Kalman update / new track
23:    write score & label to  $\text{Maps4Objects}$ 
24:  else if  $n.type = \text{HotspotResult}$  then
25:    derive  $p_m$  from  $\{\text{count}, Z, p\text{-value}\}$ ; Bayesian update
26:  else if  $n.type \in \{\text{StandardArrivalTime, FloodCalculationResult}\}$  then
27:    compute  $p_{\text{pred}}$ ; Bayesian update
28:  end if
29: end for

```

3.8 Fusing Information Derived from Social Media

Task 4.3 was also advanced in close connection with Task 3.3 (social media and text semantic analysis), through the development and validation of a multimodal analysis framework that fuses semantic, sentiment, spatial and temporal information from social media to enhance situational awareness in disaster response.

SOTA

The integration of multimodal social media data, encompassing semantic content, sentiment, and spatio-temporal information, has become an essential tool in disaster management, especially

during response and recovery phases when social media activity surges [16]. Effective information fusion from these diverse modalities offers valuable situational awareness for emergency responders [17]. A wide range of studies have combined semantic or sentiment analysis with spatio-temporal analysis of geo-referenced social media posts [18]. However, in these studies, semantics are typically only considered as a filtering mechanism or indirectly via emotional associations, leaving the actual thematic content of the discussions underexplored. Furthermore, several approaches have attempted to model semantics and sentiments jointly, often by sequentially combining topic modeling and sentiment classification [19]. These methods can provide valuable insights into topic-wise sentiment trends across time and space, but they frequently rely on keyword-filtered or geotagged posts, use bag-of-words-based topic models such as Latent Dirichlet Allocation (LDA), and perform the analyses in sequential steps. Consequently, semantic and emotional coherence is often not preserved in the final outputs. Some studies have begun to explore more integrated approaches which combine individual models for sentiment and semantic classification with spatial and temporal analyses for disaster severity assessment [20]. However, such methods often require task-specific training and are limited to monolingual applications. Thus, a key gap remains in developing a coherent, fully integrated model that simultaneously capture semantics, sentiment and spatio-temporal across different languages and disaster use cases.

Activities performed in the period M13-M18

During the first reporting period of TEMA, substantial progress was made toward addressing key gaps in the state of the art. IT:U developed a **Joint Topic-Sentiment (JTS)** framework to overcome the limitations of sequential and bag-of-words-based methods for identifying sentiment-associated topics. The framework was published in a peer-reviewed journal paper [21] and integrates semantic embedding vectors based on Sentence-BERT [22] with sentiment classification outputs to generate joint feature vectors. These vectors are clustered to form coherent groups of social media posts that reflect both thematic and emotional content. The framework is modular, supporting different language models and clustering techniques. Experimental evaluations demonstrated superior performance over traditional methods such as JST [23] and TSWE [24], validated through metrics including Topic Coherence (TC), Topic Diversity (TD), and the Sentiment-Exact Match Ratio (S-EMR). Building on this foundation, the idea has been extended to capture spatio-temporal dynamics by incorporating normalized spatial coordinates and temporal representations into the feature vectors. To maintain spatial coherence in the resulting clusters, a **Geographic Growing Self-Organizing Map (Geo-GSOM)** was developed. Unlike conventional SOMs, the Geo-GSOM dynamically expands its neuron grid and applies a two-step learning procedure that prioritizes geographical proximity. This enables the clustering of multimodal feature vectors in a way that preserves spatial structure while integrating semantic and sentiment information. The resulting clusters serve as a basis for high-level information extraction, supporting contextual analysis through predefined generative AI outputs such as summaries and extracted emergency-related information. The resulting framework is called the **Joint Spatio-Temporal Topic-Sentiment (JSTTS)**. It is capable of reducing large volumes of social media posts to a manageable set of interpretable clusters, enhancing situational awareness for emergency responders. The approach has already been applied to real-world events like the 2021 Ahr Valley flood in Germany for which findings have been disseminated in a conference paper at AGILE 2024 [25].

Activities performed in period M19-M30

In the second reporting period, IT:U has intensified their research on the JSTTS framework, focusing on understanding the geospatial properties of the Geo-GSOM algorithm, parametrisation effects and conducted comparative evaluations across four disaster use cases. A methodological overview of the JSTTS approach is available in Fig. 26.

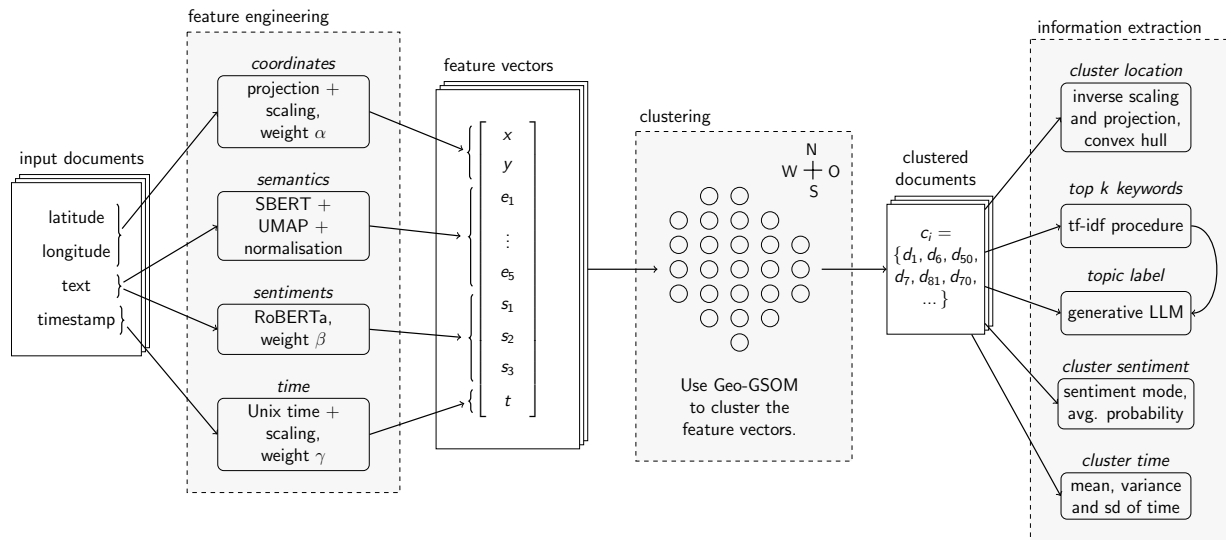


Figure 26: Methodological workflow of the JSTTS framework developed within TEMA

First, to validate the spatial coherence of the developed Geo-GSOM, an artificial data set of 400 points was used, designed to form a valley-like spatial structure. The Geo-GSOM was compared against a standard GSOM under two geographic tolerance settings ($r_{geo} = 0$ and $r_{geo} = 2$). The results showed that Geo-GSOM preserved spatial neighborhoods more effectively, with better alignment between the learned neuron structure and the underlying spatial distribution—particularly at $r_{geo} = 0$, where clustering relied purely on geographic proximity. A visual representation of this is available in Fig. 27.

Quantitative evaluation using global Moran’s I confirmed these findings. The Geo-GSOM achieved significantly higher spatial autocorrelation (0.77) than the standard GSOM (0.47), indicating improved spatial structure and reduced variance across runs. These results validate Geo-GSOM as a robust and spatially coherent clustering method, supporting its role in multimodal information fusion for disaster-related social media analysis. To evaluate the flexibility and trade-offs in the feature weighting of the JSTTS model, a parameter sensitivity analysis was conducted using a dataset of over 28,933 geo-located tweets related to Hurricane Harvey. Three feature weights for sentiment (β), space (α), and time (γ) were varied systematically to assess their influence on cluster quality. The results showed that increasing the sentiment weight (β) improved sentiment uniformity within clusters (SU), with a peak at $\beta = 0.5$, while leading to a slight drop in topic quality (TQ) and increases in spatial and temporal variance. Conversely, increasing the coordinate weight (α) reduced spatial variance in both dimensions but slightly decreased sentiment coherence. Higher

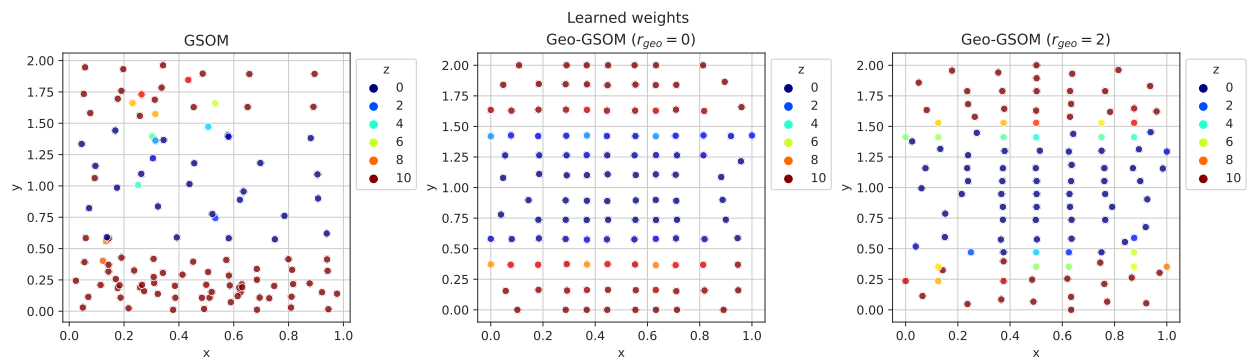


Figure 27: Learned weights of the trained (Geo-)GSOM networks in all three dimensions x , y (plotted on the axes) and z (colour) given the artificial training data

temporal weights (γ) produced clusters more concentrated in time but again led to reduced topic and sentiment quality.

A full grid search across all three parameters confirmed these patterns. The sentiment weight β showed a strong positive correlation with sentiment uniformity (Pearson $r = 0.831$), while spatial (α) and temporal (γ) weights were strongly negatively correlated with their respective variances ($r = -0.918$ and $r = -0.947$). These results demonstrate that the JSTTS model enables flexible control over the focus of clustering, allowing for more sentiment-aligned, spatially localized or temporally concentrated clusters. However, these gains involve trade-offs in other cluster dimensions, underscoring the complexity of parameter tuning in multimodal clustering tasks.

To evaluate the performance and generalisability of the JSTTS model, a comparative experiment was conducted against a state-of-the-art sequential workflow using geo-referenced tweets from four disasters: the 2014 Napa earthquake, 2017 Hurricane Harvey, 2021 Ahr Valley floods, and 2023 Chile wildfires. While the sequential baseline follows a modular pipeline which applies sentiment analysis, topic modeling, and spatial clustering independently, the JSTTS model integrates all modalities jointly into a single clustering process. The number of output clusters was aligned between both approaches to ensure fair comparison.

As summarised in Table 3, the JSTTS model consistently outperformed the sequential method in terms of semantic topic quality (TQ) and sentiment uniformity (SU). On average, JSTTS achieved a TQ of 0.145 compared to 0.034 for the sequential workflow, largely due to better topic diversity. SU scores were also significantly higher for JSTTS, averaging 0.89 versus 0.73, indicating more emotionally coherent clusters. While spatial and temporal variances were comparable across methods, JSTTS yielded slightly more balanced cluster sizes, producing fewer clusters with very small post counts. These findings are visually illustrated in the output map for the Ahr Valley floods (see Figure 28), where JSTTS generated semantically and sentimentally consistent clusters with clear spatial structure.

Beyond performance, the JSTTS model demonstrated strong adaptability across data sets with diverse geographic and temporal scopes. On average, clusters covered 7.4% of the total spatial area and 25.9% of the total time range, showing the model's ability to flexibly adjust to different scales without the need for extensive reconfiguration. These results underline the effectiveness and robustness of the JSTTS model as an integrated solution for multimodal social media analysis in disaster contexts. The above results have been published in [26]. With social media data alone, IT:U is able to handle four modalities simultaneously, specifically addressing **OC2 "Increase situational awareness in NDM"** within TEMA and significantly advancing the state-of-the-art in information fusion of geo-social media data.

In practice, the clustered outputs of the JSTTS model can be leveraged by emergency responders such as firefighters or civil protection units to enhance situational awareness during unfolding disasters. By summarising massive volumes of geo-referenced social media posts into a handful of interpretable clusters that are thematically and emotionally coherent, responders can quickly identify areas of concern, understand public sentiment and detect urgent needs or incidents reported by the public. For example, clusters with strongly negative sentiment and flood-related keywords in specific regions may help prioritise resource allocation or identify zones requiring immediate intervention.

	Ahr Valley floods		Hurricane Harvey		Chile wildfires		Napa earthquake	
	JSTTS	Seq.	JSTTS	Seq.	JSTTS	Seq.	JSTTS	Seq.
size	122.8	130.0	344.4	344.4	1,864.9	1,864.9	1,069.5	1,069.5
σ_{size}	181.2	223.3	739.3	817.3	3,146.8	4,220.1	1,024.2	1,191.8
TQ	0.165	0.029	0.191	0.042	0.142	0.034	0.081	0.030
SU	0.891	0.81	0.926	0.832	0.837	0.673	0.894	0.603
σ_x^2	0.003	0.003	0.002	0.001	0.001	0.001	0.003	0.004
σ_y^2	0.003	0.003	0.001	0.001	0.004	0.002	0.004	0.004
σ_t^2	0.067	0.065	0.056	0.061	0.002	0.002	0.076	0.067

Table 3: Evaluation metrics for the outputs produced by our JSTTS approach and the independent sequential workflow (Seq.) across four use case data sets. The metrics include the average cluster size, the standard deviation among the cluster sizes σ_{size} , the semantic topic quality TQ measured as the product of coherence and diversity, the sentiment uniformity SU, the variance among the normalised spatial coordinates σ_x^2 and σ_y^2 and the variance of the normalised time σ_t^2 . The best scores are marked in bold.

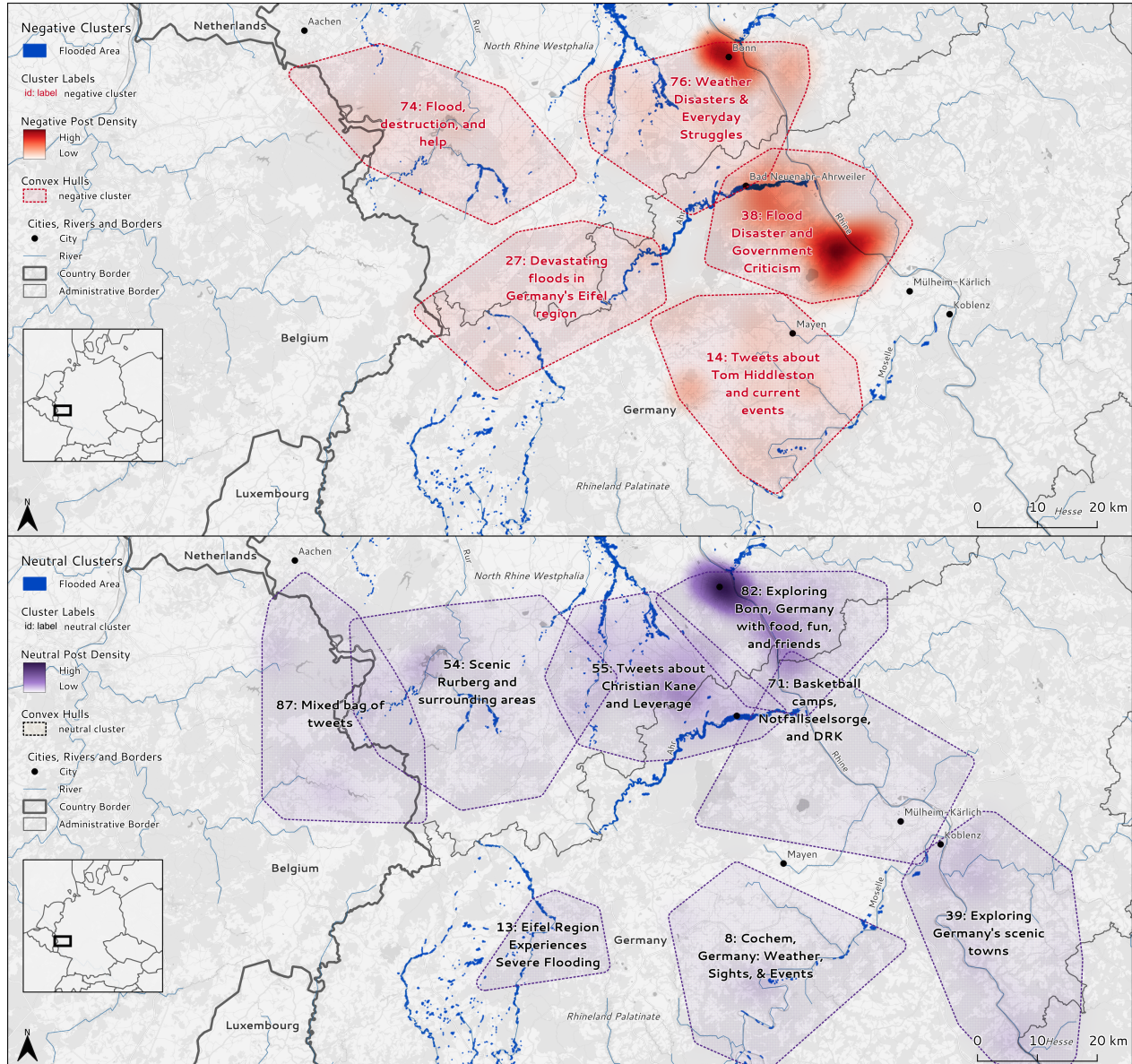


Figure 28: Visual representation of the multimodal Ahr Valley clusters identified as potentially flood-related, juxtaposed with respect to the associated sentiment (negative and neutral). The figure displays the convex hull of the clusters in geographic space, coloured by sentiment. The cluster labels in the format cluster ID:name were computed with the help of Llama-2-70b-chat and placed at the representative cluster location learned by the Geo-GSOM. The density of underlying posts is displayed using a heat map. To provide context, flooded areas identified by the Copernicus Emergency Management Service are depicted in blue.

4 Decision Support Service for Remote Sensing

Wide-spread and intense natural disasters, such as the severe floods in Western Germany and neighbouring countries and the 15.000-hectare forest fire in central Sardinia, both in 2021, force authorities to assess the disaster situation quickly and comprehensively for an adequate operational planning. SEM services such as the Copernicus Emergency Management Service (CEMS) Rapid Mapping Service (RMS) [1] provide geospatial crisis information on demand and quickly in support of authorities and responders before, during or immediately following a disaster [27]. While the standard SEM workflow has evolved in recent years, particularly in the field of satellite image analysis and delivery timeliness of the crisis information by utilising early warning systems [28], a lot of time is lost with manual work steps (e.g., searching for available data, initiating processing).

In TEMA, we have analysed and implemented different technical approaches to reduce the time between the first warning, the acquisition of satellite data and the availability of analysis results. We have developed a decision support tool that automatically processes and fuses multi-source web data (e.g. public alerts, sensor observations, weather forecasts), identifies AOIs at risk and intersects them with relevant satellite image acquisition opportunities. Our approach improves the end user's situational awareness by automatically generating decision proposals regarding EO data and product availability.

The majority of the scientific achievements described in this section have been published in [29,30], and [31].

4.1 Main Activities Performed (Months 13–30)

In TEMA, we first analysed the causes of delays in the SEM workflow and identified possible improvements. Based on the results, we developed a concept and a system mock-up to automate manual steps to improve both the timeliness and accuracy of EO-based crisis information.

Public disaster alerts are used as the primary input data source, automatically retrieved at regular time intervals. The system concept considers fire/flood simulation results as a further potential spatio-temporal input. For this purpose, DLR has been in iterative discussions and planning with NS and TSYL on the data exchange and structure of flood and wildfire simulations using web-based APIs. In collaboration with PLUS/IT:U, an evaluation showed that, due to its timeliness, geo-social media can be another suitable data source for the AOI extraction and process triggering. In order to properly integrate PDM-tech-06 into the overall TEMA platform, DLR has defined a suitable web-based service endpoint, a proposal data resource and an NGSI-LD entity definition.

Finally, we implemented our approach in the DSS for Remote Sensing (PDM-tech-06) including a proof-of-concept integration of simulation data as an additional input. Experimental work was carried out on an automated triggering of flood processing (TFA-tech-08) based on public alerts. After a continuous exchange between DLR, Lat40 and KAMK, the final prototype could be integrated into the TEMA platform via the API Gateway and decision proposals could be visualised geospatially in the SmartDesk. During the hackatons, the component was tested and further refined in the context of the TEMA platform. Furthermore, the performance and results of PDM-tech-06 were

tested internally during real disaster events that occurred within the T4.4 lifetime. One example is the severe flooding in Central and Eastern Europe that occurred in mid-September 2024. We have documented the results of the DSS during this flood disaster in an article on the TEMA project website [32]. From an end-user perspective, PDM-tech-06 will be evaluated in the German and Finnish trials. As a preparation and pre-test, we have manually created the public heavy rain warning issued by the DWD before the Ahrtal floods and ingested it into the component.

The outcomes of the activities performed are described in detail in the following sections.

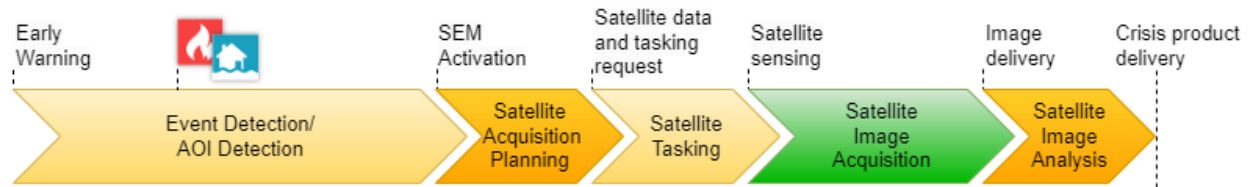
4.2 State of the Art and Advancements Made

Since 2003, the Center for Satellite-Based Crisis Information (ZKI) of the German Aerospace Center (DLR) has established one of the first rapid mapping mechanisms that continued to evolve with concurrent advances in satellite technology to provide users, typically official authorities, with precise EO-based crisis information [33]. Among other RMS providers, DLR has contributed to the predecessor of the CEMS [34]. Today, the standard SEM process of the CEMS starts with a user-driven activation, requested on average 20 hours after the user-defined event time. Upon activation, the state-of-the-art process follows the steps of

1. satellite acquisition planning and tasking
2. satellite image acquisition
3. image delivery
4. crisis map product delivery including image analysis [28]

as outlined in Figure 29. Step 1 is only necessary for EO satellites that do not collect data on a permanent basis and instead need to be tasked. Examples include commercial Very High Resolution (VHR) optical satellites (e.g. WorldView-3) and radar satellites (e.g. TerraSAR-X).

STATE-OF-THE-ART SEM WORKFLOW (e.g. CEMS)



IMPROVED SEM WORKFLOW (PDM-tech-06)

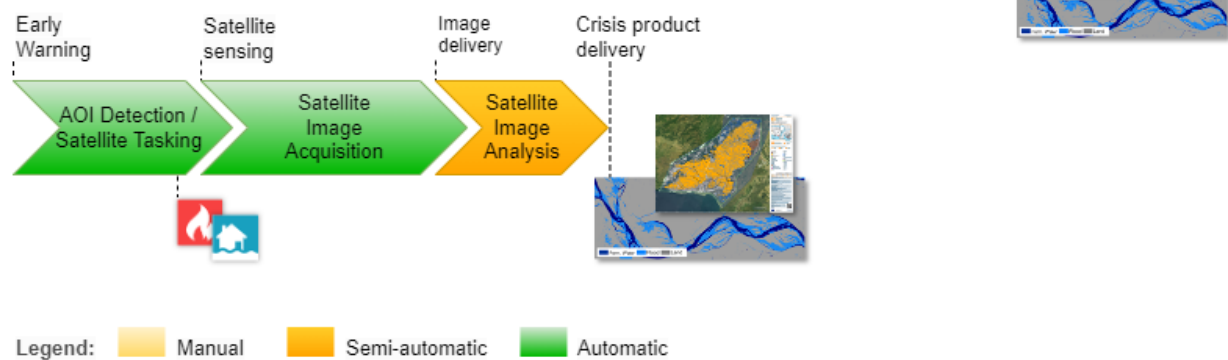


Figure 29: Comparison between state-of-the-art and proposed automated SEM workflow

To illustrate this SEM process, the timeline of the severe flooding in the Ahr valley was reconstructed. Figure 30 shows early warnings from the European Flood Awareness System (EFAS) [35] and the DWD [36,37] four, respectively, one day before the activation of the CEMS RMS. The considered timeline is largely based on [38], [39], and [40]. Upon the activation, cloud cover prevented the use of optical satellite imagery for damage assessment during first days of flooding. Meanwhile, the ZKI was activated at the request of the Bavarian Red Cross in response to the DWD warnings and was able to provide timely aerial imagery by chance [41]. An automatic flood detection based on Sentinel-1 radar satellite imagery was also published [42]. Once suitable optical satellite imagery was available, the first maps were published by the CEMS approximately 138 h after the activation. This case illustrates the time delays in the current SEM workflow due to manual activation responsibilities and handover procedures. It is important to note that the disaster response cannot be reconstructed for a theoretical case in which the SEM had been activated earlier.

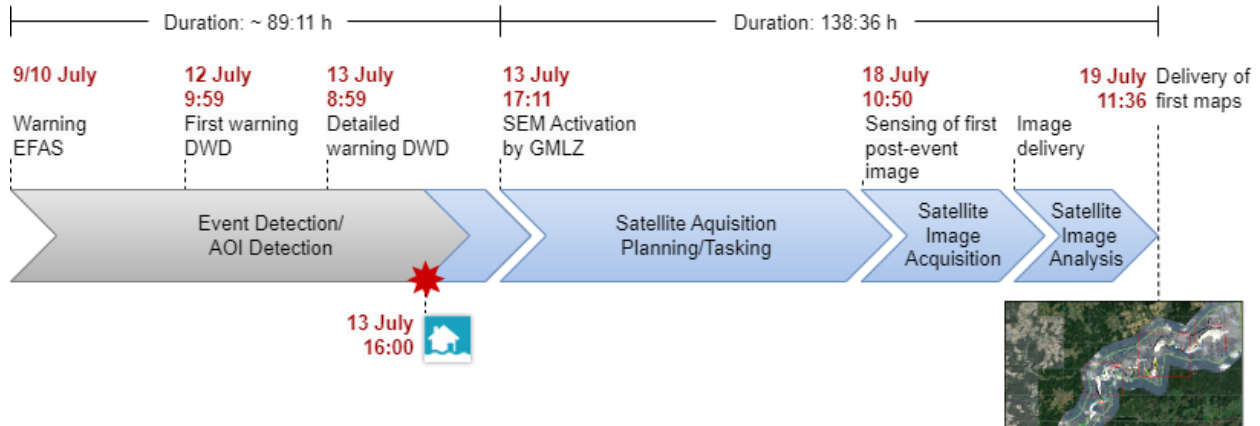


Figure 30: Condensed timeline of the CEMS activation EMSR517 for Bad Neuenahr-Ahrweiler with time in UTC.

Overall, we can identify several significant gaps in time delay 1) between the initial early warning and the SEM activation, which is performed manually by an authorised user, 2) between the activation and satellite tasking. Furthermore, 3) the latency between satellite image acquisition and delivery (e.g. through the Copernicus Data Space Ecosystem (CDSE)) and 4) the time- and labour-intensive manual and semi-automated visual image interpretation delay the SEM process at later stages. Most attention has been given to optimising the fourth gap, which remains an area for continuous improvement, such as fully automated flood detection [43, 44], and burnt area derivation [45, 46]. Such a real-time processor, which derives burned areas from medium resolution imagery (e.g. Sentinel-3), has recently been integrated into DLR’s ZKI Fire Monitoring System [47]. In T3.2 of the TEMA project, DLR has been focusing on improving flood processing (TFA-tech-08) as well as burnt area detection algorithms (TFA-tech-09) in terms of accuracy and timeliness. In addition, DLR has conducted experiments to compare the time required for data downstream through the DLR receiving station in Neustrelitz, Germany, and through the publicly available CDSE. As described in D3.2, the production of analysis-ready data through the DLR direct downlink could potentially reduce the time between acquisition and availability of Sentinel-1 satellite imagery (gap 3) by a factor of 5 compared to the CDSE.

To understand where the delays in the first steps come from, we analysed the activities of the different actors involved in the SEM process. Service providers perform the rapid mapping upon SEM activation and publish the generated crisis information, e.g. via the CEMS RMS portal. In order to produce timely and accurate mapping products such as burnt or flooded area maps, service providers need to trigger the SEM process as early as possible with clearly defined AOIs. The SEM is typically activated by end users such as civil protection authorities and emergency services. A number of early warning tools are available [28]. Similarly, [48] propose to integrate early warning alerts such as those provided by the Global Disaster Alert and Coordination System (GDACS) [49] to reduce acquisition times by up to a day. While such approaches reduce the time to trigger, they are limited to specific natural events and in some cases are not widely available. However, some critical steps prior to SEM activation remain user-driven. First, end users must manually identify the AOI, often from multiple sources of data such as warnings, weather forecasts, observations,

etc. In addition, they must make an effort to become aware of the availability of satellite data to capture the AOIs once they are affected by the event. Service providers typically use acquisition planning tools where they intersect the AOIs with planned satellite overpasses. Furthermore, it is unclear to end users when the generated products will finally become available.

Accordingly, our research question and concept examination here revolved around technical ways to improve user situational awareness, automate manual steps, and thus reduce the time needed from the initial warning to satellite data acquisition to the availability of analysis results. We developed a tool that **automatically processes and fuses multi-source web data** (e.g., public alerts, sensor observations, weather forecasts), **detects (potential) disaster AOIs and event times**, and **intersects them with relevant satellite acquisition opportunities**. Our approach improves the end-user's situational awareness by **automatically generating decision proposals regarding EO data and product availability**. Situational awareness is enhanced by the spatio-temporal format of the decision proposals including geo-referenced AOIs and satellite acquisition opportunities. This allows the decision proposals to be displayed in a GIS such as the TEMA SmartDesk application. The user is supported by **transparency of the underlying data sources, the expected (and actual) time of satellite data acquisition, relevant attributes and satellite overlap for events**.

4.3 Technical Design and Implementation of PDM-tech-06

4.3.1 Architecture and Spatiotemporal Data Fusion

Once the concept was established, we have developed a prototype of PDM-tech-06. The prototype was designed as a client-server web application. Its architecture is outlined in Figure 31. The server part consists of a data management component, an intersection component, a database and an API. The data management component automatically downloads alerts at regular (configurable) intervals from various public international providers such as the GDACS and MeteoAlarm [50] as well as with national sources such as the DWD. In addition, point information on active water levels from the German Länderübergreifendes Hochwasserportal - Cross-border Flood Portal (LHP) are analysed and the intersection component is triggered. The spatio-temporal intersection component is a Java-based extension of the operational Processing System Management (PSM) [51] deployed at DLR's ground station for satellite data reception in Neustrelitz, Germany. It correlates acquisition windows from Sentinel-1A, Sentinel-2A/B, Sentinel-3A/B, Landsat-8/9, WorldView-1/3 and GeoEye-1 satellites within the next 7 days that overlap in time and space with the identified AOIs. The outcomes of these calculations are stored in a PostgreSQL database accessible via a web API for visualisation purposes. Moreover, a dissemination service generates brief email notifications with a summary of the intersection results and suggests relevant satellite acquisition opportunities.

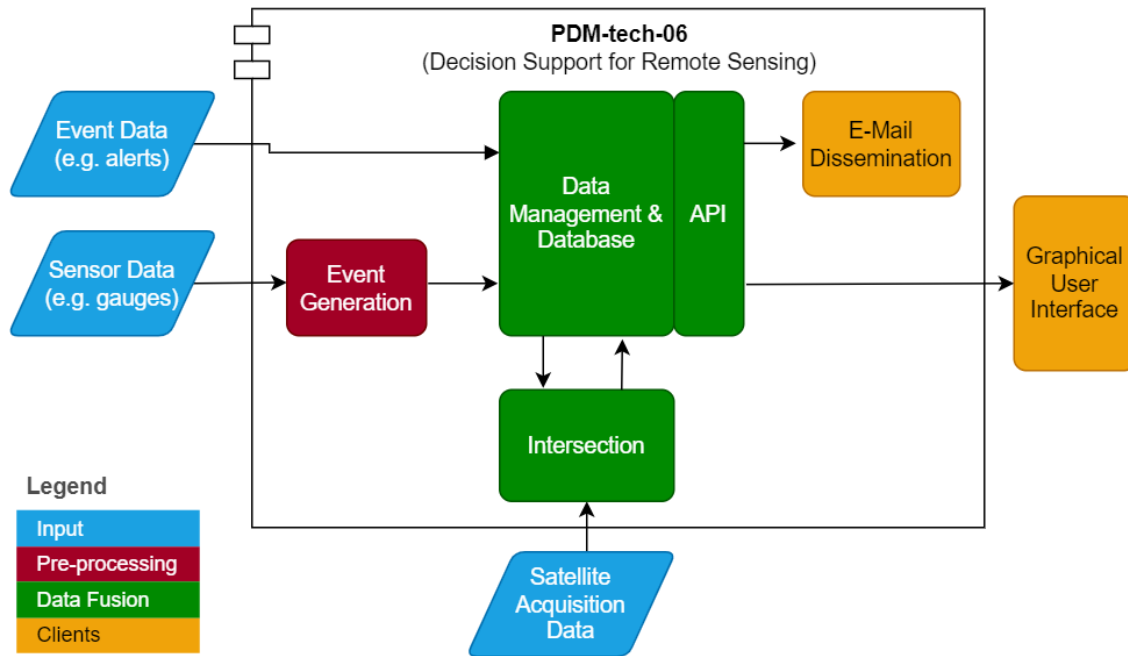


Figure 31: Architecture of PDM-tech-06

The component **determines an AOI from crisis-related web data** by detecting spatio-temporal anomalies in a given context. Sometimes web data implicitly contain AOIs, for example, the messages from numerous national and international entities such as MeteoAlarm. Sometimes, the information derived from alerts and event databases is not satisfactory or reliable. An example of a rather untrustworthy source is the Global Database of Events, Language, and Tone [52]. In such a situation, we cannot rely on just one data source. Also, an official alert may cover a vast administrative entity. However, a service provider is primarily interested in the situation in populated areas. In such cases, we suggest fusing as many data sources as necessary to determine a meaningful AOI.

Another challenge is the heterogeneity of the data. As a prerequisite for the AOI determination, we have harmonised the mapping of countries to alerts. The country code is derived from a buffered (0.01°) version of Countries 2020 1:60 Million provided by the Geographic Information System of the Commission (GISCO) (© EuroGeographics for the administrative boundaries). Prior to intersection, the component pre-filters warnings in order to present the most relevant events for SEM. Examples include:

- Filtering droughts, fog, 'high-temperature', 'low-temperature', 'coastalevent' and minor meteorological warnings which are not relevant for NDM
- Filtering 'freezing precipitation', 'black ice', 'icing', 'icy surfaces', 'freezing rain' irrelevant for satellite acquisition planning
- Filtering warnings based on keywords or phrases in the headline/description/identifier that indicate no actual warning such as "No hazardous events", "No warnings", "There are currently

no active warnings or risks" or "NOWARNING"

- Skipping warnings with severity minor
- Skipping warnings with a wrong label
- Skipping LHP warnings with urgency "past" since those point to all-clear warning information

In addition to defining AOIs for specific events, **retrieving information about satellite coverage opportunities** is essential to our approach.

1. For satellites that **collect data permanently and the data are made available free of charge** on platforms on the web each of the derived AOIs can be intersected with the potential sensing areas. No manual interaction is required and all the necessary data can be downloaded from the web. Examples of this category are the Copernicus Sentinel or Landsat missions.
2. For satellites that **provide a direct data broadcast**, such as Sentinel-1, Aqua, Terra and Suomi NPP, we additionally have to consider the direct acquisition capabilities of ground stations.
3. For satellites that **do not collect data on a permanent basis and that have to be tasked** by an authorised entity an interface with commercial satellite operators must be established to ensure that the requested AOIs can be included in the acquisition planning. Examples of this category are commercial VHR optical satellites (e.g. WorldView-3) and radar satellites (e.g. TerraSAR-X).

The overall objective is the same in all three cases: **We want to know what satellite data will be available for our AOIs, and when.** This information is of great value to decision-makers in crisis situations, based on the experience of previous ZKI activations and research projects, e.g. EU FP7 PHAROS (Community Research and Development Information Service (CORDIS), 2023) and EU H2020 HEIMDALL (CORDIS, 2022).

Not every satellite sensor is suitable for every natural disaster event. DLR is member of the International Charter "Space and Major Disasters" [53]. The Charter members have committed resources to rapidly support the so-called 'Authorised Users', typically national civil protection authorities as well as disaster relief organisations, with free of charge pre- and post-event satellite data to help mitigate the impact of major disasters on human life and property. The Charter data is evaluated either by the users themselves or by rapid mapping organisations such as the CEMS or the ZKI. Among other roles, DLR provides the rotational role of the Emergency On-Call Officer (ECO). The ECO function identifies the most timely and appropriate satellite resources. There is a procedure for this, which includes the so-called Charter scenarios. These are detailed recommendations on which Charter satellite missions should be requested in which case and with what priority. Based on these recommendations we have implemented the **satellite prioritisation** shown in Figure 32 for flood and forest fire scenarios.

	S1 A/B	S2 A/B	S3 A/B	L8	L9	WV1	WV2	WV3	GE1
Flood	1	2	3	2	2	1	1	1	1
Fire	3	1	3	1	1	1	1	1	1

Figure 32: Prioritisation of satellite sensors for flood and wildfire from highly suitable (green), over suitable (yellow) to less suitable (red). S=Sentinel, L=Landsat, WV=WorldView, GE=GeoEye

We also fuse spatially, temporally and thematically related data sources such as a meteorological warning with different active water levels indicating the same flood event. An overall incident description, the underlying alerts and overlapping satellite acquisition opportunities can be found in the decision proposal data resource exposed via the web API. Annex A: Usage of the Decision Support Endpoint contains a comprehensive decision proposal in JSON format, including information on the severity of the event, the underlying data sources, the expected (and actual) time of satellite data acquisition, the relevant attributes and the overlap of satellites for events.

As a further step towards the optimisation of the SEM process an automatic triggering of flood processing (TFA-tech-08) using an identified flood AOIs has been experimentally evaluated. The idea is to trigger the processing of existing satellite data on the one hand, but also the scheduling of the processing of data available in the future. Currently, the flood processor automatically analyses data across Europe with a stable frequency. Further research is needed in order to offer intelligent, targeted processing in the future that makes efficient use of processing resources when and where most needed.

A detailed description of the architecture and applied algorithms is provided in [29].

4.3.2 Interaction

In the context of the TEMA platform, shown in Figure 33, the DSS accesses fire and flood simulations provided by PDM-tech-01 and PDM-tech-02 as a further input. The communication was realised by a direct request via the respective web interfaces of the simulators. In order to be aware of updates to the simulations, PDM-tech-06 performs periodic requests (i.e. pulling).

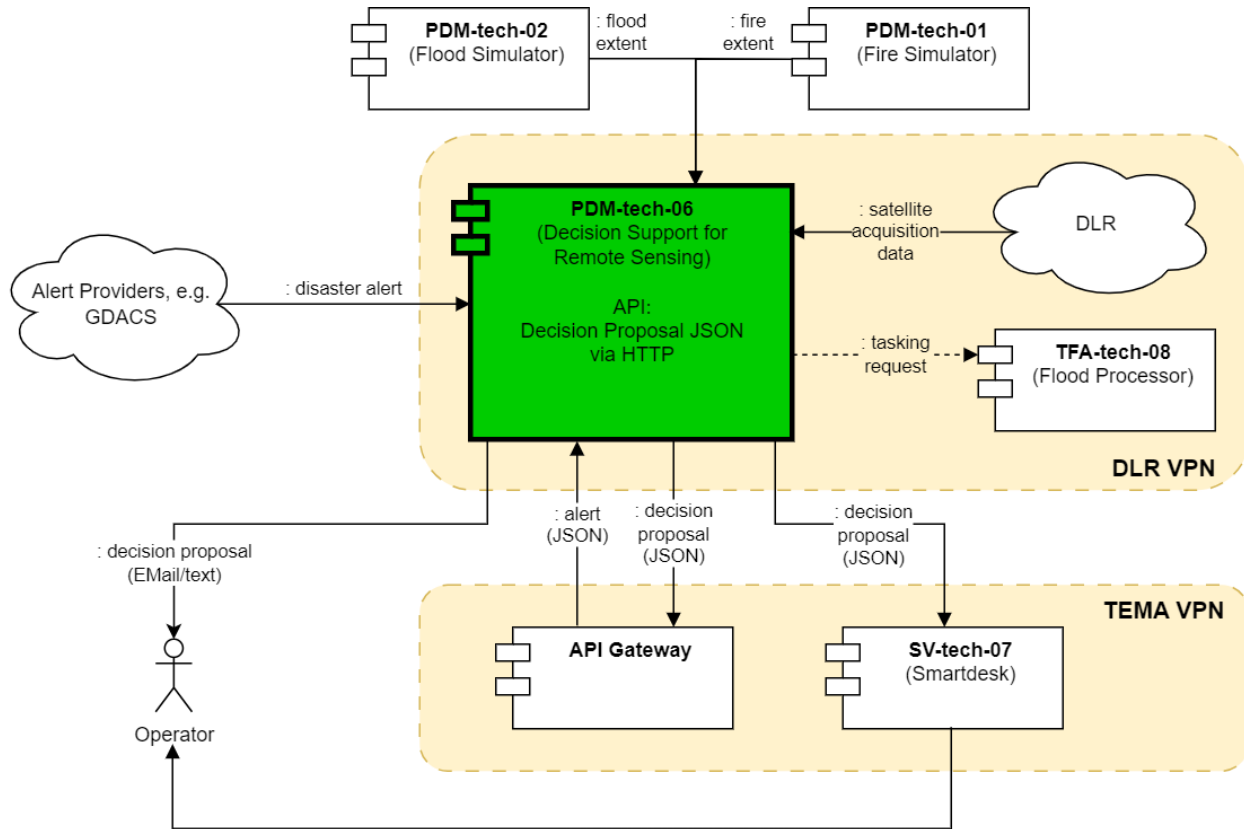


Figure 33: Interactions of PDM-tech-06 in the context of the TEMA platform

Integrating FireSim (PDM-tech-01) outputs into the DSS

TSYL’s FireSim outputs, such as Arrival Time, Rate of Spread, Flame Length, Fireline Intensity or Firepath, provide high-resolution simulations of wildfire behaviour. These outputs can be leveraged to improve the DSS, enhancing remote sensing workflows in NDM. In this sense, FireSim’s outputs enable automated delineation of geographically and temporally relevant AOIs, focusing satellite tasking or UAV monitoring on zones with the highest expected fire activity or areas with early impacts.

In the TEMA project, FireSim continuously updates its outputs based on real-time weather data from ground sensors and control points for simulation adjustment based on fire fronts actual positions. This continuous refinement can provide feedback into satellite tasking logic, for example, adjusting monitoring targets as fire conditions evolve. The way TEMA interacts with FireSim is through an API Gateway that has been developed by Lat40.

When the Gateway receives an Alert from the Fire Monitoring Mission, the information contained in the Alert is used to trigger the simulation. Since FireSim is a component built for CRUD Requests interactions, the corresponding gateway component requests FireSim outputs and sends them to the TEMA platform via MinIO object storage. Basically, the request that is sent to the FireSim API to create a simulation is a payload with all the information needed, such as ignition points,

timestamp, weather information and other adjustment parameters. Internally, FireSim randomly generates a `sim_id` (GUID) that is the only reference to the simulation that is being generated. When the simulation is successfully calculated, the outputs can be requested via the FireSIM API by anyone knowing the corresponding `sim_id`. This field is mandatory to get any output from the API since there is no other way to reference the simulation. In the actual implementation of FireSim inside the TEMA architecture, the only component that has access to the `sim_id` value is the API gateway. If the DSS (or any other component) needs access to FireSim outputs from outside the TEMA platform, some development should be considered by the partners involved to be able to access the `sim_id` internally.

Integrating flood simulation software (PDM-tech-02) outputs into the DSS

PDM-tech-02 calculates the propagation of a flood and its associated water levels over a specified period of time. The results of a simulation are written to a NetCDF file that follows the CF conventions. This requires the 2D and 1D mesh data to be stored in separate parts of the file. These files contain snapshots of all relevant flow variables for a defined output time step. The node variables of the NetCDF files include volumes, water levels and all the source and sink terms. Water levels are expressed in meters above Mean Sea Level (MSL).

Once an end-user activates an Alert on the TEMA platform, an NGS-Entity is created and sent to PDM-tech-02. The coordinates of the Alert are used as input to set up a scenario for the flood simulation. Based on these coordinates and the location of the Alert, PDM-tech-02 automatically retrieves the boundaries of the hydrological catchment area (or watershed). A hydrological catchment is an area or land where all the rainfall and surface water naturally drains into a single water body, such as a river. The edges of such catchments are defined by topography (such as hills or ridges) or man-made structures such as dikes or dams. Based on the derived hydrological area, a scenario is created to simulate the flood in this region.

Similar to the data management component of DSS which downloads public alerts and active water levels as input, PDM-tech-02 uses weather forecast data from DWD: the ICON (Icosahedral Nonhydrostatic) Model, which is a global Numerical Weather Prediction (NWP) model. The state-of-the-art approach in weather forecasting involves generating a new ensemble forecast for ICON Europe (ICON-EU) every 3 hours, with a spatial resolution of 7 km. For the use case of the Ahr valley in TEMA, PDM-tech-02 uses ICON-D2 forecast data, which is updated hourly with a spatial resolution of 2.2 km for Germany. This provides PDM-tech-06 with hourly updated flood predictions based on the latest weather forecast data.

PDM-tech-02 generates water level rasters for each output timestep, which can be retrieved by API. These rasters showcase snapshots of the maximum flood extent for a specified time step (see Fig. 34 as an example). These temporal rasters are stored in the data warehouse of Nelen & Schuurmans (NS) and are retrieved by DLR via pull request to available endpoints of the raster data (<https://demo.lizard.net/api/v4/timeseries/1bcb36e-781d-4339-9632-00d5398c3b15/>). Depending on the output time step of the simulation, a loop request will result in the retrieval of each output time step and the associated water levels and flood extent per specified time step (for example: $t = 0$, $t = + 1h$, $t = +2h$). These water level rasters provide a maximum extent where flooding is expected.

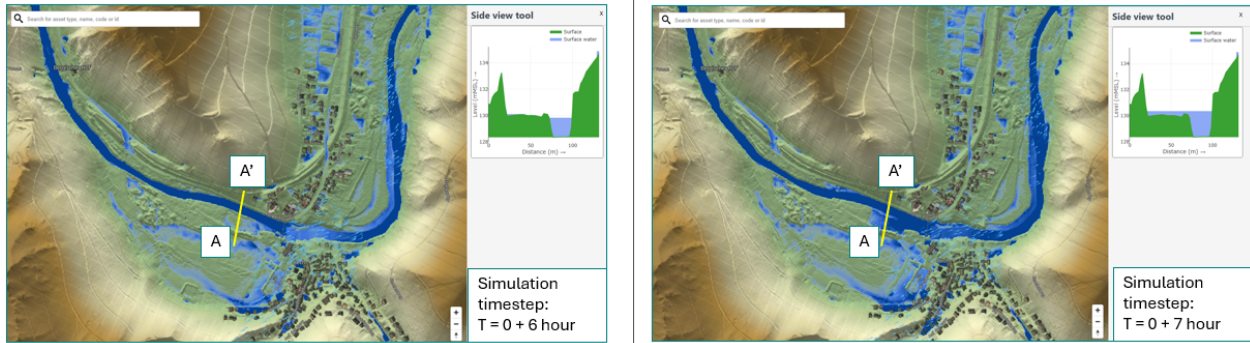


Figure 34: Different time steps with various flood extents.

Due to organisational constraints the DSS could not be deployed in external Virtual Private Networks (VPNs). Therefore, a solution had to be found to be able to push new results into the TEMA platform. Like TFA-tech-08 and TFA-tech-09, PDM-tech-06 provides a **web-based API** that can be accessed by any client. We have restricted access to the prototype API using basic auth. This gives us a **self-contained, sustainable service** that can be easily integrated into other contexts, system architectures and information flows, such as existing systems used by government agencies. While TEMA aims at developing a platform at TRL 5-6, the DSS will be open for future extension in the context of future research and development initiatives. The API Gateway developed by Lat40 resides within the TEMA VPN. The Gateway requests proposals from PDM-tech-06 and distributes decision proposals to all interested TEMA components via the Digital Enabler component. For this purpose, DLR has defined an NGSI-LD entity that is created by the Gateway as soon as it receives new data from PDM-tech-06. A more specific description of the DSS endpoint as well as the proposal resource can be found in Annex A: Usage of the Decision Support Endpoint.

4.3.3 Visualisation

The benefit of an open web API becomes clear when considering the different ways in which decision proposals can be visualised. One option is to load the data resource into a GIS. We have used one of our custom-built GIS applications to display our results as a proof-of-concept. For the Ahrtal use case, we have manually created an alert based on the original DWD warning and ingested it into the DSS. Different visualisations of the resulting proposal are shown in Figures 35, 36 and 37.

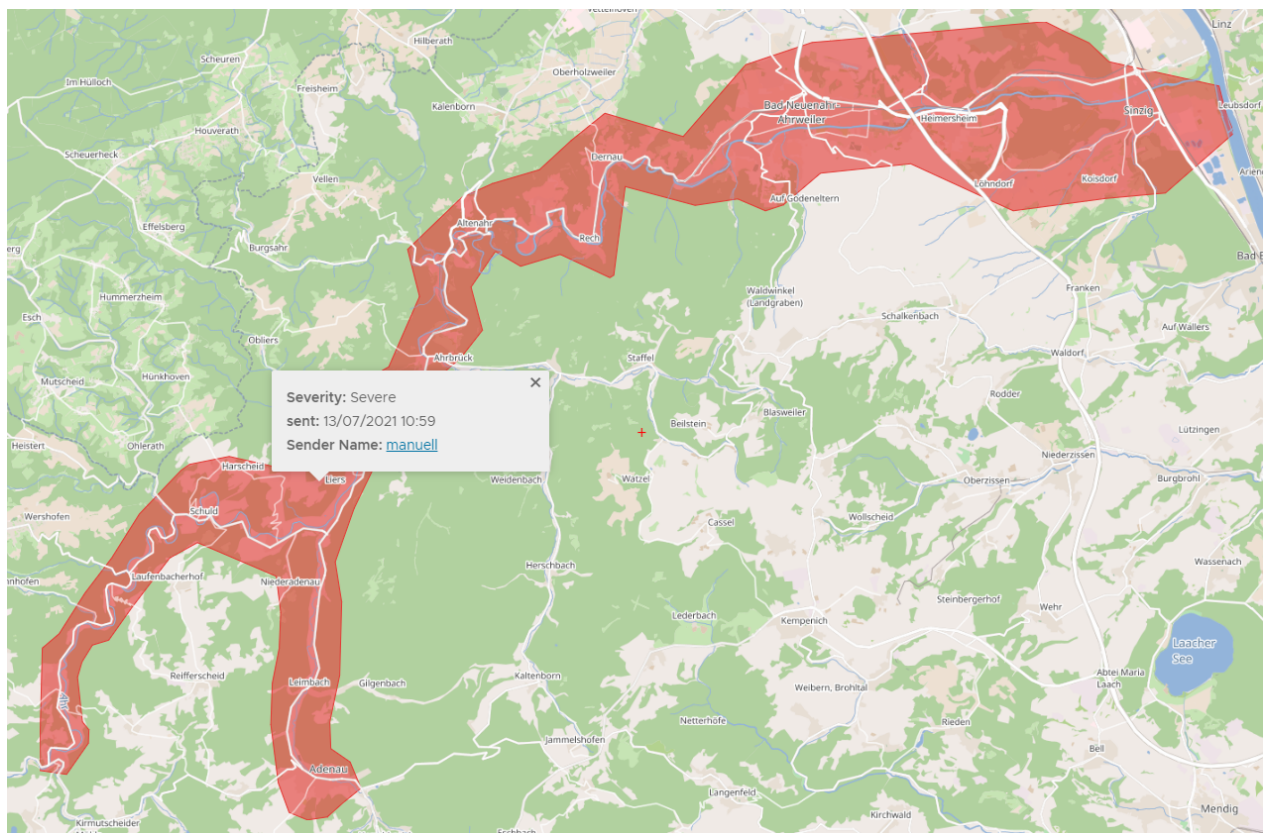


Figure 35: Possible geospatial map visualisation of an AOI derived from a manually ingested Ahrtal warning

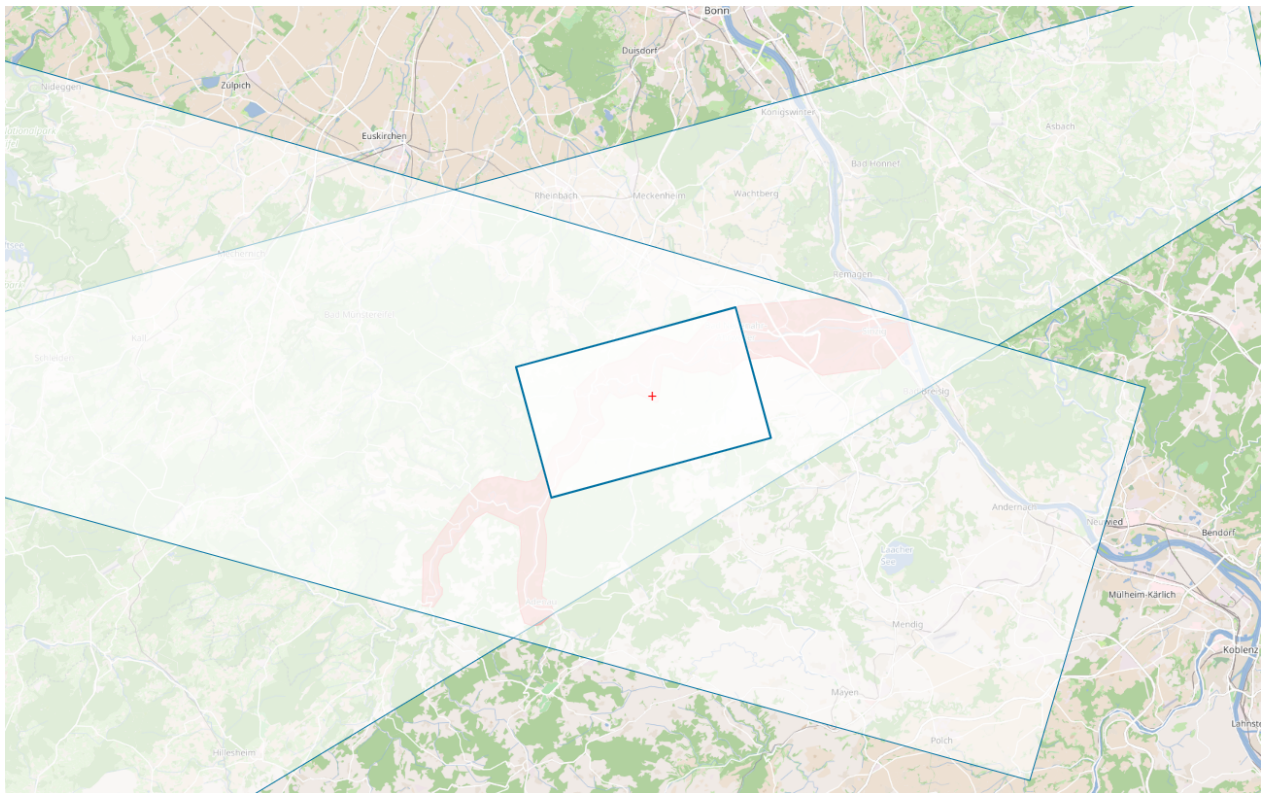


Figure 36: Possible geospatial map visualisation of selected relevant satellite overpasses

Satellite scenes		Warnings				
	👁	Satellite Name	⚠	📄	Mission Status	Acquisition date ↓
>	👁	Sentinel-1A	1	6%	planned	22/09/2024
>	👁	Sentinel-1A	1	15%	planned	21/09/2024
>	👁	Sentinel-2A	2	86%	planned	21/09/2024
∨	👁	Sentinel-1A	1	76%	planned	20/09/2024
<p>Sentinel-1A Satellite Priority for Flood: Highly relevant Begin time: 20/09/2024 05:03 End time: 20/09/2024 05:15</p> <p>📖 HIDE SCENE ON MAP</p>						
>	👁	Sentinel-2B	2	44%	planned	19/09/2024
>	👁	Sentinel-1A	1	19%	acquired	18/09/2024

Figure 37: Possible list visualisation of relevant satellite overpass windows. The table shows for each satellite the prioritisation for the disaster event, overlap in percent, an indication whether the acquisition is "planned" or "acquired" and the acquisition time.

Further screenshots are shown in Section 4.4.

During testing and the TEMA trials in Germany and Finland we will demonstrate the direct interaction between the **DSS's web API and the SmartDesk (SV-tech-07)**. The SmartDesk visualises a decision proposal on the map by highlighting the warning AOIs and overlaying the tracks of relevant satellite overpasses. The information may help users to make a decision based on information from the Alert message and determine smaller AOIs to run TEMA business missions. Figures 38 and 39 show screenshots of the SmartDesk with a first version of a visualised decision proposal.

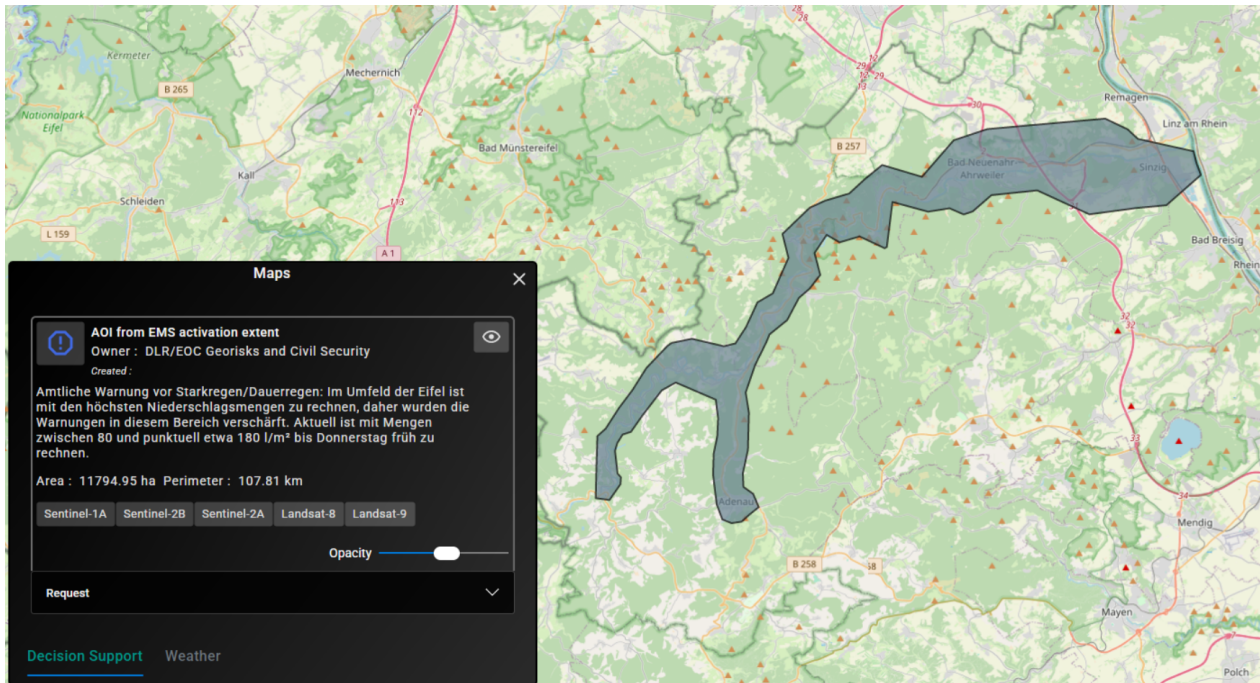


Figure 38: SmartDesk showing an official warning as issued by the DWD in July 2021 for the Ahrtal valley, Germany. The box contains the warning text and the identified overlapping satellites.

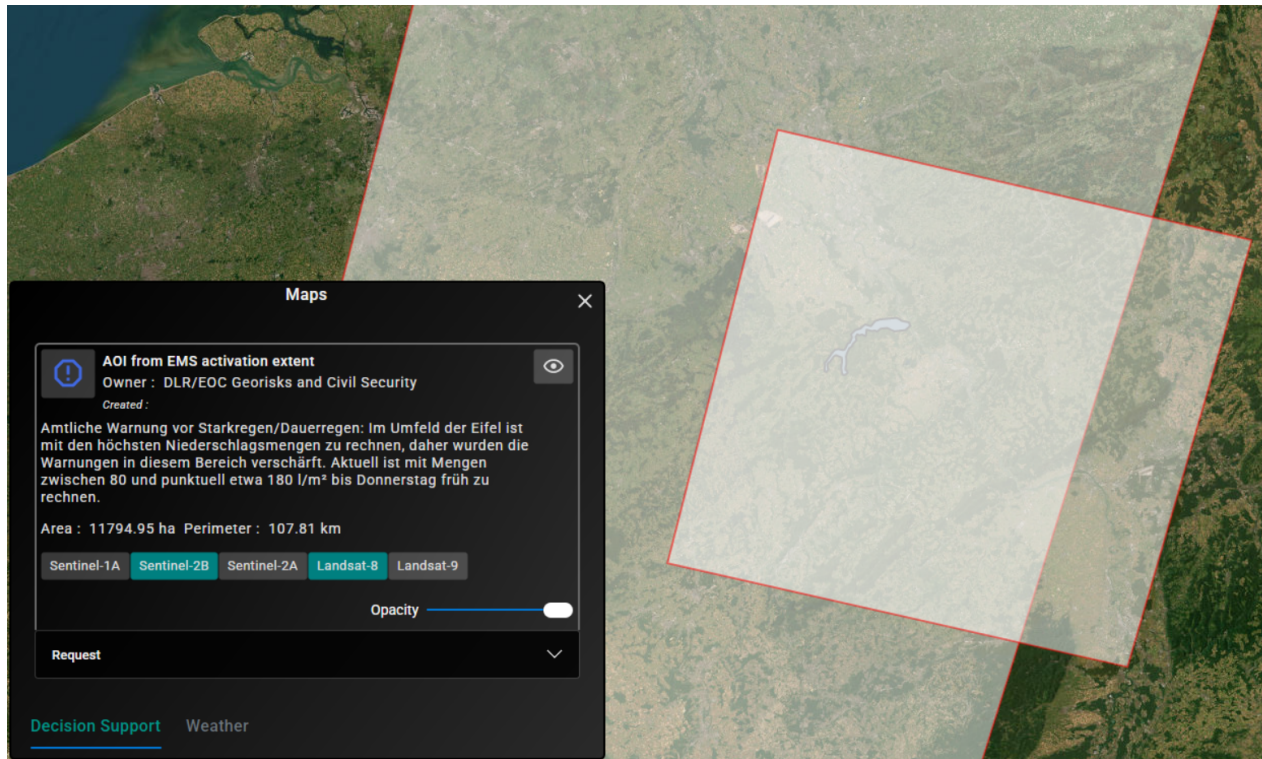


Figure 39: SmartDesk showing the swaths of the two satellites Sentinel-2B and Landsat-8 relevant for the Ahr valley warning AOI.

In addition, during the upcoming trials in Germany and Finland end-user partners will be subscribed to receive text **notifications via email**. Figure 40 shows an example notification with a summary of warnings and overlapping satellite acquisition opportunities for a specific incident.

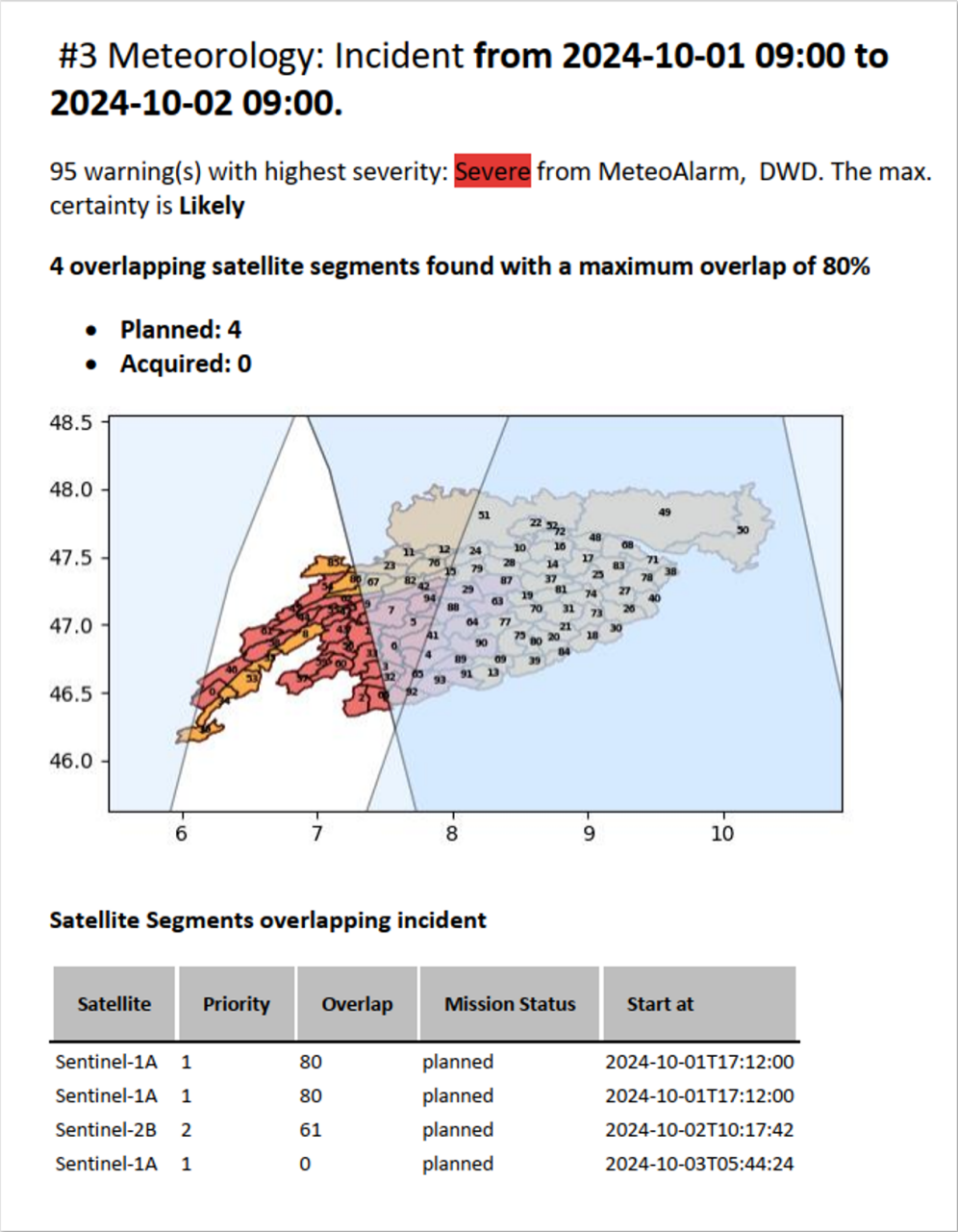


Figure 40: E-Mail notification showing the analysis results in a human-readable format.

4.4 Performance in Real Events

Since the start of T4.4, release versions of the DSS for Remote Sensing have been running continuously in the DLR infrastructure. During the latest project lifetime, PDM-tech-06 has recorded and analysed several real events around the world, such as a local flood warning for Lithuania in March 2024, regional floods in Bavaria in June 2024, inter-regional floods in Central and Eastern



Europe in September 2024, and Cyclone Chido that had devastated the French island of Mayotte in December 2024. Figures 41 and 42 show the results for the regional flood event in September 2024.

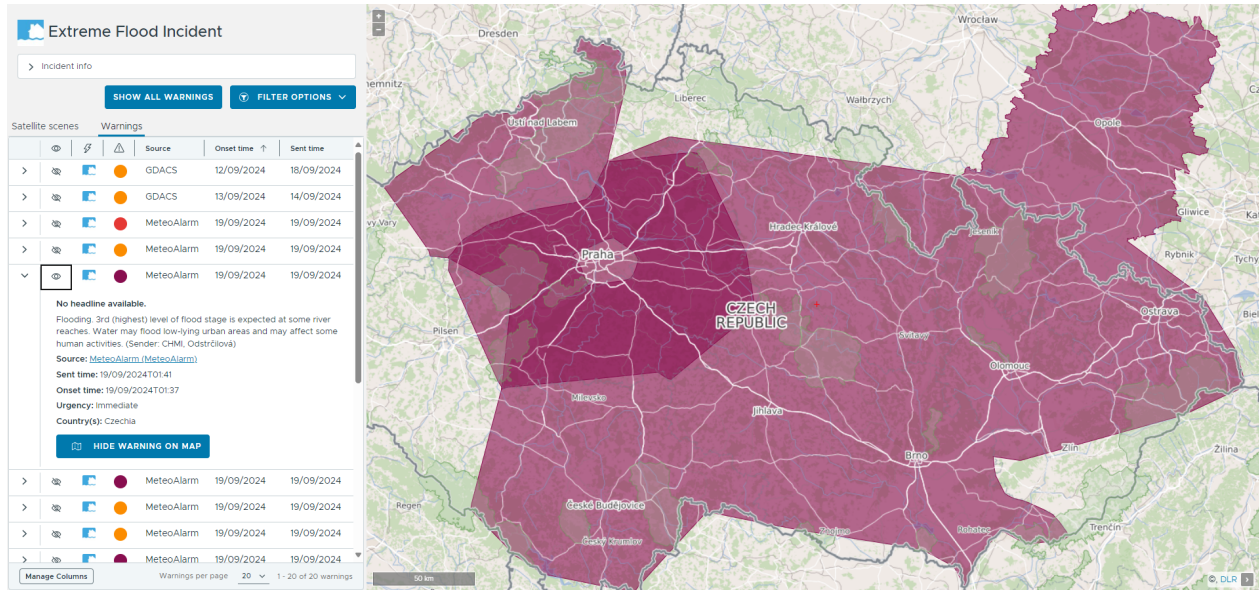


Figure 41: Screenshot showing the list of public warnings captured by PDM-tech-06 and the resulting clustered AOIs in a map for the regional floods in Central and Eastern Europe in September 2024 utilizing a test GIS.

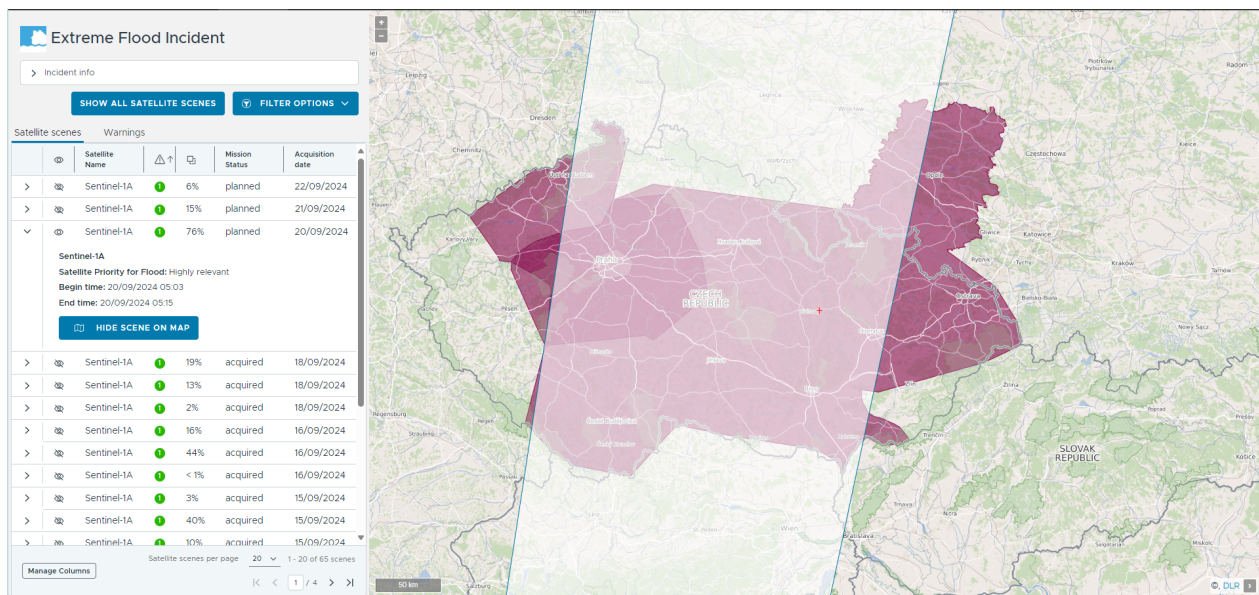


Figure 42: Screenshot showing the list of relevant satellite acquisition opportunities generated by PDM-tech-06 for the regional floods in Central and Eastern Europe in September 2024. In a test GIS app satellite windows are visualised in a table and on the map.

On the one hand, real events such as those mentioned above are used to test and to refine the functionality and performance of the component. For example, pre-filtering rules as listed in Section 4.3.1 were consecutively extended. On the other hand, first insights into the timeliness of our approach were gained. The time required for AOI detection is 5-10 minutes on average. The total time for AOI detection and correlation of AOIs with satellite overpasses is between 1.5 and 2 h. The longer duration is attributed due to the fact that all trajectories must be recalculated for each query, and this applies to a relatively large number of satellites.

4.5 Impact and Future Prospects

Compared to the manual process, the time required to determine the AOI of a disaster event and the relevant satellite overpasses is reduced from several days to a few hours due to automation. TEMA objective **OC3 “Reduce mental load for human operators in NDM”** is addressed by automating manual tasks through the TEMA platform. By augmenting established SEM processes with automation and open data, the platform enhances the timeliness and quality of the resulting EO products. This approach allows operators to focus more on critical data analysis rather than data retrieval, thereby improving situational awareness. The DLR technology Decision Support for Remote Sensing generates transparent decision proposals in both textual and geospatial formats, facilitating easy access and communication between service providers and end-users, thereby meeting KPIs for automation and transparency in disaster response.

Together with related achievements for the flood and burnt area processors made in T3.2 and documented in D3.1 and D3.2, PDM-tech-06 strongly supports TEMA objective **OC1 to “Reduce latency in NDM”** between warning and map product delivery. Besides the automated determination of AOIs the experimental automatic triggering of flood and burnt area processing needs to be explored in order to use processing capabilities more efficiently and targeted. Future work also includes a further systematic quantification of the time taken for each step in the SEM workflow including worst-case durations. With this information, we expect to gain more insight into the expected time of product availability.

PDM-tech-06 will be evaluated in trials in Ahrtal, Germany (regional flood) and Finland (forest fires).

5 Conclusions

Deliverable D4.2 Report on information fusion and decision support is the second deliverable of the fourth Work package (WP4) of the TEMA project. This document reports the main research results of Tasks T4.3 Information fusion and T4.4 Data-fusion-based decision support and process triggering. The main outputs of the research and development carried out were 3 technological components supporting the TEMA platform functionalities described in Deliverable D2.2. These TEMA technologies and the related ones developed in WP3 and WP5 will be interlinked and orchestrated through the developed TEMA Core in Task T6.2. In Tasks T6.3 and T6.4 the TEMA technologies will be trialed and evaluated by the end users.

Section 3 summarised the implementation of the Information fusion module of the TEMA platform architecture as well as the development and evaluation of the JSTTS framework that fuses semantic, sentiment, spatial and temporal information from social media. Section 4 presented the approach and implementation of a decision support service that automatically processes and fuses multi-source web data (e.g., public alerts, sensor observations, weather forecasts), identifies AOIs at risk and intersects them with relevant satellite image acquisitions for an improved situational awareness of SEM providers and end-users.

Moreover, 6 publications (3 journal papers, 3 conference papers) were submitted to academic journals and conferences that are listed in Annex B: Related publications. Further publications related to the work presented in this document are planned in the scope of WP7. Finally, as a public deliverable, D4.2 assists in the dissemination of the project results to the scientific community.

References

- [1] CEMS RMS, “Copernicus Emergency Management Service on-demand mapping.” <https://mapping.emergency.copernicus.eu/>, 2025. Accessed April 9, 2025.
- [2] O. Baysal and G. Zhou, “Uav-based multi-sensor data fusion for time-critical disaster response,” in *ISPRS Workshop on Geospatial Data for Emergency Response*, 2009.
- [3] S. Mandyam, S. Priya, S. Suresh, and K. Srinivasan, “Natural disaster analysis using satellite imagery and social-media data for emergency response situations,” *arXiv preprint arXiv:2311.09947*, 2023.
- [4] S. A. Kashinath, S. A. Mostafa, A. Mustapha, H. Mahdin, D. Lim, M. A. Mahmoud, M. A. Mohammed, B. A. S. Al-Rimy, M. F. M. Fudzee, and T. J. Yang, “Review of data fusion methods for real-time and multi-sensor traffic flow analysis,” *IEEE Access*, vol. 9, pp. 51258–51276, 2021.
- [5] F. Nex and F. Remondino, “UAV for 3D mapping applications: A review,” *Applied Geomatics*, vol. 6, no. 1, pp. 1–15, 2014.
- [6] N. Said, K. Ahmad, M. Regular, K. Pogorelov, L. Hassan, N. Ahmad, and N. Conci, “Natural disasters detection in social media and satellite imagery: A survey,” *Multimedia Tools and Applications*, vol. 78, no. 1, pp. 1–27, 2019.
- [7] G. A. Mills-Tettey, A. Stentz, and M. B. Dias, “The dynamic Hungarian algorithm for the assignment problem with changing costs,” *Robotics Institute, Pittsburgh, PA, Tech. Rep. CMU-RI-TR-07-27*, 2007.
- [8] S. Thrun, W. Burgard, and D. Fox, *Probabilistic Robotics*. Intelligent Robotics and Autonomous Agents, Cambridge, MA: MIT Press, 2005.
- [9] Y. Bar-Shalom, X. Li, and T. Kirubarajan, *Estimation with Applications to Tracking and Navigation*. Wiley, 2009.
- [10] E. Winarno, W. Hadikurniawati, and R. N. Rosso, “Location-based service for presence system using Haversine method,” in *2017 International Conference on Innovative and Creative Information Technology (ICITech)*, pp. 1–4, IEEE, 2017.
- [11] H. W. Kuhn, “The Hungarian method for the assignment problem,” *Naval Research Logistics Quarterly*, vol. 2, no. 1–2, pp. 83–97, 1955.
- [12] C. Dick, J. H. Krüger, and R. Westermann, “GPU ray-casting for scalable terrain rendering,” in *Eurographics (Areas Papers)*, pp. 43–50, Citeseer, 2009.
- [13] B. Santana, E. K. Cherif, A. Bernardino, and R. Ribeiro, “Real-time georeferencing of fire front aerial images using iterative ray-tracing and the bearings-range extended Kalman filter,” *Sensors*, vol. 22, no. 3, p. 1150, 2022.
- [14] G. ETSI, “Context information management (CIM); NGSI-LD API,” *Context Information Management (CIM)*, pp. 1–159, 2019.

- [15] R. Rai, *Socket.IO real-time web application development*. Packt Publishing, 2013.
- [16] J. Phengsuwan, T. Shah, N. B. Thekkummal, Z. Wen, R. Sun, D. Pullarkatt, H. Thirugnanam, M. V. Ramesh, G. Morgan, P. James, and R. Ranjan, “Use of social media data in disaster management: A survey,” *Future Internet*, vol. 13, p. 46, Feb. 2021.
- [17] Z. Wang and X. Ye, “Social media analytics for natural disaster management,” *International Journal of Geographical Information Science*, vol. 32, pp. 49–72, Jan. 2018.
- [18] K. Camacho, R. Portelli, A. Shortridge, and B. Takahashi, “Sentiment mapping: Point pattern analysis of sentiment classified Twitter data,” *Cartography and Geographic Information Science*, vol. 48, pp. 241–257, May 2021.
- [19] I. AlAgha, “Topic Modeling and Sentiment Analysis of Twitter Discussions on COVID-19 from Spatial and Temporal Perspectives,” *Journal of Information Science Theory and Practice*, vol. 9, pp. 35–53, Mar. 2021.
- [20] M. Parimala, R. M. Swarna Priya, M. Praveen Kumar Reddy, C. Lal Chowdhary, R. Kumar Poluru, and S. Khan, “Spatiotemporal-based sentiment analysis on tweets for risk assessment of event using deep learning approach,” *Software: Practice and Experience*, vol. 51, no. 3, pp. 550–570, 2021.
- [21] D. Hanny and B. Resch, “Clustering-based Joint Topic-Sentiment Modeling of social media data: A neural networks approach,” *Information*, vol. 15, p. 200, Apr. 2024.
- [22] N. Reimers and I. Gurevych, “Sentence-BERT: Sentence embeddings using Siamese BERT-networks,” in *Proceedings of the 2019 Conference on Empirical Methods in Natural Language Processing and the 9th International Joint Conference on Natural Language Processing (EMNLP-IJCNLP)*, (Hong Kong, China), pp. 3980–3990, Association for Computational Linguistics, 2019.
- [23] C. Lin and Y. He, “Joint sentiment/topic model for sentiment analysis,” in *Proceedings of the 18th ACM Conference on Information and Knowledge Management, CIKM '09*, (New York, NY, USA), pp. 375–384, Association for Computing Machinery, Nov. 2009.
- [24] X. Fu, H. Wu, and L. Cui, “Topic Sentiment Joint Model with word embeddings,” in *DMNLP@PKDD/ECML*, 2016.
- [25] D. Hanny and B. Resch, “Multimodal geo-information extraction from social media for supporting decision-making in disaster management,” *AGILE: GIScience Series*, vol. 5, pp. 1–8, May 2024.
- [26] D. Hanny and B. Resch, “Multimodal GeoAI: An integrated spatio-temporal topic-sentiment model for the analysis of geo-social media posts for disaster management,” *International Journal of Applied Earth Observation and Geoinformation*, vol. 139, p. 104540, 2025.
- [27] S. Voigt, F. Giulio-Tonolo, J. Lyons, J. Kučera, B. Jones, T. Schneiderhan, G. Platzeck, K. Kaku, M. K. Hazarika, L. Czarán, S. Li, W. Pedersen, G. K. James, C. Proy, D. M. Muthike, J. Bequignon, and Debarati Guha-Sapir, “Global trends in satellite-based emergency mapping,” *Science (New York, N.Y.)*, vol. 353, no. 6296, pp. 247–252, 2016. [tex.eprint: https://www.science.org/doi/pdf/10.1126/science.aad8728](https://www.science.org/doi/pdf/10.1126/science.aad8728).

- [28] A. Wania, I. Joubert-Boitat, F. Dottori, M. Kalas, and P. Salamon, “Increasing timeliness of satellite-based flood mapping using early warning systems in the Copernicus Emergency Management Service,” *Remote Sensing*, vol. 13, no. 11, 2021. Number: 2114.
- [29] M. Mühlbauer, M. Friedemann, J. Roll, T. Riedlinger, F. Henkel, L. D. Angermann, M. Böck, T. Kaminski, and K. Barginda, “Improved Satellite-Based Emergency Mapping through automated triggering of processes,” pp. 1–9, May 2024.
- [30] S. Schmidt, M. Friedemann, D. Hanny, B. Resch, T. Riedlinger, and M. Mühlbauer, “Enhancing satellite-based emergency mapping: Identifying wildfires through geo-social media analysis,” *Big Earth Data*, vol. 0, no. 0, pp. 1–23, 2025.
- [31] M. Friedemann, M. Mühlbauer, F. Henkel, T. Wilke, and T. Riedlinger, “Supporting situational awareness for an improved triggering of satellite-based emergency mapping,” *Abstracts of the ICA*, vol. 9, 2025.
- [32] M. Friedemann and M. Wieland, “Satellite-based decision support and mapping of floods in central Europe in September 2024.” <https://tema-project.eu/articles/satellite-based-decision-support-and-mapping-floods-central-europe-september-2024>, 2024.
- [33] M. Gähler, “Remote sensing for natural or man-made disasters and environmental changes,” in *Environmental Applications of Remote Sensing* (M. Marghany, ed.), ch. 11, Rijeka: IntechOpen, 2016.
- [34] T. Schneiderhan, M. Gähler, O. Kranz, and S. Voigt, “Insights to the Emergency Mapping Service within the GMES project SAFER - Highlights, main achievements and challenges,” in *Conference Proceedings*, pp. 1–5, June 2010.
- [35] EFAS, “EFAS.” <https://www.efas.eu>, 2025. Accessed April 9, 2025.
- [36] Deutscher Wetterdienst (DWD), “Tweet: "Aktuelle Unwetterwarnung: Sehr starke Regenfälle und Überschwemmungen in Rheinland-Pfalz, Nordrhein-Westfalen und Teilen von Hessen. #Unwetter" (July 12, 2021).” https://twitter.com/DWD_presse/status/1414524803273400323, 2021. Accessed April 9, 2025.
- [37] Deutscher Wetterdienst (DWD), “Tweet: "Sehr starke Regenfälle und überschwemmungen in Rheinland-Pfalz und Nordrhein-Westfalen. #Unwetter" (July 13, 2021).” https://twitter.com/DWD_presse/status/1414872018005241857, 2021. Accessed April 9, 2025.
- [38] CEMS, “EMSR517: Flood in Western Germany,” 2021. European Union.
- [39] CEMS, “The Copernicus Emergency Management Service forecasts, notifies, and monitors devastating floods in Germany, Netherlands, Belgium and Switzerland,” July 2021. European Union.
- [40] A. Weidinger, “Was ist in der Flutnacht passiert?– Ein Protokoll.” <https://www.swr.de/swraktuell/rheinland-pfalz/flut-rekonstruktion-ahrtal-protokoll-100.html>, June 2023. Südwestrundfunk (SWR).
- [41] E. Holzheimer, U. Kippnich, M. Kippnich, K. Lechner, and M. Wieland, “Erkundung im Ahrtal mit Unterstützung von Verfahren der künstlichen Intelligenz,” *Die Flut im Juli 2021. Erfahrungen*

- gen und Perspektiven aus dem Rettungsingenieurwesen und Katastrophenrisikomanagement*, vol. 1, pp. 22–26, 2022.
- [42] ZKI, “Unwetter in Nordrhein-Westfalen und Rheinland-Pfalz, Deutschland.” <https://activations.zki.dlr.de/en/activations/items/ACT152.html>, July 2021. German Aerospace Center (DLR), Earth Observation Center. Retrieved February 14, 2024.
- [43] M. Wieland and S. Martinis, “A modular processing chain for automated flood monitoring from multi-spectral satellite data,” *Remote Sensing*, vol. 11, pp. 1–23, October 2019.
- [44] M. Berezky, M. Wieland, C. Krullikowski, S. Martinis, and S. Plank, “Sentinel-1-based water and flood mapping: Benchmarking Convolutional Neural Networks against an operational rule-based processing chain,” *IEEE Journal of Selected Topics in Applied Earth Observations and Remote Sensing*, vol. 15, pp. 2023–2036, 2022.
- [45] M. Nolde, S. M. Plank, and T. Riedlinger, “An adaptive and extensible system for satellite-based, large scale burnt area monitoring in near-real time,” *Remote Sensing*, vol. 12, pp. 1–20, July 2020.
- [46] L. Knopp, M. Wieland, M. Rättich, and S. Martinis, “A deep learning approach for burned area segmentation with Sentinel-2 data,” *Remote Sensing*, vol. 12, pp. 1–22, July 2020.
- [47] ZKI, “Fire monitoring and management.” <https://services.zki.dlr.de/fire>, 2025. Accessed April 9, 2025.
- [48] A. Ajmar, A. Annunziato, P. Boccardo, F. G. Tonolo, and A. Wania, “Tsunami modeling and satellite-based emergency mapping: Workflow integration opportunities,” *Geosciences*, vol. 9, no. 7, p. 314, 2019.
- [49] GDACS, “GDACS.” <https://gdacs.org/>, 2025. Accessed April 9, 2025.
- [50] Meteoalarm, “Meteoalarm - European severe weather alerts.” <https://meteoalarm.org/>, 2025. Accessed April 9, 2025.
- [51] M. Boettcher, R. Reißig, E. Mikusch, and C. Reck, “Processing management tools for Earth Observation products at DLR-DFD,” in *DASIA 2001 Data Systems in Aerospace* (T. N. European Space Agency Publications Division ESTEC, P.O. Box 299 2200 AG Noordwijk, ed.), vol. SP-483 of *Data Systems in Aerospace*, European Space Agency, 2001.
- [52] GDELT Project, “GDELT Project - Global Data on Events, Language, and Tone.” <https://www.gdeltproject.org>, 2025. Accessed April 9, 2025.
- [53] S. Martinis, A. Twele, S. M. Plank, H. Zwenzner, J. Danzeglocke, G. Strunz, H.-P. Lüttenberg, and S. Dech, “The international ‘Charter Space and Major Disasters’: DLR’s contributions to emergency response worldwide,” *Photogrammetrie, Fernerkundung, Geoinformation*, vol. 85, pp. 317–325, November 2017.
- [54] OASIS Emergency Management Technical Committee, “Common Alerting Protocol Version 1.2.” <http://docs.oasis-open.org/emergency/cap/v1.2/CAP-v1.2-os.html>, 2010. Accessed: 2025-04-11.

Annex A: Usage of the Decision Support Endpoint

The endpoint to be interrogated to search for the item of interest is available here:

- <https://services.zki.dlr.de/tema-api>

In order to narrow down an AOI and timeframe the following query can be used:

- [https://services.zki.dlr.de/tema-api?intersects=\{%22type%22:%22Polygon%22,%22coordinates%22:\[\[6.823104892,50.37160887\],\[6.823104892,50.568673976\],\[7.28591315,50.568673976\],\[7.28591315,50.37160887\],\[6.823104892,50.37160887\]\]\}&from_date=2024-06-11T00:00:00&to_date=2024-06-20T00:00:00](https://services.zki.dlr.de/tema-api?intersects=\{%22type%22:%22Polygon%22,%22coordinates%22:[[6.823104892,50.37160887],[6.823104892,50.568673976],[7.28591315,50.568673976],[7.28591315,50.37160887],[6.823104892,50.37160887]]\}&from_date=2024-06-11T00:00:00&to_date=2024-06-20T00:00:00)

When the endpoint above is queried, it may return either no item, i.e. the data the client is looking for is not available or has not yet been calculated, or a list containing the data of interest. The data consists of a list of 0-n “proposal” items. These consist of 1-n “warning” elements and 0-n “segment” elements. The latter represent the satellite acquisition segments. The document is likely to be updated over time once new input data becomes available referring to the very same disaster event. Figure 43 shows the main section of a proposal containing information on the disaster event such as the severity, the expected or actual onset time and a geometry which outlines the total AOI clustered from the individual warning-based AOIs. Each warning element is attributed by a textual description, the disaster type, severity and certainty of the alert. The standard format for warning messages is the Common Alerting Protocol (CAP) standard [54]. We have adopted corresponding attributes and values where applicable. The representation of a satellite segment is shown in Figure 44.

```

"proposal": [
  {
    "severity": {
      "name": "Severe"
    },
    "onset_at": "2024-06-12T12:39:02",
    "expire_at": null,
    "countries": [
      {
        "country": {
          "name": "Germany",
          "iso3_code": "DEU"
        }
      }
    ],
    "geom": {
      "type": "Polygon",
      "coordinates": [...]
    },
    "warnings": [
      {
        "warning": {
          "headline": "AOI from EMS activation extent ",
          "description": "Amtliche Warnung vor Starkregen/Dauerregen: Im Umfeld der Eifel ist mit den höchsten Niederschlagsmengen zu rechnen, daher wurden die Warnungen in diesem Bereich verschärft. Aktuell ist mit Mengen zwischen 80 und punktuell etwa 180 l/m² bis Donnerstag früh zu rechnen.",
          "onset_at": "2024-06-12T12:39:02",
          "expires_at": null,
          "category": {
            "name": "Flood"
          },
          "severity": {
            "name": "Severe"
          },
          "certainty": {
            "name": "Observed"
          }
        }
      }
    ]
  }
]

```

Figure 43: Main part of a proposal as provided via the Web API

```
"satellites": [  
  {  
    "priority": 2,  
    "overlap": 100,  
    "segment": {  
      "from": "2024-12-02T21:19:42.856534",  
      "to": "2024-12-02T21:19:45.334066",  
      "satellite": {  
        "name": "Sentinel-2B"  
      },  
      "geom": {  
        "type": "Polygon",  
        "coordinates": [...]  
      }  
    }  
  },  
  ...  
]
```

Figure 44: Example of a satellite segment as listed for warning elements inside a proposal

Annex B: Related publications

No.	Title	Reference	Type
1	Clustering-Based Joint Topic-Sentiment Modeling of Social Media Data: A Neural Networks Approach	[21]	Article
2	Multimodal Geo-Information Extraction from Social Media for Supporting Decision-Making in Disaster Management	[25]	Article
3	Multimodal GeoAI: An integrated spatio-temporal topic-sentiment model for the analysis of geo-social media posts for disaster management	[26]	Article
4	Improved Satellite-Based Emergency Mapping through Automated Triggering of Processes	[29]	Article
5	Enhancing satellite-based emergency mapping: Identifying wildfires through geo-social media analysis	[30]	Article
6	Supporting Situational Awareness for an Improved Triggering of Satellite-Based Emergency Mapping	[31]	Article



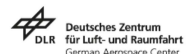
Disclaimer

This document contains material, which is the copyright of certain TEMA contractors, and may not be reproduced or copied without permission. All TEMA consortium partners have agreed to the full publication of this document if not declared “Confidential”. The commercial use of any information contained in this document may require a license from the proprietor of that information. The reproduction of this document or of parts of it requires an agreement with the proprietor of that information.

This document does not represent the opinion of the European Community, and the European Community is not responsible for any use that might be made of its content.

Copyright Notice

© 2025 by the authors, the TEMA consortium.



Funded by
the European Union